DEVELOPMENT OF A NEW COALBED METHANE (CBM) COMPUTER ANALYSIS MODEL TO EVALUATE CBM RESERVOIRS AT THE DRUNKARDS WASH UNIT, UINTA BASIN, UTAH

by

YUANHAI YANG

A thesis submitted to the Faculty and the Board of Trustees of the Colorado School of Mines in partial fulfillment of the requirements for the degree of Doctor of Philosophy (Petroleum Engineering).

Golden, Colorado

Date _Sep. 10, 2004_

Signed: _Yuanhai Yang_
Yuanhai Yang

Approved: _Craig W. Van Kirk_
Dr. Craig W. Van Kirk
Thesis Advisor

Golden, Colorado

Date _September 10, 2004_

Craig W. Van Kirk
Dr. Craig W. Van Kirk
Professor and Head,
Department of
Petroleum Engineering

ABSTRACT

This work presents a new computer analysis model and methodology using well logging data to evaluate coalbed methane (CBM) reservoirs in general, with specific application demonstrated at the Drunkards Wash Unit (DWU), Uinta basin, Utah. The input data includes log curves provided by a standard logging tool, which include bulk density, resistivity, and gamma ray. The major output results consist of coal lithology, coal thickness, gas content, ash content, and gas-in-place.

This new CBM computer analysis model is constructed on the basis of new observations and new algorithms in the following aspects:

- A diverse coal lithology system at DWU

- Logging responses in CBM reservoirs under adverse logging environments

- Gas desorption/adsorption characteristics

- Applications of the new CBM computer analysis model

After examining the Proximate Analysis results of more than 200 coal samples retrieved from 23 core holes, a new coal lithology system was determined. Compared to the original coal lithology system, the new one introduced two new coal lithologies and encompassed the representative coal lithologies present at DWU. For the first time, the new coal lithology system quantitatively relates the coal lithology with its ash content.

As one of the major research tasks, in-depth investigations into log responses in CBM reservoirs at DWU have been performed. New observations have been obtained with respect to three major aspects (1) petrophysical properties of various coal lithology; (2) corresponding log parameters of these geophysical properties; and (3) log environments that affect the log responses in various coal lithology. As the result of these new observations, a new "dynamic log cutoff system", whose applications are automatically determined by the specific log conditions, has been introduced to replace the previous "static log cutoff system" that was utilized indiscriminately on all kinds of

log environments. Therefore, the reliability of the new analysis model to interpret coal lithology using log data has been greatly enhanced.

The investigations into the gas desorption/adsorption behavior have revealed the representative gas desorption/adsorption characteristics of the coals present at DWU, which include the observed deviation between the Extended Langmuir Equation predicted gas content and the actual desorbed gas contents in lower quality coals. As a result of this research, the gas contents and gas-in-place values can be more accurately calculated by the new analysis model.

This new analysis model has been accepted by the operator as a working tool to evaluate the CBM reservoirs at DWU for individual well completion designs and field-wide reservoir evaluations. Recently, a log data set consisting of 460 CBM wells has been processed using this new analysis model. Subsequently, the analysis modeling results were utilized to perform a CBM reservoir evaluation for the DWU as a further investigation proprietary to the operator. This evaluation has yielded significant new observations and understanding with respect to reservoir properties and well performance. While this new analysis model and the accompanying new observations are specific to the DWU in the Uinta basin, they are also, to various extents, instructive for CBM exploration and development in other CBM deposit provinces.

TABLE OF CONTENTS

LIST OF FIGURES

LIST OF TABLES

DEDICATIONS

I would like to dedicate this work to my wife, Qimin, for her five-year sacrifice, and to my daughter, Anqi, for the encouragements she gave me.

ACKNOWLEDGEMENTS

CHAPTER 1

INTRODUCTION

This chapter begins with a brief discussion of the general information about the Drunkards Wash Unit (DWU) and addresses the fact that further development of the field needs a more sophisticated wireline log evaluation CBM model, which is the major task of this research. Finally, the research objectives and the major research tasks are presented.

1.1   General information about DWU

This section presents general information about geologic character, operational practices, and the evolution of coal grade identification methods.

1.1.1   Geology and reservoir characteristics

DWU, the largest coalbed methane (CBM) play in the Uinta basin, is located in the southeast part of Utah. As indicated in Figure 1-1, the unit boundary is adjacent to the city of Price. The target coal beds occur in the Upper Cretaceous Ferron Sandstone, which is a sequence of interbedded fluvial-deltaic sandstones, shales, and coals. The depth of the Ferron formation at DWU varies between 1,100 feet and 3,500 feet. The reservoir comprises high quality coal, lower quality coal, carbonaceous shale, and gas-charged sand. This diversity is rarely reported in other CBM basins.

In addition to its diversity in coal grade, the CBM reservoirs at the DWU exhibit several other characteristics. The thickness of each coal seam varies from less than half a foot to more than 10 feet, while the thickness of total coal (high quality and lower quality coals) averages 20 feet. Based on its vitrinite reflectance, the coal rank is classified as High Volatile B Bituminous coal. In contrast to its relatively low thermal maturity, the in-situ gas content is uncommonly high, varying between 300 and 500 scf/ton. Pressure

transient and other well tests indicate the permeability of the coal is in the range of 4 to 20 mD. Figure 1-2 illustrates a typical coal-seam profile present at DWU.
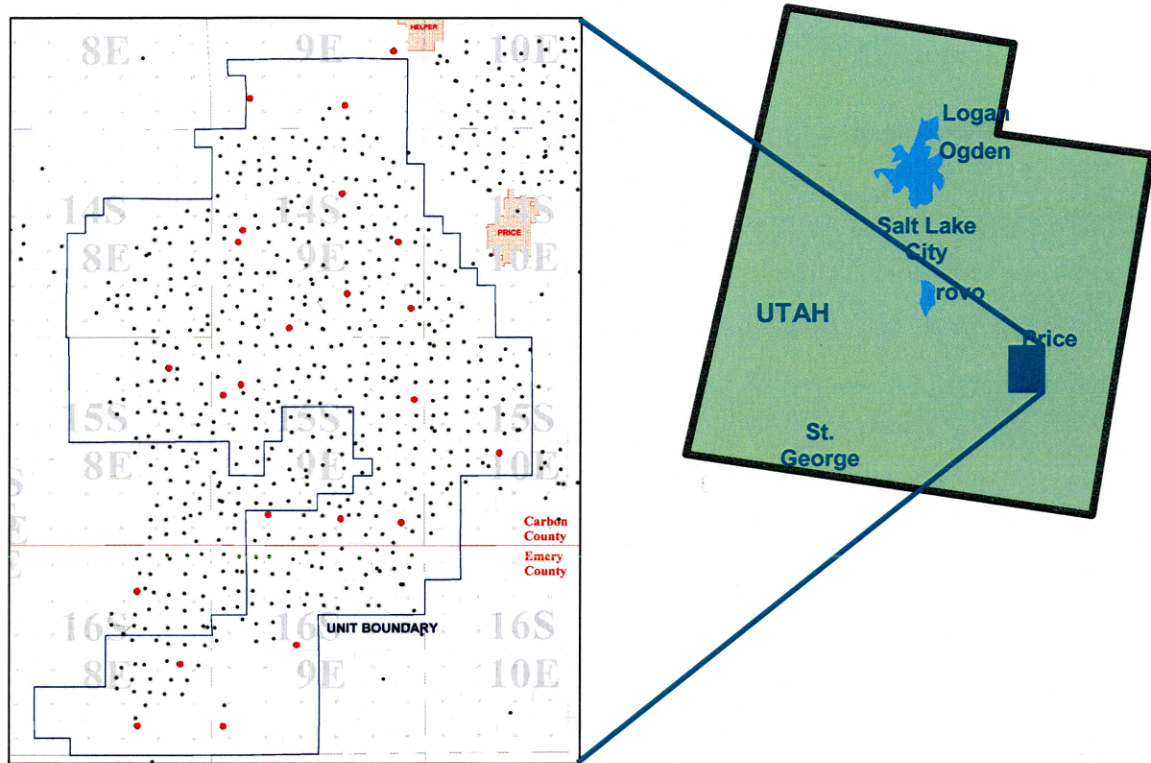
Figure 1-1:   Unit map
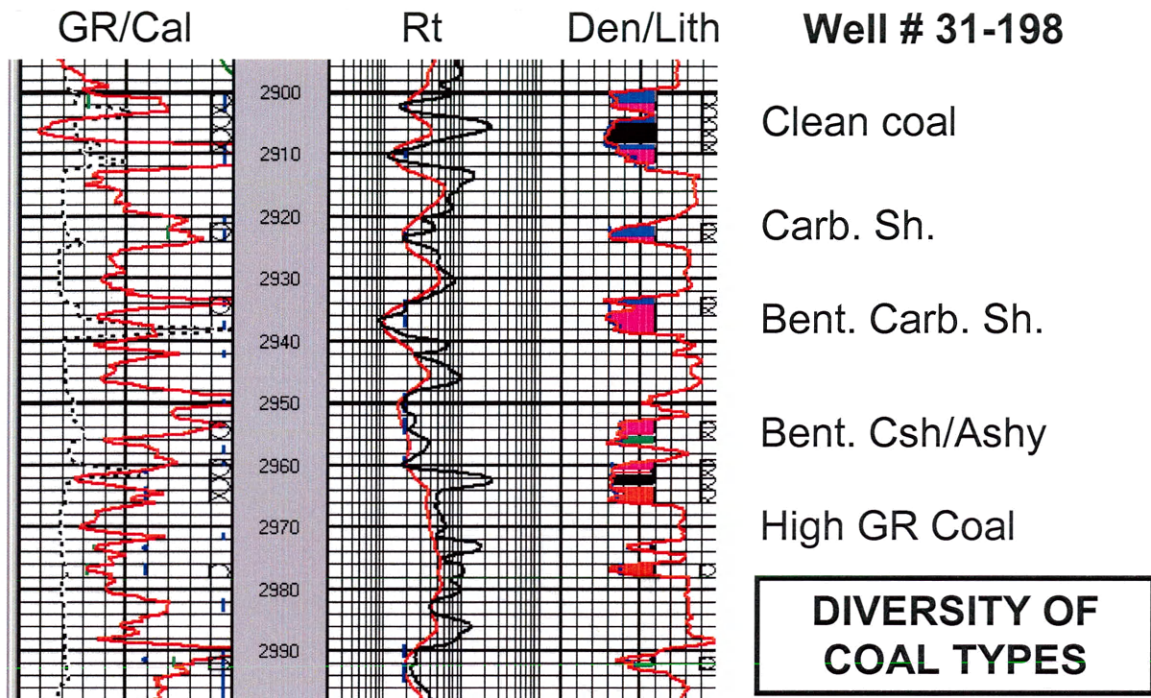
Figure 1-2: Representative coal lithologies present at DWU (Rt, resistivity of deep induction log; Den, density log; Lith, lithology; GR, gamma ray log; Cal, caliper log)

1.1.2 Existing operational practices

Since its discovery in 1991, the DWU has steadily developed into a large CBM play. By the end of May 2003, 485 producing wells had been drilled under the existing well spacing of 160 acres. As displayed in Figure 1-3, the gas production rate at the end of May 2003 was 190 MMCFD, and the cumulative gas production was 364 BCF. The latest available gas production data of September 2003 indicate that gas production rate was maintained at the same level as that of May 2003.
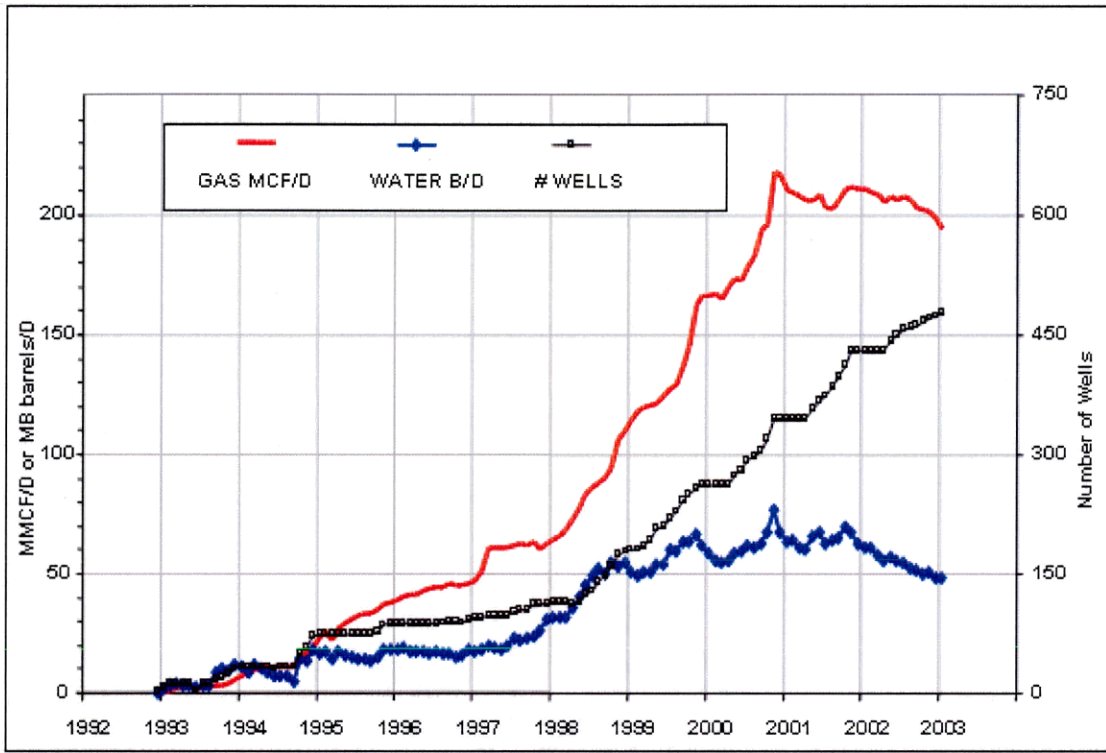
Figure 1-3:   Drilling history and the corresponding gas and water productions

After a decade of development, a comprehensive operational practice had been established at the DWU. In order to minimize formation damage and reduce costs, air drilling has been employed. For the purposes of wellbore stabilization and stimulation control, the total depth is cased and cemented. Figure 1-4 depicts a commonly used well completion design. The perforations are arranged in a way that will facilitate hydraulic fracturing in stages. Usually, the hydraulic stimulation involves two to three stages. Cross-linked gel and moderate size (200k lbs proppant and 100k gal slurry) is a typical treatment design. The dewatering process may cover a span of 20 to 30 months, depending on the reservoir conditions. Water disposal involves a combination of injection wells and evaporation into the atmosphere.
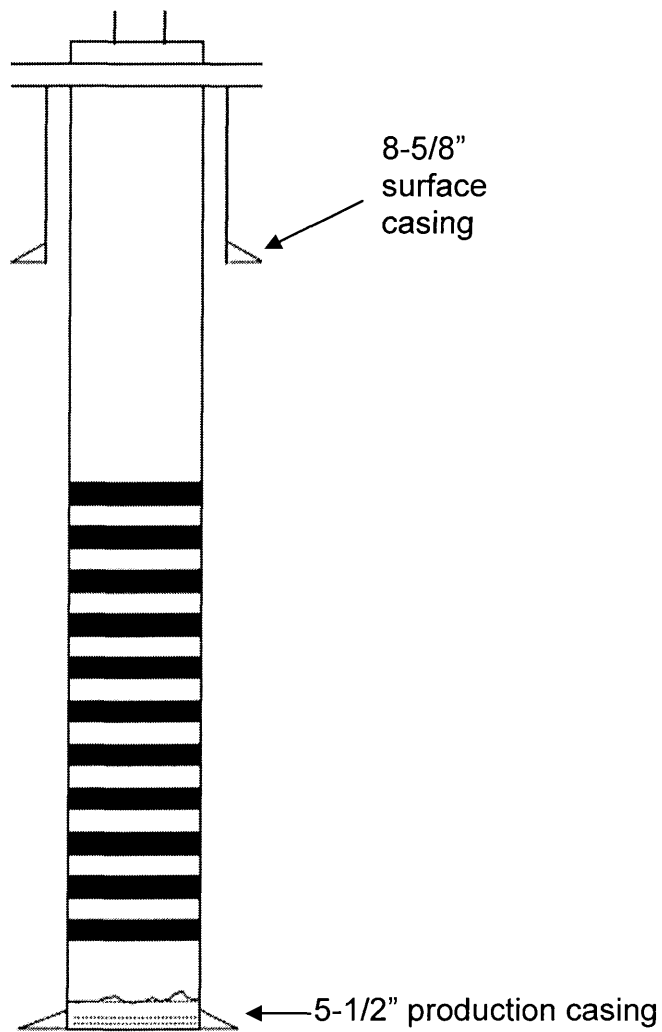
Figure 1-4:   Typical wellbore diagram

Under the current well spacing of 160 acres, the majority of the unit has been drilled. Further operations comprise new wells around the unit boundary, infill drilling with closer well spacing, and re-stimulation on subperformance wells using more effective and economic hydraulic fracturing methods. All of these future operations

require a high quality reservoir evaluation effort and more accurate knowledge about the existing field-wide distribution of coal grade and gas reserves. Considering the huge amount of logging and production data recorded at more than 460 CBM wells, a new CBM computer model is the only practical choice to carry out this field-wide CBM reservoir evaluation.

1.1.3 Evolution of coal identification methods at DWU

Since the commencement of CBM operations at DWU, coal evaluation had been carried out using petrophysical logging data. Prior to development of the new model, the evolution of coal evaluation methods had experienced two stages.

In the first stage, the coal evaluation method had relied heavily on the bulk density curve. A bulk density of 1.75 g/cc was chosen as the log cutoff of "total coal", making no distinction between high quality and low quality coals.

In the second stage, three major modifications were made to the previous method. First, a bulk density of 2.00 g/cc was adopted in order to encompass high quality coal, low quality coal, and carbonaceous shale. Second, the low resistivity parameter was incorporated into the criteria to discriminate carbonaceous shale from coals. Third, in order to separate high quality coal from lower quality coal, a gamma-ray (GR) cutoff corresponding to 40 percent ash content was introduced. Using this technique, the procedures below were followed to identify coal lithologies.

(1) hand pick "total coal" using the bulk-density cutoff of 2.00 g/cc

(2) identify high gamma-ray coal (HGC) using a given gamma-ray log cutoff (usually between 51-55 API units, depending on the gamma ray magnitude of the representative shale formation)

(3) use a low resistivity parameter to separate carbonaceous shale from the remaining coals

6

For both individual well and field-wide reservoir evaluation purposes, there are five major limitations associated with this coal evaluation method described above.

First, this method heavily relies on the bulk density curve, which is very sensitive to wellbore irregularity. Wellbore irregularity is a common and severe problem for a large area of this unit. In cases where coal is interbeded within incompetent bentonitic shale, the enlarged bore hole renders coal evaluation impossible when using bulk density.

Second, the given gamma-ray cutoff used to identify HGC can significantly underestimate high quality coal thickness. When thin coal beds occur in relatively thick shale formations, there will be a high gamma-ray environment influence on the entire interval occupied by both coal and shale. Under these circumstances, the given gamma-ray cutoff will inevitably underestimate the high quality coal thickness.

Third, the information revealed by the resistivity parameters was not being fully utilized. It was observed through this research that each coal grade exhibits a characteristic resistivity. Furthermore, the shallow resistivity curve demonstrates high vertical resolution. These two facts make the resistivity curves a good indicator of grade changes.

Fourth, obviously this "hand pick" method is subject to human errors. Therefore, the validity of a field-wide reservoir evaluation could be significantly compromised.

Finally, abnormally high resistivity associated with coals and abnormally high GR related to shale makes the logging responses within the Ferron formation elusive. Logging responses are not only controlled by lithologies but are also influenced by formation configurations (the relative positions and their thicknesses). Therefore, the previous "static log cutoff system" was replaced by a "dynamic log cutoff system" that can accommodate the adverse influence resulting from undesirable coal grade configuration.

The analysis presented above indicates that the previous coal grade identification method failed to fully integrate the unique CBM reservoir situations and their corresponding log responses. Therefore, significant errors in coal grade interpretation

were inevitable. On the contrary, the new model consists of two major modules, coal grade identification and gas-in-place calculation. The construction of the first module called for investigations into the CBM reservoir characters and their corresponding log responses. To set up the second module, a comprehensive examination of gas desorption/adsorption was required. As a result of this research, the new model can more accurately predict the diverse coal grades and the gas reserves at DWU. To demonstrate the advantages associated with the new model, a comparison between the new model and the old model has been provided in Chapter 8: Model Application at DWU.

1.2 Research objectives and major research tasks

This section discusses the research objectives and major research tasks associated with the development of the new CBM analysis model.

1.2.1 Research objectives

This research was initiated with three major research objectives.

(1) The new model should be able to identify the diverse coal grade system present at DWU, which includes clean coal, high gamma-ray coal, ashy coal, carbonaceous shale, and bentonitic carbonaceous shale.

(2) This model should more accurately calculate the gas content of individual coal seams. As a result, field-wide distribution of gas reserves would then be estimated with more accuracy.

(3) The model should be capable of providing such information as individual coal seam characteristics, petrophysical parameters, and certain reservoir properties.

1.2.2 Major research tasks

In order to realize the research objectives, six major research tasks have been carried out, including 1) the classification of a new coal lithology system; 2) examination of petrophysical log responses in CBM reservoirs; 3) study of the gas desorption/adsorption

tests; 4) development of a new log cutoff system to delineate coal lithology and a method to calculate gas-in-place (GIP); 5) programming of the new model; and 6) application of the new model at DWU.

1.2.2.1 Classification of a new coal lithology system

This research concluded that there is a more diverse coal lithology system present at DWU than was originally perceived. As a result of this study, a new comprehensive coal lithology system has been defined on the basis of investigations into coal sample Proximate Analysis, gas desorption/adsorption tests, and core sample descriptions. To overcome the major drawbacks associated with the old system discussed in the previous section, the new system has fulfilled two needs. First, this new system encompasses all the representative coal grades present at DWU. Second, the definition of each coal grade quantitatively reflects the particular coal quality.

There are three major factors calling for the classification of the new coal grade system. First, different coal grade represents different gas desorption capacity. For instance, at DWU clean coal gas content has a range of 300 to 500 scf/ton, while ashy coal gas content can vary between 100 and 200 scf/ton. Almost all carbonaceous shale has a gas content of no more than 100 scf/ton. Second, different coal grade represents different CBM reservoir properties in terms of porosity and permeability. For instance, high quality coals possess a well developed cleat system and display relatively high permeability and porosity, whereas lower quality coals, as a result of increased ash content, manifest deteriorated porosity and permeability. Finally, different coal lithologies display different geomechanical properties, which are the governing factors of hydraulic stimulation designs.

1.2.2.2 Examination of the petrophysical logging responses in CBM reservoirs

Improved log examination is one of the most fundamental and important tasks for this research, because of two facts. First, successful interpretation of coal grades depends

on an accurate analysis of log responses in CBM reservoirs. Second, the diverse coal grade system and the adverse log environments present at DWU make the log responses elusive.

To fulfill this subtask the following logging parameters, as well as the mechanisms behind logging perturbations, have been investigated.

Bulk density (Den):

a) Coal bulk density of each coal lithology

b) Log bulk density of each coal lithology

c) The factors that caused the deviation of log bulk density from coal bulk density, which include: enlarged wellbore effect, thin bed effect, and log algorithm

Resistivity (Rt):

a) Factors that influence coal formation resistivities, which include:

- Coal formation fluid resistivity

- Wellbore fluid resistivity

- Effect of permeability

- Effect of ash content

- Effect of mineral types

b) Log resistivity responses in CBM reservoirs, which include:

- High quality coals (clean coal and high GR coal (HGC))

- Low quality coal (ashy coal)

- Carbonaceous shale (CSH)

- Bentonitic CSH

Gamma-ray(GR):

a) Regional gamma-ray magnitude

b) Correlation between GR log and ash contents of coal samples

c) Thin bed effect on GR log

To facilitate this examination, a comprehensive logging strategy has been adopted at this unit, which includes bulk density, resistivity, gamma-ray, sonic, photo electronic factor, neutron, micro resistivity image, and nuclear magnetic resonance. In addition to the diversity of logging parameters, the logging environment has changed from a high resistivity domain (produced water or fresh water) to a low resistivity domain (KCL wellbore fluids). Furthermore, a logging database consisting of more than 460 wells by the end of May 2003 has been built by the operator.

1.2.2.3 Study of gas desorption/adsorption behaviors and calculate the gas content (GIP)

This task entails two subtasks. First, the existing theories governing gas desorption/adsorption are derived on the basis of high quality coals. However, in addition to high quality coals, the CBM reservoirs at DWU contain a significant amount of lower quality coals, such as ashy coal and carbonaceous shale. Therefore, the applicability of these theories to the lower quality coals has been investigated. As a result of this research, it has been concluded that applying the old method to calculate gas content of lower quality coals can result in significant errors.

Second, two existing methods for calculating gas contents have been widely accepted in the industry: the direct method and the indirect method. The direct method relies on gas desorption characteristics and the indirect one depends on gas adsorption behaviors. In this study, both methods have been evaluated in order to select the more reliable one for gas reserves calculations.

1.2.2.4 Establish the logging cutoffs to delineate coal lithology

A log cutoff system consists of a group of log parameters representing the petrophysical properties of each coal lithology. By applying a log cutoff system to a given log set, the coal lithologies encountered by this log set can be identified and interpreted. To establish a reliable log cutoff system which can accommodate the adverse

log environment and accurately delineate the diverse coal lithologies present at DWU, investigations in three aspects have been carried out.

First, the responses of individual log parameters in the CBM reservoir have been examined. As a result, the petrophysical properties of different lithology (coal and non-coal formations) reflected by individual log parameters were characterized. Second, the response of multiple log parameters in CBM reservoirs has been correlated to different lithologies (coal and non-coal formations). Thus, the log signature of a given lithology in CBM reservoirs was defined. Third, the major components of the log environment, as well as their effects on log parameters, have been evaluated. At DWU, there are several unique reservoir characteristics, such as thin coal beds, stratigraphic configuration, and enlarged wellbore, significantly affecting log responses.

1.2.2.5 Program the new model

To construct the new computer model, five major programming projects using C++ have been performed: input log curve management, log curve correction, log cutoff system, GIP calculation, and individual coalbed specifications.

Input curve management involves the setup of an input log curve set which contains all the log parameters which have been recorded at DWU. Thus, different logging sets provided by different vendors in different wells can be processed by the computer model. The log curve correction is primarily performed on the bulk density log to mitigate the thin bed effects. The programming work of the log cutoff system entails the routines delineating coal lithologies by comparing the log cutoff system against the input log curves. The GIP calculation includes the algorithms to calculate the vertical distribution of gas content, as well as the GIP of each coal seam. The individual coalbed specifications provided such information as coal lithology, thickness, coal percentage, GIP, and burial depth.

1.2.2.6 Apply the new model at Drunkards Wash Unit

The new CBM computer model has been applied at DWU for two major purposes. First, this computer model has been accepted by the operator as a working tool to process the log data in individual wells. After a new CBM well is drilled and logged, this model is used to evaluate the coal conditions in terms of coal lithology, thickness, GIP, and burial depth. Second, the operator has applied this model to process the log data collected from the existing 460 wells drilled at DWU. The modeling results were utilized to perform a field-wide CBM reservoir evaluation.

CHAPTER 2

LITERATURE REVIEW

For the purpose of this research, the literature review has been conducted in two major areas: (1) coalbed methane (CBM) reservoir characteristics, and (2) evaluation of CBM reservoir characteristics using wireline logs.

2.1 CBM reservoir characteristics

Coal, which contains more than 50 percent by weight and 70 percent by volume of carbonaceous material including inherent moisture (Bates and Jackson, 1987), has been recognized as both source rock and reservoir rock for natural gas. The fundamental CBM reservoir characteristics lie in three major aspects: (1) gas generation capacity, (2) gas storage capacity (gas adsorption characteristics), and (3) gas producing capability (gas desorption characteristics).

2.1.1 Gas generation capacity

Natural gas is generated in coal by two distinct processes: biogenic and thermogenic (Rice, 1991). Biogenic gas usually is generated in the early stage of coalification, while the thermogenic gas is formed in the late stage of coalification (Kim and Douglas, 1972). Even though both of them have been reported in CBM production throughout the world, thermogenic gas has been predominant. These two types of gases demonstrate different characteristics in many ways, such as gas generation environments, gas composition, and gas generation capacity.

Biogenic gas is primarily composed of methane and carbon dioxide. It is produced by the decomposition of organic matter by micro-organisms and is commonly generated in peat swamps (Woese et at., 1990). The principle requirements for the generation of significant amounts of biogenic gas are: anoxic environment, low sulfate

concentrations, low temperatures, abundant organic matter, high pH values, adequate pore space, and rapid sedimentation (Rice and Claypool, 1981; Zhang and Chen, 1985; Rice, 1992). Therefore, biogenic gas usually is formed early in the burial history of low-rank coal, peat to sub-bituminous in rank (Rice and Claypool, 1981). Compared to the thermogenic gas, the biogenic gas generation capacity from coals is less (Levine, 1992).

Thermogenic gas is formed as the result of extraction of light hydrocarbon elements from the macro-molecular fraction of carbonaceous materials under the effects of catagenesis and metagenesis processes, initiated from sub-bituminous coal and ended in anthracite (Hunt, 1979). Thermogenic gas usually consists of methane, other hydrocarbon components, carbon dioxide, and nitrogen. As indicated in Figure 2-1, significant amounts of methane are generated from coal during the entire coalification process. The estimates are variable (approximately 100 to 300 standard cubic centimeters per gram of coal), depending on the elemental data employed, starting rank, and assumptions made about the products (Juntgen and Karweil, 1966; Hunt, 1979; Welte et al., 1984; Levine, 1987).
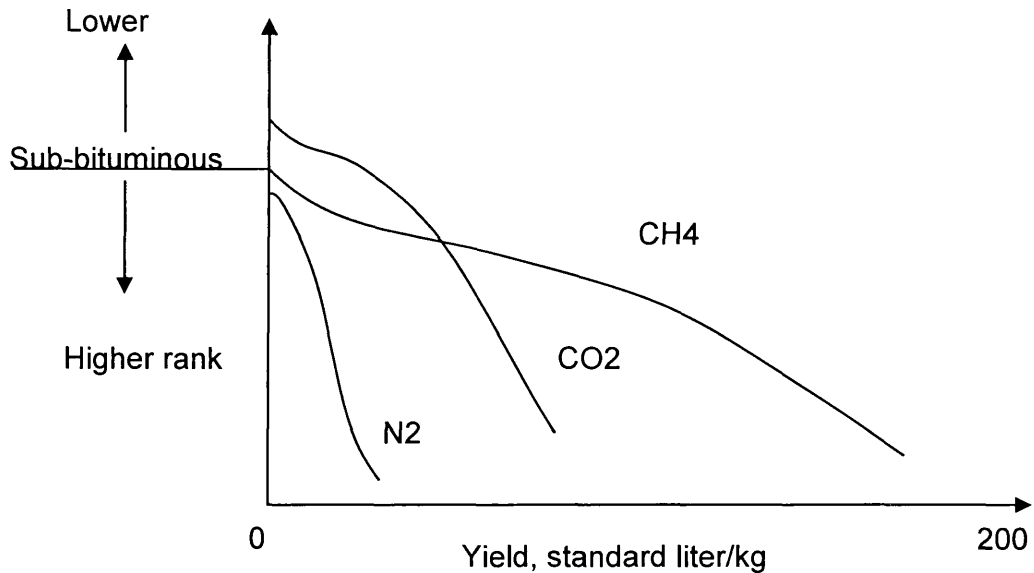
Figure 2-1:   Calculated amount of gas generated from coal during coalification (Hunt, 1979)

2.1.2   Gas storage capacity (gas adsorption characteristics)

Because coal is a microporous solid possessing a large internal surface area, it has the ability to adsorb natural gas (Vinnokurova, 1978). Many studies show that natural gas storage on coals is a physical sorption process, which involves weak intermolecular attraction due to van der Waals and electrostatic forces (Jolly et al., 1968; Rupppel et al., 1972; and Yang and Saunders, 1985). Two outstanding features associated with the physical adsorption of natural gas in coal enable coal to function as reservoir rocks: (1) the rapid attainment of equilibrium of the adsorption process, and (2) the desorption process.

The rapid attainment of equilibrium refers to the rate of adsorption at the surface of a micropore. Some diffusion is probably occurring in all experimental measurements. Nevertheless, equilibrium times of a few hours are very typical for most of the

documented coals (Jolly et al., 1968), indicating that equilibrium is quite rapid even though some diffusion is inevitable.

There is also plenty of evidence that the gas sorption process is reversible (van der Sommen et at., 1955; Gunther, 1965; Mavor et al., 1990). Reversible means that the adsorption and desorption curves are the same. Adsorption refers to increasing sorption due to increasing free gas pressure, while desorption refers to decreasing sorption due to decreasing free gas pressure.

The discussion above suggests two critical characteristics of coal as a reservoir formation. First, the rapid attainment of equilibrium enables the coal to efficiently adsorb and store natural gas on the free surface in the coal matrix. Second, the reversibility of adsorpion implies that the total amount of natural gas adsorbed into the coal matrix can be released completely from the coal under desirable conditions. These two features make coal a natural gas reservoir. In addition to these two general features, the gas storage capacities of coals are affected by six major factors discussed below.

2.1.2.1 Coal rank effect on gas storage capacity

Gas storage capacity is proportional to coal rank, and gas storage capacity increases as coal rank increases (Selden, 1934). This trend can be correlated with the increased carbon content, which is the primary sorbent of natural gas. During the coalificaiton process, the carbon content of coal increases while hydrogen content and oxygen decrease. As Figure 2-2 indicates, both the hydrogen/carbon ratio and the oxygen/carbon ratio diminish while coal rank increases from peat to anthracite coals (Tissot and Welte, 1984).
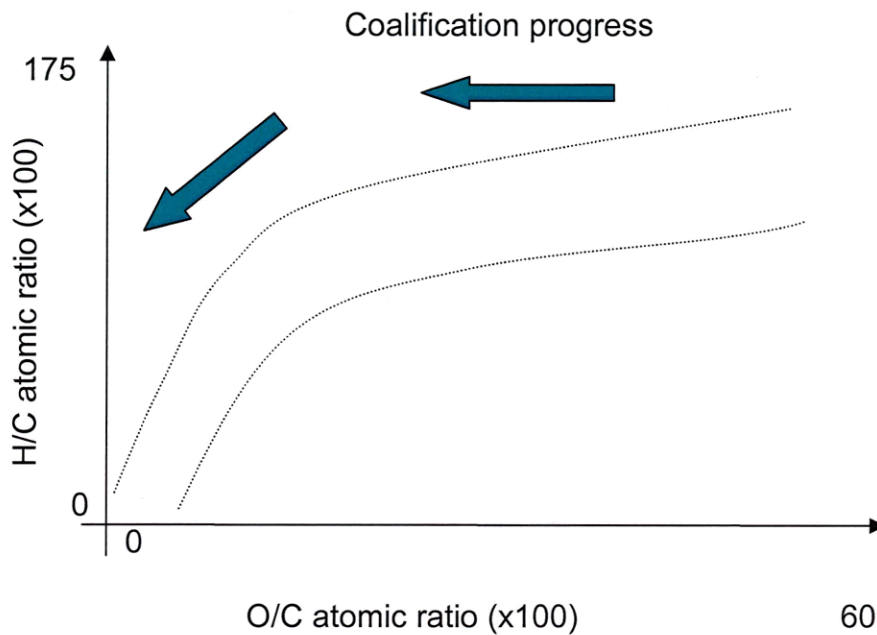
Figure 2-2: Variation in H/C and O/C atomic ratio during the coalificaiton process (after Durand and Paratte, 1983)

2.1.2.2 Coal petrology effect on gas storage capacity

The petrology refers to compositions of the maceral groups, which consists of vitrinite, inertnite, and liptonite. Each maceral group represents the different supply resource for peat preservations. Work performed by Schwarzer (1983) suggests that vitrinite and inertnite are the primary maceral groups that adsorb natural gas.

2.1.2.3 Pressure and temperature effects on gas storage capacity

For a given temperature, gas sorption capacity increases with pressure during the adsorption process, while the increase occurs at a decreasing rate as the sorption capacity approaches the saturation limit (Kim, 1977). This adsorption behavior is usually represented by the Langmuir Equation.

High temperature favors more gas in the free-state than in the sorbed state (Ruppel et at., 1974). In other words, the gas adsorption capacity decreases as the temperature increases. The effect of temperature on gas adsorption capacity can be demonstrated by the Langmuir isotherm Equation.

Langmuir isotherm Equation:

$$V = VL \frac{bP}{1+bP}$$ 2.1

Where:

V = adsorption capacity, scf/ton

VL = Langmuir volume, scf/ton

b = Langmuir constant

P = pressure, kPa

Langmuir constant:

$$b = e^{\frac{Q}{RT}} / \sqrt{T}$$ 2.2

Where:

Q = heat of sorption, Joule per thousand mole (J/ Kmol)

R = universal gas constant

T = temperature, K

As represented by Equation 2.1 and Equation 2.2, the gas adsorption capacity is proportional to the Langmuir constant. Also, the Langmuir constant is inversely proportional to temperature. Therefore, when temperature increases, the gas adsorption capacity decreases.

2.1.2.4 Mineral effect on gas storage capacity

Mineral matter refers to the non-coal components that are commonly seen in coal, which usually consist of kaolinite, illite, chlorite, and bentinite, depending on the depositional environment under which the coal is preserved. Gunther (1965) noted that mineral matter acted as an inert dilutent with respect to gas adsorption capacity. This suggests that mineral matter does not contribute to gas adsorption. This observation indicates the importance of coal quality for the gas storage capacity analysis.

2.1.2.5 Moisture effect on gas storage capacity

Bell and Racop (1986) showed that moisture plays an important role in gas adsorption on coals. It has been observed that the presence of moisture reduces the sorption of natural gas until a critical moisture content is reached. Above this critical moisture content, moisture will not further affect the gas adsorption capacity. Figure 2-3 displays the moisture effect on gas adsorption capacity on coal samples collected from the Vermejo coal in the Raton basin.

The work of Jouber et at. (1974) suggests that the critical moisture is the equilibrium moisture. The equilibrium moisture is determined by saturating coal samples with water at 96 to 97 percent relative humidity and 30 degrees Celsius (ASTM, 1979). Also, he noticed that the critical moisture can be correlated to the coal oxygen content. This is consistent with the physical adsorption of water which is related to the presence of oxygen.

2.1.2.6 Gas species effect on gas storage capacity

The gas adsorption capacity of different gas species on coal has been presented by Arri et al. (1992). The adsorption capacity for each component of natural gas, such as methane, carbon dioxide, and nitrogen, are demonstrated in Figure 2-4. It can be seen in this Figure that methane sorbs more than nitrogen, while carbon dioxide sorbs more than methane. Ettinger et al. (1996) suggest that the adsorption strength of various gases can

be determined by their boiling points at atmospheric pressure. This means that increasing boiling points correspond to increasing adsorption strength. For common gases, this trend on increasing sorption ranges from hydrogen, nitrogen, methane, ethane to carbon dioxide.
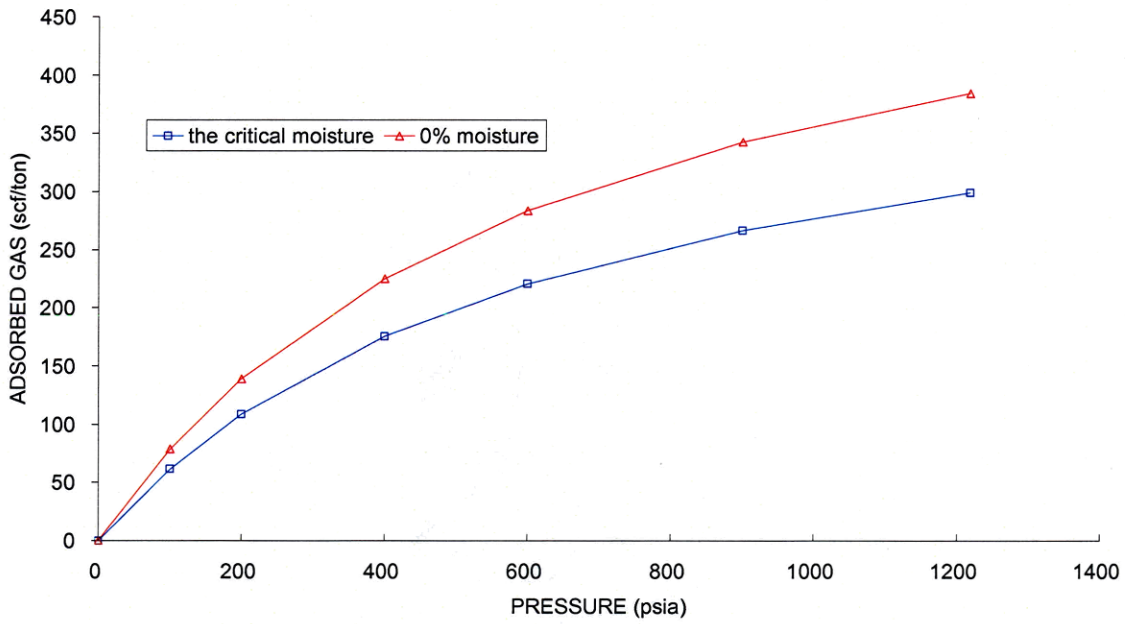
Figure 2-3:   Effect of moisture on gas sorption (after Yee, 1991)
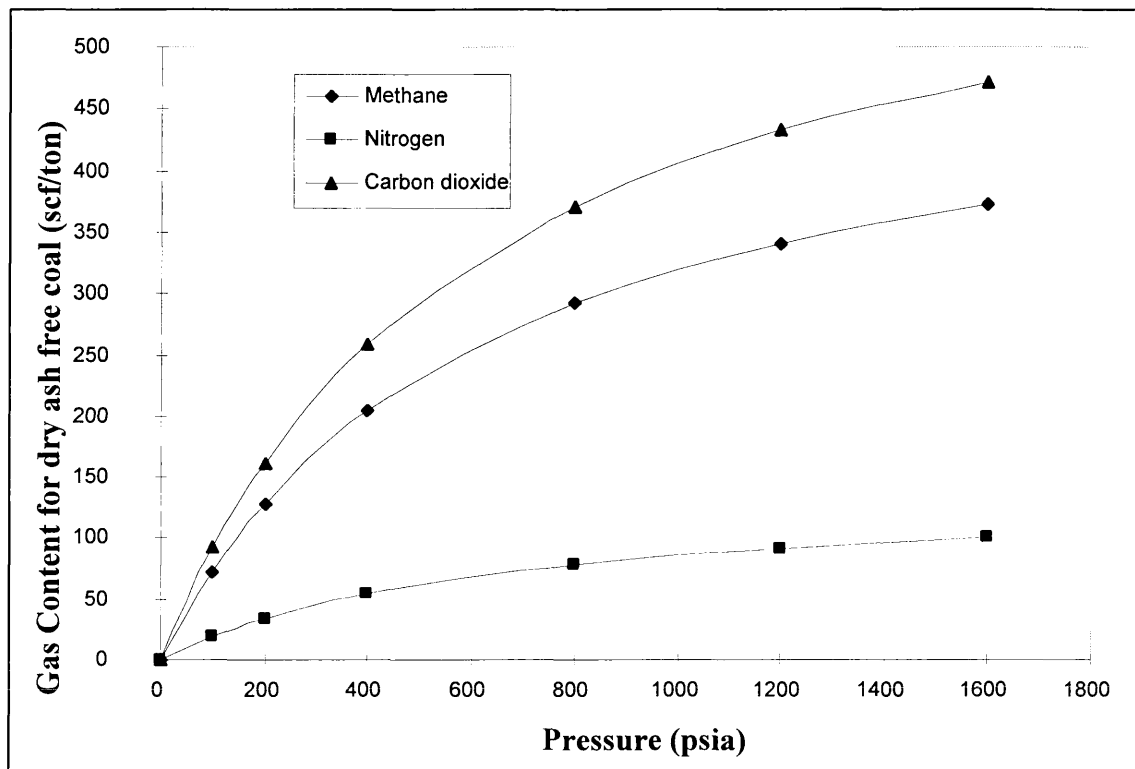
Figure 2-4: Gas sorption of different gas species on coal (after Yee, 1991)

2.1.3 Gas producing capability

Gas production is determined by gas migration in the binary porosity system present in the coal formation: which consist of (1) the micro porosity (coal matrix), and (2) macro porosity (natural fracture) (Little, 1991). Since the gas migration in the coal matrix (gas desorption) is the reverse process of gas adsorption (van der Sommen et at., 1955; Gunther, 1965; Mavor et al., 1990), the six major factors that influence gas adsorption capacity discussed in the preceding section will also affect the gas desorption characteristics. To evaluate the gas producing capacity in the micro porosity system, the combined effect of these six major factors can be presented by the desorption time, which is a measure of the gas desorption rate in the coal matrix.

Gas migration in the macro porosity system is determined by the development of the natural fracture-cleat system. The cleat system provides the major conduits for gas migration in coal reservoirs. The development of the cleat system determines the relative permeability to gas. Therefore, for a given CBM reservoir where the gas desorption rate is fixed at a high level, the development of the cleat system dictates the gas producing capability.

2.1.3.1 Desorption rate

The desorption rate indicates how quickly the adsorbed gas can desorb from the free surfaces of the coal matrix and diffuse toward the cleat system. The desorption rate is usually represented by the characteristic sorption time in days, as defined by Equation 2-3 (Sawyer et al., 1987).

$$T = 1.1052 \frac{D}{r^2} \qquad\qquad 2.3$$

Where:

T = characteristic time, days

D = diffusion coefficient, cm^2/min

r = characteristic diffusion length, cm

The characteristic sorption time is further defined as the time it takes for 63 percent of the gas to diffuse out of the coal. For practical applications, the characteristic sorption time can be obtained by the desorption test.

2.1.3.2 Development of the cleat system

Cleats are natural fractures in coal that serve as conduits for Darcy flow of gas and water to the wellbore during depressurization (Gray, 1987; Kolesar et al., 1990).

Darcy flow of gas and water in cleats has been verified by numerous researchers in the laboratory using whole cores, and in the field during drill-stem and production tests (Mavor and Close, 1989; Close et al., 1992; Mavor et al., 1991).

As illustrated in Figure 2-5, face and butt cleat systems are the primary and secondary natural fracture permeability avenues, respectively, for gas and water flow in coals. Face and butt cleat systems are commonly mutually orthogonal, or nearly orthogonal, and are essentially perpendicular to bedding surfaces. Shorter length butt cleats terminate against longer length face cleats. As a result of these geometric relationships, there is commonly a significant face and butt cleat permeability anisotropy in coal reservoirs.
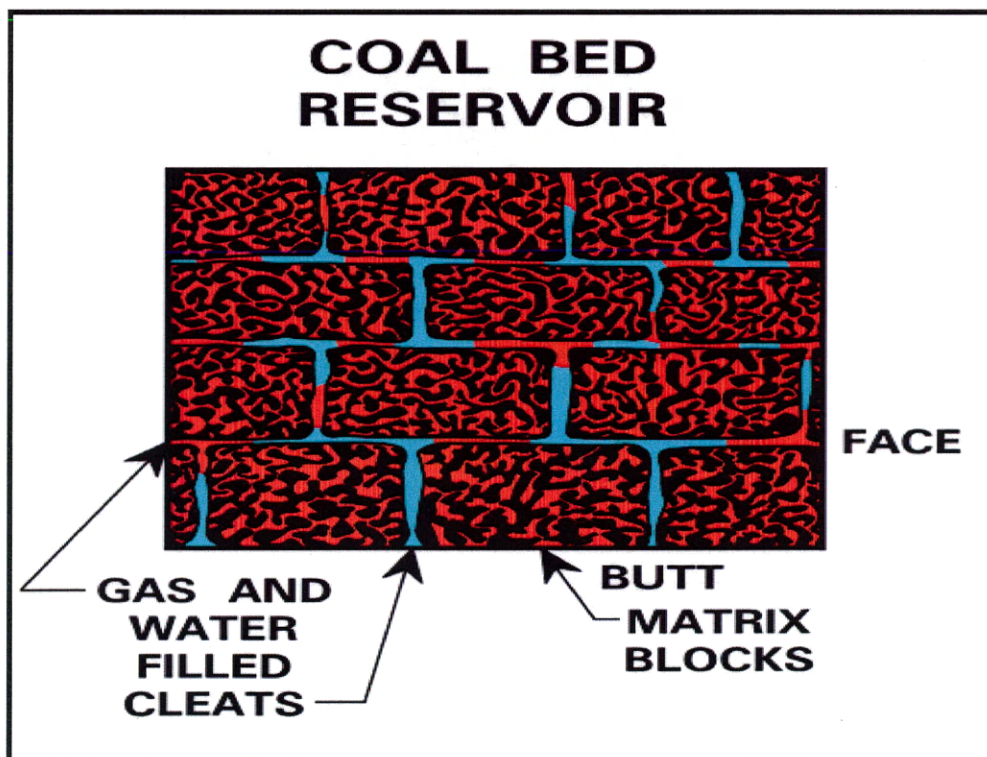
Figure 2-5:   The cleat system

Cleat occurrence and geometry have been verified as a function of coal rank, coal petrology, structure features, burial depth, tectonic history, and secondary mineralization and maceral filling (Hobbs et al., 1976; Grout, 1991; Poe et al., 1987; Tissot, 1984).

2.2   Evaluation of CBM reservoir characteristics using wireline logs

The primary objective of a CBM reservoir evaluation is to generate the field-wide distribution of the fundamental reservoir properties, such as the coal lithology, coal thickness, gas content, and gas-in-place. This information can be obtained by drilling core holes and performing a series of tests on the retrieved coal samples in laboratories. A standard test set consists of proximate analysis, ultimate analysis, desorption test, and adsorption experiment. While the coring and testing approaches are the most reliable ways to acquire the fundamental CBM reservoir properties, they are prohibitively expensive and extremely time-consuming for a field-wide reservoir evaluation campaign. Alternatively, wireline logs provide petrophysical properties of the CBM reservoir and have proven to be the most cost effective means to perform a CBM reservoir evaluation (Mullen, 1988). Subsequently, intensive literature reviews have been carried out in two areas for this research: wireline log responses in CBM reservoirs and CBM reservoir evaluation methods using wireline log data.

2.2.1   Wireline log responses in CBM reservoirs

Three wireline logging parameters have been used most commonly in CBM reservoir evaluations: bulk density, gamma ray, and resistivity (Mullen 1988; Johnston 1990, Johnston and Scholes, 1991; Mavor et al., 1990; Ellis et al. 1988).

2.2.1.1 Bulk density

The bulk density log has been the principle log to identify coals because of the low matrix density of coals. A 1.55 g/cc bulk density log cutoff has been widely employed to identify coals.

The ash content of coal can significantly affect the bulk density log of coals, depending on the mineral type and the concentration of ash content. Since the ash content affects the gas storage capacity of coals, it is always critical to distinguish it from the pure coal using the bulk density log.

2.2.1.2 Gamma ray (GR)

The GR log in coals usually reads low API units because of the lack of naturally radioactive elements in pure coals. The GR log in pure coal rarely exceeds 15 API units.

Clay minerals that constitute the ash content contain naturally radioactive elements. Therefore, the presence of ash content will cause higher GR readings in coals. Because the majority components of ash content are clay minerals, the GR log has been used as an indicator of ash content.

2.2.1.3 Resistivity

The resistivity of pure coal is extremely high because of the limited electrical conductivity of carbonaceous material. The two substances that increase the conductivity of coal are the salinity of the formation water in the cleats and the ash content in the coal matrix. Therefore, in high quality coals, which contain limited amounts of ash and relatively low salinity formation water, high resisitivity is a characteristic log signature.

2.2.2   CBM reservoir evaluation method using wireline log data

As an inheritance from the coal industry, the log analysis method has been used to measure the petrophysical properties of coal since the inception of CBM exploration and production. To evaluate the coal lithology, coal thickness, gas content, and gas-in-place, Mullen (1988) proposed the use of correlations for calculating these parameters from the bulk density log.

The basic theory of the log analysis method involves correlations between log responses with the measured results of the coal sample tests. Based on these correlations,

the log measurements can be used to interpret the coal quality, coal thickness, gas content, and gas-in-place.

Specifically, eight steps are followed to arrive at the desired CBM reservoir properties.

(1) Use the bulk density to calculate the ash content

(2) Derive the moisture content from ash content

(3) Subtract the ash content and moisture content to arrive at the total coal percentage

(4) Calculate the maximum gas content by dividing the total desorbed gas by the total coal percentage (direct method), or

(5) Calculate the maximum gas content using the Extended Langmuir Equation (indirect method)

(6) Obtain the in-situ gas content of a given coal seam from its ash content

(7) Volumetrically compute the gas-in-place of individual coal seams

(8) Sum up the gas-in-place of individual coal beds to arrive at the total gas-in-place for each well.

2.3 Further investigations

Since the CBM reservoirs at DWU demonstrate many unique characteristics, more research is required in order to develop a useful CBM computer model on the basis of existing theories.

2.3.1   Relatively high quality coals vs. lower quality coals

The existing log analysis methods have been derived from the experimental results on relatively high quality coal samples. For example, the reported lower density boundary of the coal samples is 1.75 g/cc (Mavor, 1994; Mullen, 1991). However, the CBM reservoirs at DWU comprise a significant amount of lower quality coals, such as ashy coal and carbonaceous shale. To determine whether the existing log analysis

27

methods were applicable to those lower quality coal reservoirs, more research was required.

2.3.2   Ideal conditions versus real conditions

The existing log analysis method evolved from CBM reservoirs that possess ideal conditions, such as relatively thick coal seams, simple stratigraphic profiles, and in gauge wellbores. Under these ideal reservoir conditions, the log parameters are subject to insignificant negative influences and the log responses can closely reflect the actual reservoir petrophysical properties. In contrast, the CBM reservoirs at DWU demonstrate far more complex situations. For example, approximately 70 percent of the coal seams are less than 3 feet in thickness. Additionally, a diverse coal grade system constitutes a more complex CBM reservoir system than most other CBM fields. Furthermore, the thin coal seams that are interbeded within shale and sand laminates form a complex stratigraphic column. Thus, the log responses are inevitably affected by these adverse log environments.

2.3.3   Single log parameter versus multiple log parameters

The existing log analysis method primarily uses the bulk density for the construction of CBM models. The information measured by other tools is greatly disregarded. In addition to the bulk density, a standard log tool suite measures other log parameters, such as gamma ray, resistivity, and caliper. This research indicates that these log parameters provide valuable supplementary information that can significantly enhance the accuracy of a CBM model.

CHAPTER 3
COAL LITHOLOGY CLASSIFICATION

Since the proximate analysis is the most commonly used experiment to evaluate coal lithology, this chapter discusses proximate analysis results and the establishment of a new coal lithology system.

3.1 Proximate Analysis

Proximate Analysis is a testing method that determines the four primary constituent components of coal: fixed carbon, moisture, volatile matter, and ash content. It is the principle means to evaluate coal quality and coal lithology. The results of Proximate Analysis of coal samples retrieved from 23 core holes at DWU have greatly facilitated the classification of the new coal lithology system.

By heating coal samples at different temperatures and observing the weight loss, each component can be calculated. For example, heating the coal at low temperature, the moisture first evaporates away and its volume is equal to the initial weight loss. At the second level of temperature, the volatile matter is expelled out of the coal samples and its volume can be estimated by the corresponding weight loss. When the remaining coal sample is burned at high temperature, the fixed carbon is exhausted. The fixed carbon and the ash content can be calculated by measuring weight of the remaining material (ash content).

Since all these major components affect the capability of natural gas absorption of coal, as well as the coal quality, the knowledge of them is critical for coal classification. Moisture:

The moisture content represents the average moisture holding capacity of the organic and inorganic fractions of coal. The moisture holding capacity of coal is the amount of moisture the coal can hold at 100 percent relative humidity without any free

moisture present on the surfaces of coal particles. Since the moisture competes against natural gas for adsorption positions on the free surface of coal matrix, its content influences the overall gas adsorption capacity of the coal.

According to the proximate analysis results, the moisture content of Ferron coal at DWU falls in the range of 1 to 3 weight percent.

Volatile matter:

The volatile matter primarily reflects the light hydrocarbon fraction of coal, which is determined by the level of thermal maturity and the stage of coalification. On the basis of dry-ash-free (DAF), the volatile matter of Ferron coal at DWU is approximately 40 weight percent of the toatal weight. Therefore, it is classified as high volatile coal.

Fixed carbon:

Fixed carbon constantly increases during the process of coalification. Since fixed carbon is the primary gas sorbent, it represents the natural gas adsorption capacity of coal. The fixed carbon content of Ferron coal at DWU is approximately 60 weight percent of the total weight.

Ash content:

Ash content refers to the non-coal materials, which is predominantly clay while trace amount of quartz is reported. The major constituent components include kaolinite, chlorite, illite, and montmorillinite.

Since ash does not absorb any measurable amount of natural gas, the ash content is inversely proportional to the overall natural gas adsorption capacity of coal. Practically, ash content is a reliable indicator of coal quality for a given rank of coal. To evaluate the coal quality, the ash content distribution of coal samples retrieved from 23 core holes were examined and are presented in the following section.

3.2 The previous coal lithology evaluation system

Previously, the Ferron coal was classified as clean coal, high gamma-ray coal (HGC), and carbonaceous shale, according to its log responses. Table 3-1 displays the specifications of the previous coal lithology system.

Investigations into coal sample testing results indicate that there are three major limitations associated with the originally classified coal lithology system. First, the system was not complete enough to encompass all the representative coal lithologies present at DWU. Second, the old coal lithology classification failed to correlate coal lithologies with their corresponding ash contents, which is the primary parameter determining coal lithology. Third, the bulk density of carbonaceous shale (CSH) of 2.0 g/cc is not correct. According to the proximate analysis results, the correct bulk density for carbonaceous shale is between 2.0 to 2.2 g/cc.

Coal lithology	Specifications
Clean coal	bulk density log is less than 1.75 g/cc, and GR is less than that corresponding to 40 percent shale
High gamma ray coal (HGC)	bulk density log is less than 1.75 g/cc, and GR is more than that corresponding to 40 percent shale
Carbonaceous shale (CSH)	Bulk density log is between 1.75 g/cc and 2.0 g/cc

Table 3-1: The previous coal lithology system at DWU

3.3 The new coal lithology sytem

The new coal lithology system has been developed based on the proximate analysis results: ash content, bulk density, and mineral type.

3.3.1 Ash content distribution in the Ferron coal at DWU

As displayed in Figure 3-1, the measured ash contents of the CBM reservoirs at DWU vary from 6 percent to 76 percent by weight. The ash content of 65 percent of the coal samples is less than 35 percent by weight. The ash content of 10 percent of the coal samples is between 35 percent and 50 percent by weight. The ash content of 25 percent of the coal samples is between 50 percent and 76 percent by weight.

In this study, ash content has been utilized as the principle criterion to classify coal lithologies because of three factors: (1) ash content is the main coal quality indicator; (2) ash content strongly affects the gas content of coals; (3) there is adequate amount of coal samples for each specified ash content range.
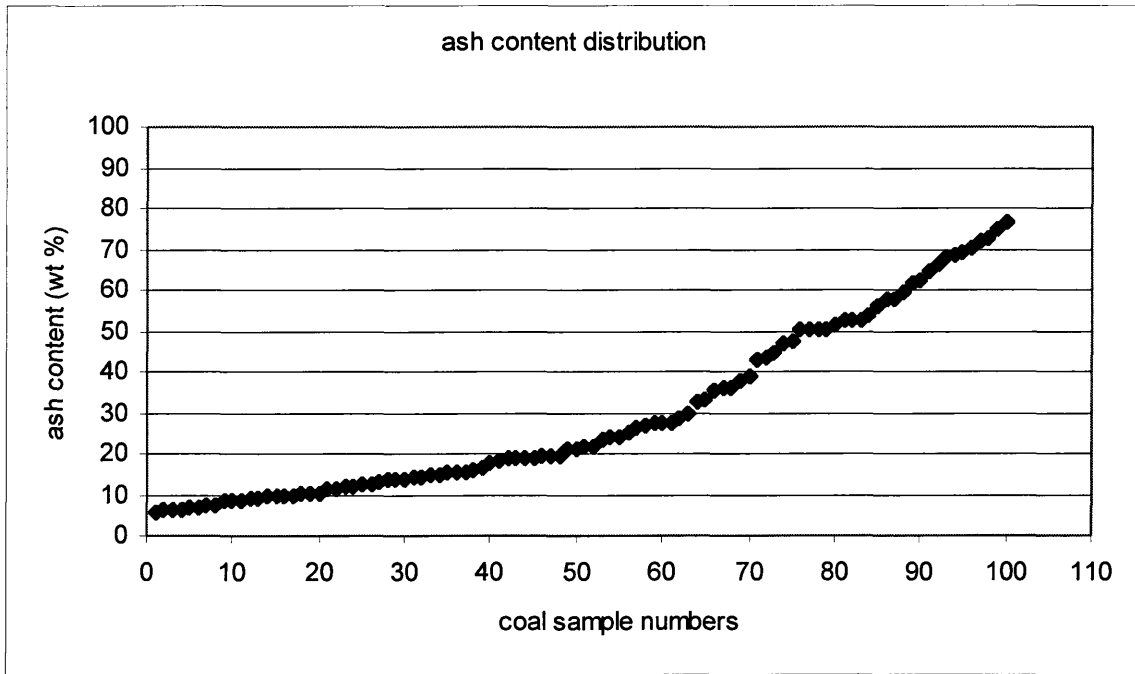
Figure 3-1:   The ash content distribution in the Ferron coals at DWU

32

3.3.2 The correlation between ash content and bulk density

The Proximate Analysis results indicated in Figure 3-2 show a very strong correlation between the coal bulk density and its corresponding ash content. The accuracy of this correlation can be demonstrated by the high regression coefficient of 0.98. The significance of this correlation lies in two factors. First, since the ash content is the main coal quality indicator, this correlation enables us to evaluate coal quality and lithology using the bulk density. Second, since the ash content is inversely proportional to the gas content, the gas content can be correlated to the bulk density.
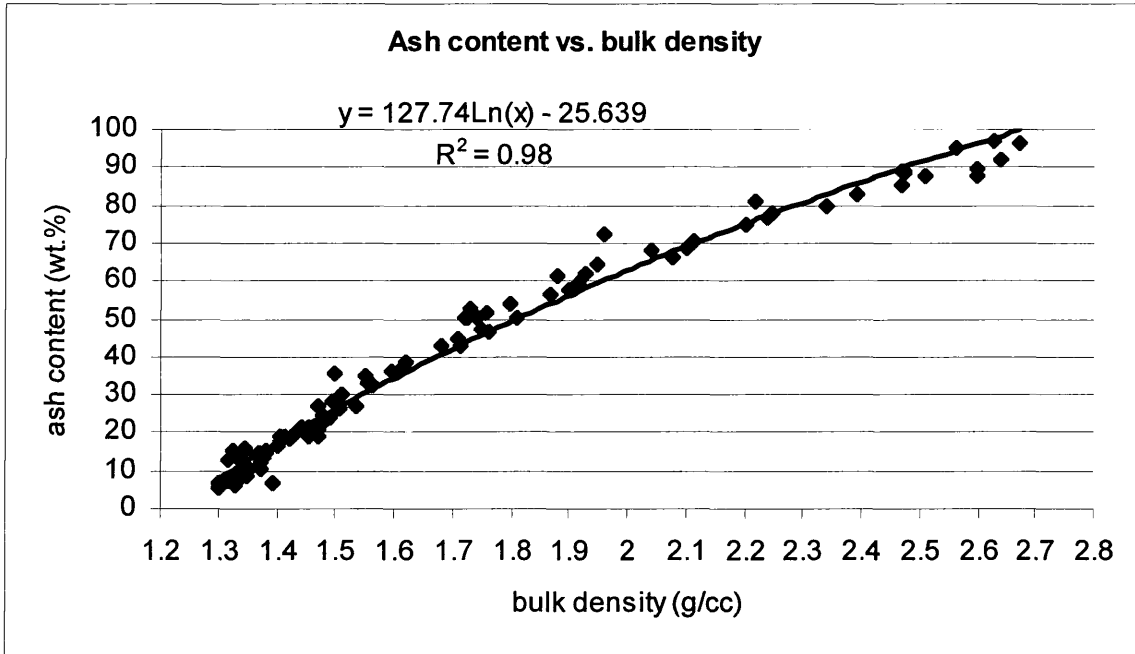
Figure 3-2:   The correlation between coal bulk density and ash content

3.3.3 Different type of minerals in the carbonaceous shale

At DWU, it has been observed that there are formation streaks comprising organic carbon and tonstein (predominantly bentonite). Because these formation streaks contain large amounts of minerals and a fair amount of organic carbon, which has the capability of holding gas, it fell into the category of carbonaceous shale. But in contrast to conventional carbonaceous shale, the bentonitic carbonaceous shale is predominantly composed of bentonite. The distinction between the conventional carbonaceous shale and bentonitic type of carbonaceous shale should be made for two major reasons.

First, the gas content of conventional carbonaceous shale has been tested by numerous gas desorption experiments. Thus, the gas content of conventional carbonaceous shale has been confirmed. Therefore, the conventional carbonaceous shale has been classified as CBM reservoir. In contrast, few coal samples of bentonitic carbonaceous shale have ever been tested for gas content. Therefore, its gas content has not been confirmed yet. Second, the bentonitic carbonaceous shale is prone to collapse and results in enlarged bore hole. This situation is a hazard to gas production. Therefore, it is operationally beneficial to discriminate bentonitic carbonaceous shale from conventional carbonaceous shale.

3.3.4 The new coal lithology system

As a result of this study, a new coal lithology system was developed based on the examinations of coal sample testing results. In contrast to the previous system, the new system encompasses all representative coal lithologies. Additionally, the definition of each coal lithology quantitatively reflects its ash content. Thus, the new system is conducive to the construction of a new CBM model and any CBM reservoir evaluation efforts.

Coal lithology	Ash content (wt. percent)	Bulk density (g/cc)
Clean coal	0-35	1.27-1.55
High gamma-ray coal (HGC)	35-50	1.55-1.75
Ashy coal	50-66	1.75-2.00
Carbonaceous shale (CSH)	66-76	2.00-2.20
Bentonitic Carbonaceous shale (BCSH)	66-76	2.00-2.20

Table 3-2:   The new coal lithology system

This new coal lithology classification system is supported by three major factors associated with the Ferron coal at DWU.

First, according to the modeling results of all the CBM wells drilled at DWU, there is an appropriate coal sample population to justify each coal lithology category. For instance:

Clean coal	72 percent of total coal
HGC	22 percent of total coal
Ashy coal	6 percent of total coal

Second, the conventional coal definition was incorporated into the new coal lithology categorization. By definition, coals contain more than 50 percent by weight of fixed carbon (Bates and Jackson, 1987). This criterion is consistent with the threshold of HGC.

Third, this classification matches the coal description practices applied at DWU. The correlation between the new coal classification and the coal description practices is displayed in Table 3-3.

The new coal classification	Coal description
Clean coal (0-35 percent ash)	black, bright, and rubble
HGC (35-50 percent ash)	black, dull
Ashy coal (50-65 percent ash)	solid, heavy
Carbonaceous shale (65-76 percent ash)	dark scratches

Table 3-3: Correlations between the new coal classification and coal description practices at DWU

CHAPTER 4

PETROPHYSICAL LOG RESPONSES IN THE CBM

RESERVOIRS AT DWU

In order to characterize the log responses in the CBM reservoirs at DWU, the major investigations have been concentrated on three aspects: 1) petrophysical properties of various coal grades; 2) the corresponding log parameters of these petrophysical properties; and 3) log environments that affect the log responses in various coals.

This investigation has resulted in the construction of a new log cutoff system which can more accurately identify the coals present at DWU. Since the new log cutoff system consists of bulk density, resistivity, and GR, this chapter will present the new observations associated with these log parameters.

4.1 Bulk density

For a given rank of coal, its bulk density is the result of the composition of its constituent components. According to the Proximate Analysis, coal is composed of fixed carbon, volatile matter, moisture, and ash content. Because the volatile matter and moisture are functions of fixed carbon, the major components of coal can be classified as ash content and pure coal which consists of fixed carbon, volatile matter, and moisture. Therefore, the coal bulk density is proportional to the ash content. Since the grade of coal (coal quality) is determined by its ash content, coal bulk density is the indicator of coal qualities. Therefore, usually log bulk density has been used as the principle log tool to evaluate the grade of coals, or the coal quality.

Before the log bulk density can be accepted as the tool to evaluate coal grade, two factors associated with coal bulk density and log bulk density have to be investigated. First, the bulk density of a given grade of coal is not constant. Instead, it varies from basin to basin where different depositional environments provide different minerals with

37

different densities. For example, the three commonly reported minerals (kaolinite, chlorite, and illite) demonstrate appreciable differences in their bulk density (kaolinite, 2.41 g/cc; chlorite, 2.76 g/cc; and illite, 2.52 g/cc). Therefore, for a given CBM play, the bulk density of each grade of coal has to be verified on the basis of the composition of its constituent components.

Second, because the bulk density log is a sidewall logging tool with limited investigation depth, it is extremely vulnerable to the challenging log environment caused by the thin coal seams and irregular wellbores present at DWU. Under such undesirable situations, the bulk density measurement can significantly deviate from the true bulk density of the corresponding coals. In response, vigorous investigations have been practiced to characterize the effects of hostile log situations on the log responses.

To fulfill the investigations related to coal bulk density and its corresponding log bulk density, the following tasks have been completed:

- Using sufficient Proximate Analysis results, the relationship between coal bulk density and its ash content was established. Based on this relationship, the bulk density of each grade of coal has been quantitatively defined.

- By comparing the bulk density of each grade of coal with its corresponding log bulk density under different log environments, the errors caused by major adverse situations were characterized.

- As a result of this investigation, correction methods were developed to alleviate the errors in log bulk density caused by hostile log environment. These methods will be discussed in subsections in this chapter.

4.1.1 Coal bulk density

At DWU, Proximate Analysis has been performed on 116 coal samples, which were retrieved from core holes throughout the unit. As part of the tests, coal bulk density and its corresponding ash content have been measured. Using these test results, the relationship between coal bulk density and ash content volume has been established.

As depicted in Figure 4-1, the reciprocal of coal bulk density is inversely proportional to its corresponding ash content.

Because the moisture contents measured on these 116 coal samples are consistently minimal (below 2 percent), the coal sample density (moisture free) can be treated as the coal bulk density.

This strong correlation between coal bulk density and ash content, which is supported by the high regression coefficient of 0.98, can serve two purposes. First, the bulk density of each grade of coal has been quantitatively defined. Second, the log bulk density can be verified against the corresponding coal bulk density for given coal samples whose ash contents are known.

Ash content vs. bulk density

$y = 127.74Ln(x) - 25.639$

$R^2 = 0.98$
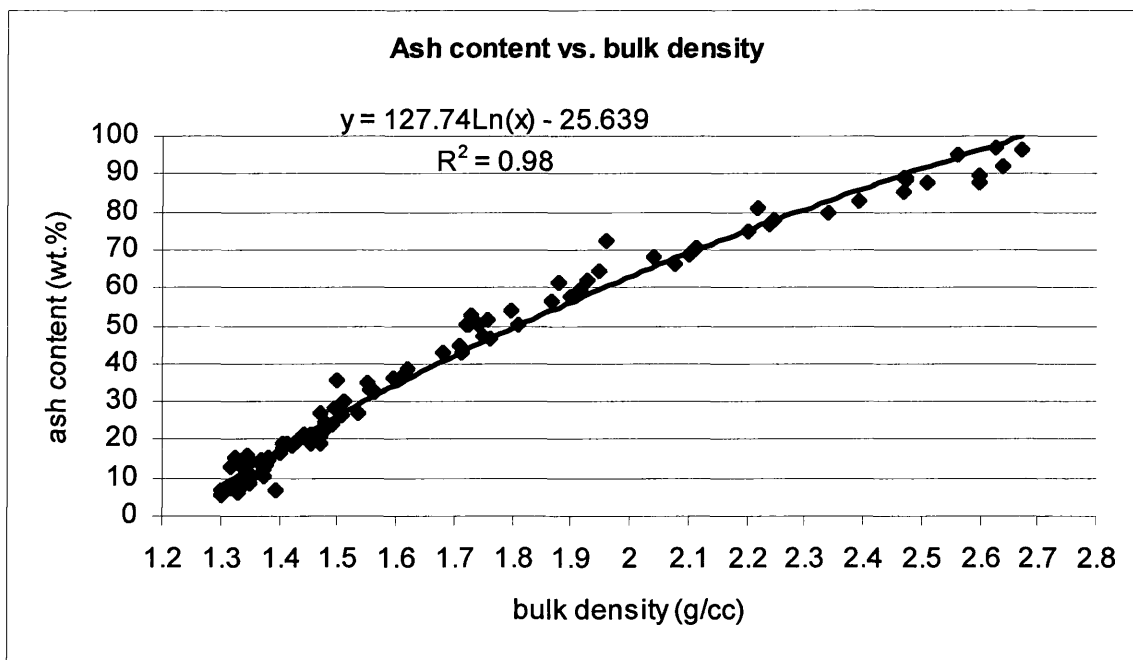
Figure 4-1   Correlation between coal sample density and ash content (the same Figure as Figure 3-2)

To extrapolate the curve in Figure 4-1 to the far left where ash content equals zero, the density of pure coal is read as 1.22 g/cc. When the ash content equals 100 percent, the resultant density of ash is 2.67 g/cc.

According to the coal lithology classification established in Chapter 2, the bulk density of each grade of coal has been assigned as follows:

Clean coal: 1.22 – 1.55 g/cc

HGC: 1.55-1.75 g/cc

Ashy coal: 1.75-2.00 g/cc

CSH: 2.00-2.20 g/cc

4.1.2   Log bulk density responses in CBM reservoirs

To characterize the log bulk density response in the CBM reservoirs at DWU, the coal bulk densities measured on more than 200 coal samples have been compared with the corresponding log bulk densities which were run under different log environments. It has been observed that, while the log bulk density is able to reasonably reflect the coal bulk density under favorable borehole situations, the log bulk density can be significantly affected by three major factors associated with DWU: 1) thin bed effect; 2) enlarged wellbore; and 3) the existing algorithm for processing log data. In order to alleviate the impact of erroneous log bulk density on the new CBM computer model, the effects of these three factors have been addressed and presented in the ensuing sections.

4.1.2.1 Thin bed effect

During the early stage of CBM development at DWU, the vertical resolution of most of the log bulk density was approximately 2 feet, which was determined by the logging tools. This means that the log bulk density reading at the center of a 3.5-foot interval is equal to the averaged log bulk density readings for this 3.5-foot interval. In other words, the true bulk density of the formation can be fully reflected only when the

coal seam is 3.5 feet or more in thickness. At a later stage, the high-resolution bulk density log was adopted, which improved the vertical resolution to approximately 1.5 feet.

The differences between the high resolution density log and the conventional one are illustrated in Figure 4-2. On the far right track of "Density", the red curve represents the high resolution log bulk density and the blue line is the log bulk density curve with normal resolution. The other four tracks, from right to left, are tracks of "interpreted coal lithology", "resistivity", "depth", and the "correlation" which contains GR, SP, and caliper. Corresponding to the coal lithology to the left, the high resolution curve more closely reflects the coal bulk density than the conventional curve does. It is obvious that the conventional resolution bulk density log failed to reflect the changes of lithologies of small intervals. As indicated in Figure 4-2, the high resolution bulk density log is able to better evaluate coal seams in terms of density and the boundaries between coal and non-coal formations.
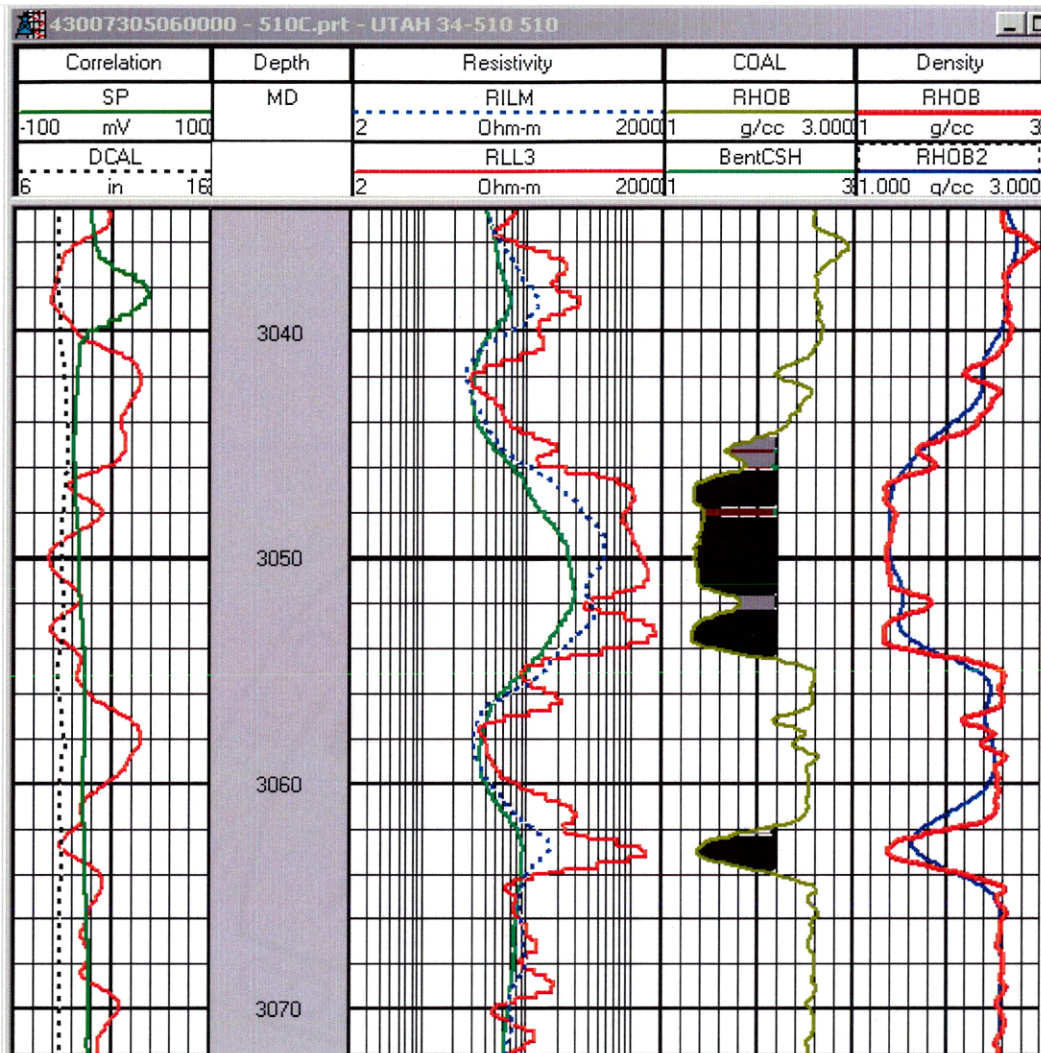
Figure 4-2   Log bulk density curves with different resolutions

Although the high resolution bulk density log can better evaluate the coal seams which are 3 feet or more in thickness, its credibility has been compromised within thinner coal beds. According to the statistics of coal samples collected from 23 core holes, there are a large number of coal seams thinner than the 3 feet. This situation is depicted in Figure 4-3.

As Figure 4-3 displays, 84 coal seams out of 112 cored coal seams are thinner than 3 feet. Approximately 30 percent of cored coal beds have a thickness above the resolution of the bulk density log, while 70 percent of them are thinner than the log resolution. These thin coal seams comprise approximately 28 percent of the total coal thickness.
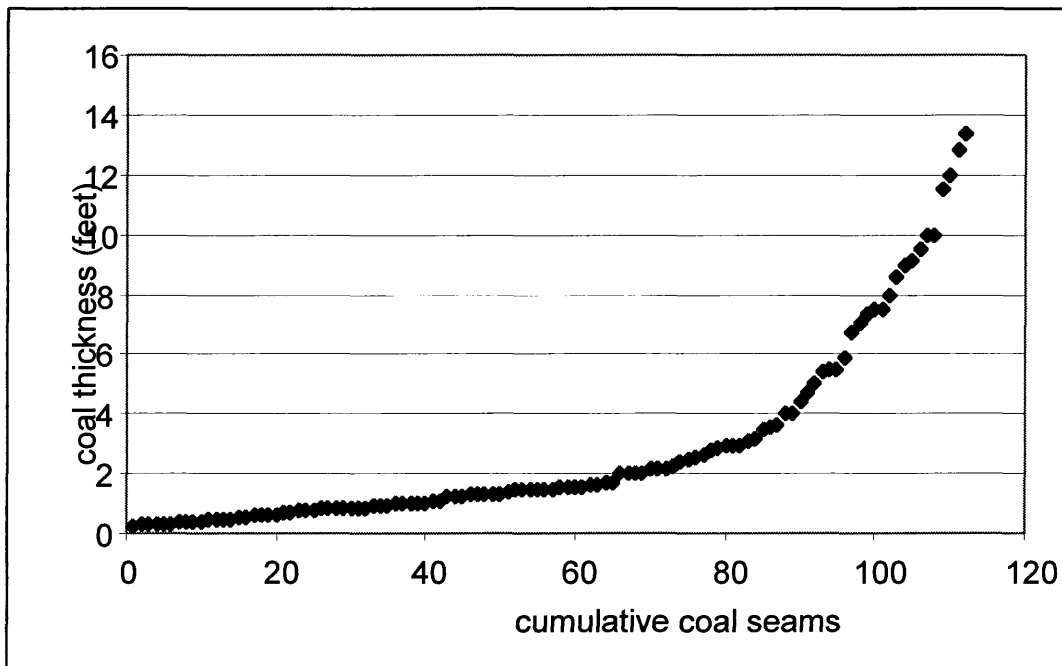
Figure 4-3   Statistics of coal thickness measured on 112 coal seam samples

There are two negative impacts of thin-bed effects on coal evaluation: underestimated coal quality and the difficulty to define the boundary between coal and non-coal formations.

The first negative effect is that the log bulk density is always higher than the actual coal bulk density. When the log bulk density is utilized for coal evaluation, the

coal quality will be underestimated. This underestimation will result in errors in the calculation of gas reserves. Figure 4-4 displays the thin bed effect on a typical thin coal seam at DWU.

As illustrated in Figure 4-4, there are 5 major coal seams in this well. According to the proximate analysis, the coal bulk densities of these coal seams are approximately the same. However, the bulk density log of these coal seams is different. The bulk density log of the thick coal bed between 3108 feet and 3118 feet is 1.32 g/cc, while the readings of the thin coal beds occurring at 3088 feet, 3122 feet, 3142 feet and 3158 feet vary from 1.46 g/cc to 1.64 g/cc.
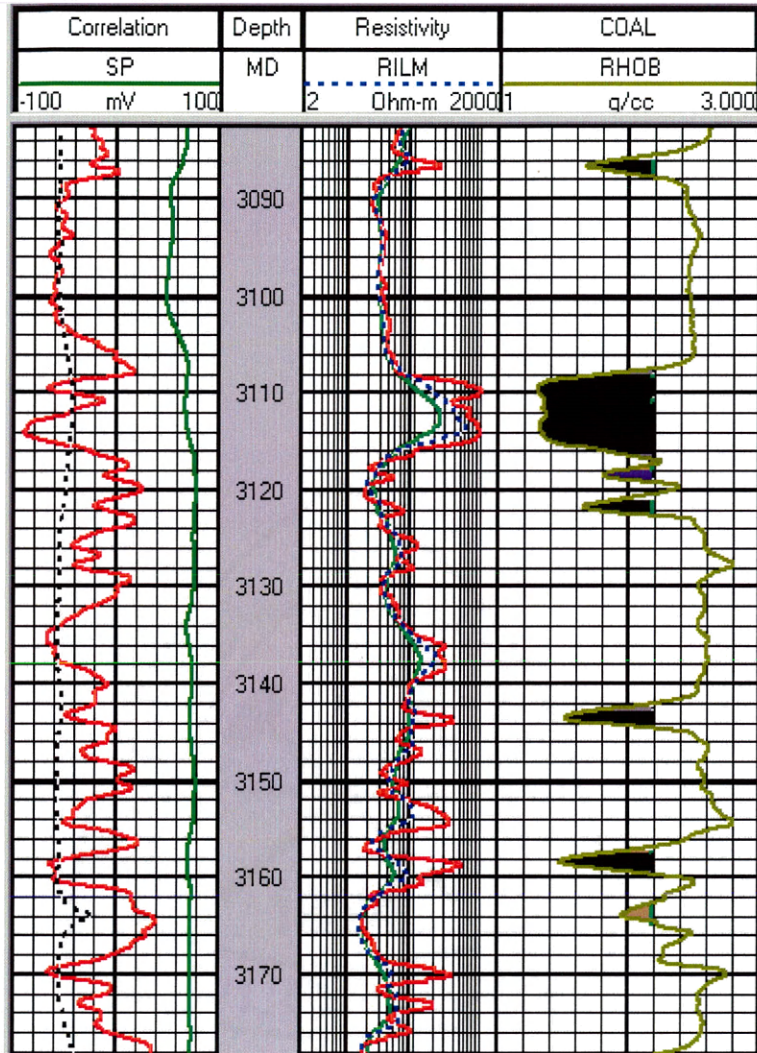
Figure 4-4   Thin bed effect on log bulk density

For the coal bed approximately 2 feet in thickness as Figure 4-4 displays, its log bulk density is 1.39 g/cc while the actual coal bulk density is 1.34 g/cc.

To characterize the thin bed effect, the coal bulk densities were compared with their corresponding log bulk densities of a group of thin coal seams. It is observed that, for the thin beds with a thickness between 1 and 2.5 feet that are commonly recorded at

DWU, the coal bulk density is proportional to its corresponding log bulk density. This relationship is demonstrated in Figure 4-5 and Equation 4-1.
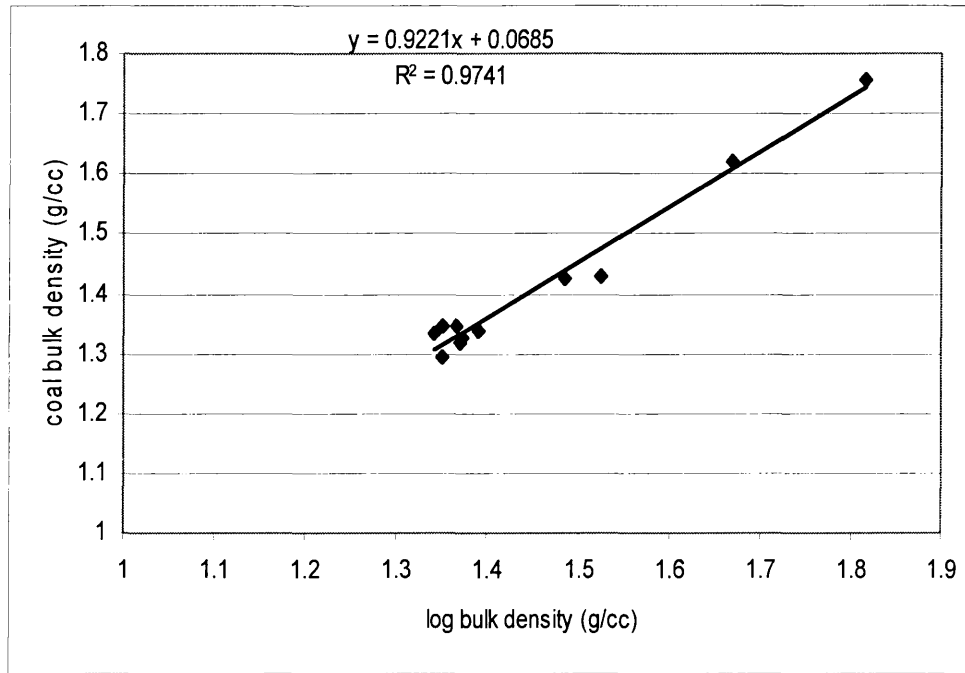
Figure 4-5   Correlation between log bulk density and coal bulk density in thin coal beds

$$\rho_b(coal) = 0.9221\rho_b(\log) + 0.685 \hspace{3cm} 4.1$$

Where:

ρ_b (coal) = high quality coal bulk density, g/cc

ρ_b (log) = log bulk density, g/cc

In order to mitigate the thin bed effect on logs and restore the true bulk density of thin coal seams, this equation has been incorporated in the new CBM computer model to evaluate coal quality and calculate the original gas-in-place.

4.1.2.2 Enlarged wellbore effect

The bentonitic carbonaceous shale that is interbedded within the Ferron coals (northwest part of the unit) is prone to collapse and forms an enlarged wellbore within the coal intervals. The caliper log in this area indicated that washouts range from 0.5 inch to 13 inches. The comparison between the density log and its corresponding core samples implied that a significant density log error would be introduced when the washout is more than 1 inch. The caliper log (dotted line in the first track on the left) in Figure 4-6 portrays a typical enlarged wellbore interval caused by bentonitic carbonaceous shale in the depth interval from 3058 to 3082 feet.
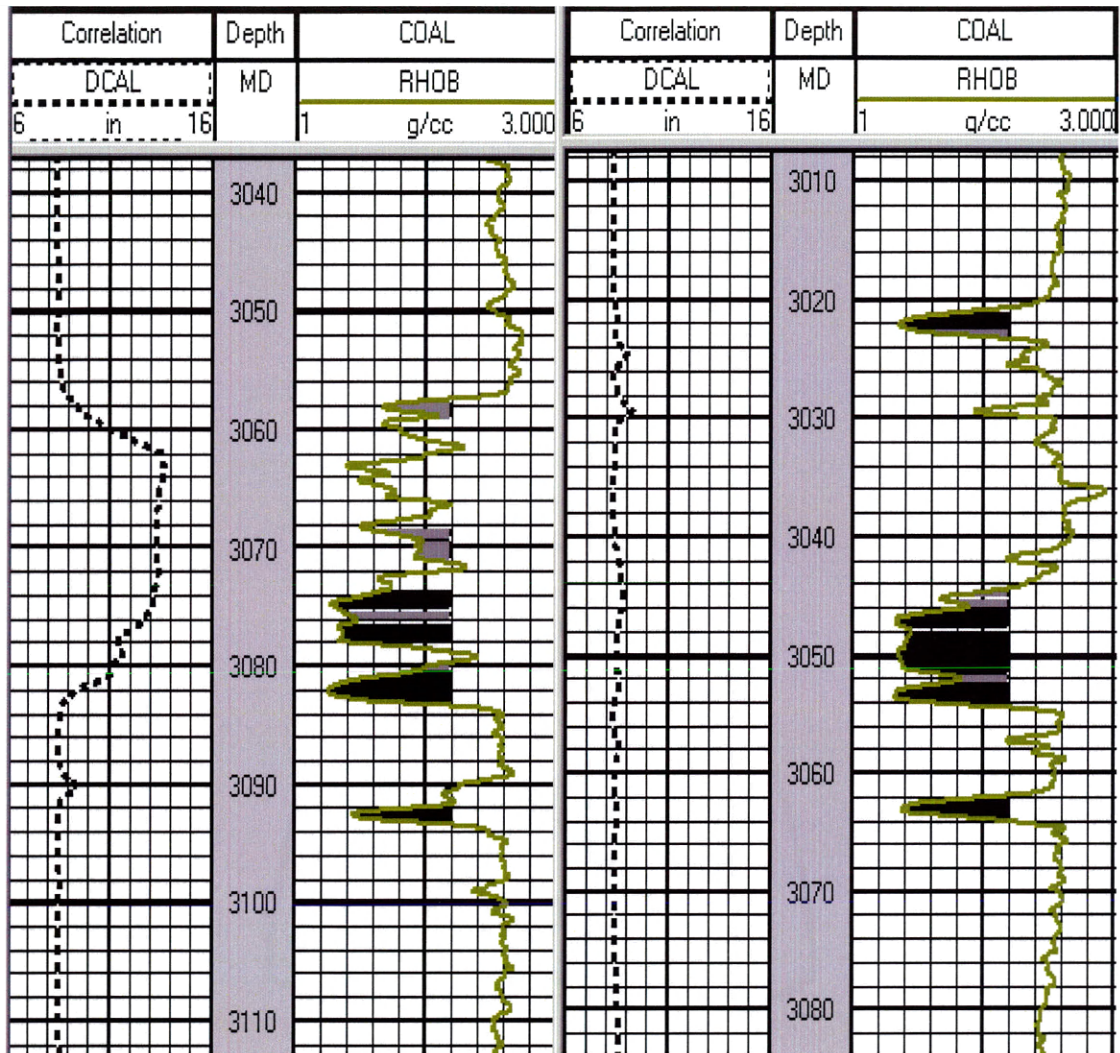
Figure 4-6   Enlarged wellbore effect on log bulk density

In this case, wellbore size indicated by the caliper log (DCAL) in the far left track increased from the bit size of 7 and 7/8 inches to 13.5 inches. The bulk density log in the offset well (left track) is compared to the core description provided from the core hole (right track). According to the lithology description displayed in the right "COAL" track, the interval between 3060 feet and 3070 feet in the offset well is a non-coal formation

48

whose bulk density is always above 2.5 g/cc. Due to the effect of the enlarged bore hole, the log bulk density of this interval is reduced to 1.38 g/cc, approaching the magnitude of the bulk density of the clean coals located below. As this example indicates, an enlarged wellbore can substantially reduce the log bulk density, which is caused by increased clearance between the tool face and the formation. Therefore, the caliper log has been incorporated into the new CBM computer model as a quality check to avoid misinterpretation of coal lithologies.

Because of its deeper investigation depth, log resistivity tools can tolerate most of the wellbore irregularity encountered at DWU. In cases of appreciable wellbore irregularities, the resistivity log is applied to distinguish coal from non-coal formations.

4.1.2.3 The effect of existing log algorithms on log bulk density

The log bulk density responds to the electron density of the formations, instead of the true density of the formations. The electron density is related to bulk density by the following equation:

$$\rho_e = \rho_b \left[\frac{2Z}{A} \right] \qquad 4.2$$

Where:

ρ_e = Electron density

ρ_b = Bulk density

A = atomic number

Z = molecular weight

For the most common sedimentary formations, the bracket term is very close to unity. For example, it is 0.9985 for quartz. Therefore, for liquid filled sandstones, the log density is practically identical to actual density. In contrast, this term for coal is 1.06,

instead of unity. As a result, an error of 6 percent is introduced into the log readings for coals and the log reading is 6 percent lower than the true density.

4.2 Resistivity

This section discusses (1) resistivity logging tools and wellbore effects; (2) factors that influence CBM reservoir resistivity; and (3) resistivity measurements in different coal lithologies.

4.2.1   Resistivity logging tools and borehole effects

The standard resistivity logging tools applied at DWU consist of a shallow lateral (short guard) and dual induction logs. The shallow laterolog used at DWU resembles a spherical focussed log (SFL) and has a relatively small depth of investigation of 12 inches to 20 inches. Because of its focusing nature, the shallow lateral logging tool is suitable for the resistivity environment formed by CBM reservoirs and borehole fluids, and is able to tolerate significant wellbore washouts, which is a common problem at DWU. In addition, the thin measuring-current beam (13 inches) warrants a satisfactory vertical resolution for coalbed identification. Therefore, the shallow lateral is a reliable logging tool to evaluate the resistivity of CBM reservoirs. In the following subsections, the reliability of the shallow lateral tool will be elaborated with respect to the resistivity environments, wellbore washouts, and investigation depth within CBM reservoirs. Also, the borehole effects on dual induction tools are discussed.

4.2.1.1 The resistivity environment and borehole corrections

Compared to conventional sandstone formations, CBM reservoirs demonstrate high resistivities in the 100 to 2000 Ohm-m range. Under the resistivity environment formed by the CBM reservoirs and borehole fluids at DWU, the shallow lateral tool yields reliable measurements. This premise has been verified by the relevant "borehole

correction chart" provided by the logging tool manufacturer (Figure 4-7), as discussed below.

The abscissa of the borehole correction chart is the ratio between shallow lateral measurement (Rlls) and the borehole fluid resistivity (Rm). Within CBM formations at DWU, the shallow resistivity measurement (Rlls) varies between 100 Ohm-m and 2000 Ohm-m. The corresponding borehole fluid resistivities (Rm) range is approximately 1 Ohm-m to 10 Ohm-m. Consequently, the Rlls/Rm ratio falls in the range of 100 to 200.

The cluster of blue curves represents the borehole correction for different borehole sizes. The standard borehole size at DWU is 8 inches (bit size: 7-7/8 inches).
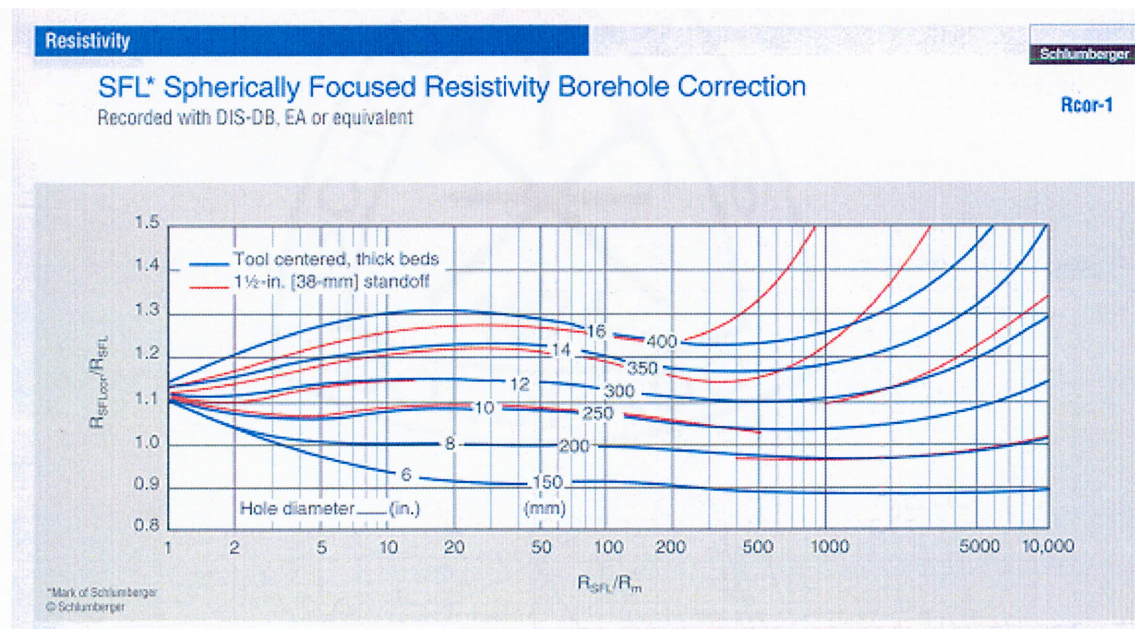
Figure 4-7   SFL Spherically focused resistivity correction chart
(Schlumberger Log Interpretation Charts, 1998)

The ordinate of the chart is the correction factor for the shallow lateral measurement. In an 8-inch borehole and with ratio Rlls/Rm between 100 and 200, the correction factor for the shallow lateral measurement is less than 20 percent, even for washouts as large as 6 inches, which enlarge the hole to 14 inches. Statistics of caliper logs demonstrate that most washouts are between 10 inches and 14 inches, with an occasional maximum of 16 inches.

4.2.1.2 Investigation depth

The investigation depth of 50 percent signal for the shallow lateral (short guard) is approximately 12 inches (according to the service company) for relatively low resistivity borehole fluids. Since there is a low porosity nature of the cleat system within coals, a relatively deep invasion of borehole fluids can be expected. Therefore, the measurement of the shallow lateral log primarily reflects the resistivity of the borehole fluid within the invaded zone. This suggestion will be further corroborated in the following section by the variation of shallow lateral logs in wells with different borehole fluid resistivities.

4.2.1.3 Borehole effect on dual induction logs

The combined effects of low conductivity of the coal formation and relatively high borehole fluid conductivity have significantly degraded the reliability of dual induction logging tools. Borehole corrections are often much larger than the magnitude of the coal bed conductivity. Comparing the field-wide deep induction log distribution to the corresponding borehole resistivity, a consistent observation has been made that the deep induction resistivity log closely corresponds to the borehole fluid resistivity. As the direct result, the true resistivity of the coal formation has been masked by the borehole effect.

4.2.2   Factors influencing coal resistivity

In the foregoing it was concluded that the shallow lateral log remains a reliable resistivity logging tool even under the adverse logging conditions present at DWU.

Subsequently, the shallow lateral log was used to evaluate the factors that influence the resistivity of the coal formations. Through this study, it has been observed that the resistivity of CBM reservoirs depends on two major factors: (1) the resistivity of the fluid within the cleat system and (1) the ash content of the coals.

4.2.2.1 The effect of cleat fluids

Because of the shallow investigation nature of the shallow lateral log, the resistivity of the borehole fluids controls the shallow resistivity measured in the flushed zone where the borehole fluids have replaced the original formation fluids. A substantial difference in shallow lateral measurements has been observed comparing wells in which different borehole fluid conductivities are used. This result is suprising considering the low volume (up to 4 percent) of the cleat system. However, the huge contrast of borehole fluid resistivity (1 to 10 Ohm-m) within clean massive coal (>2000 Ohm-m) explains the significant effect of such a small volume.
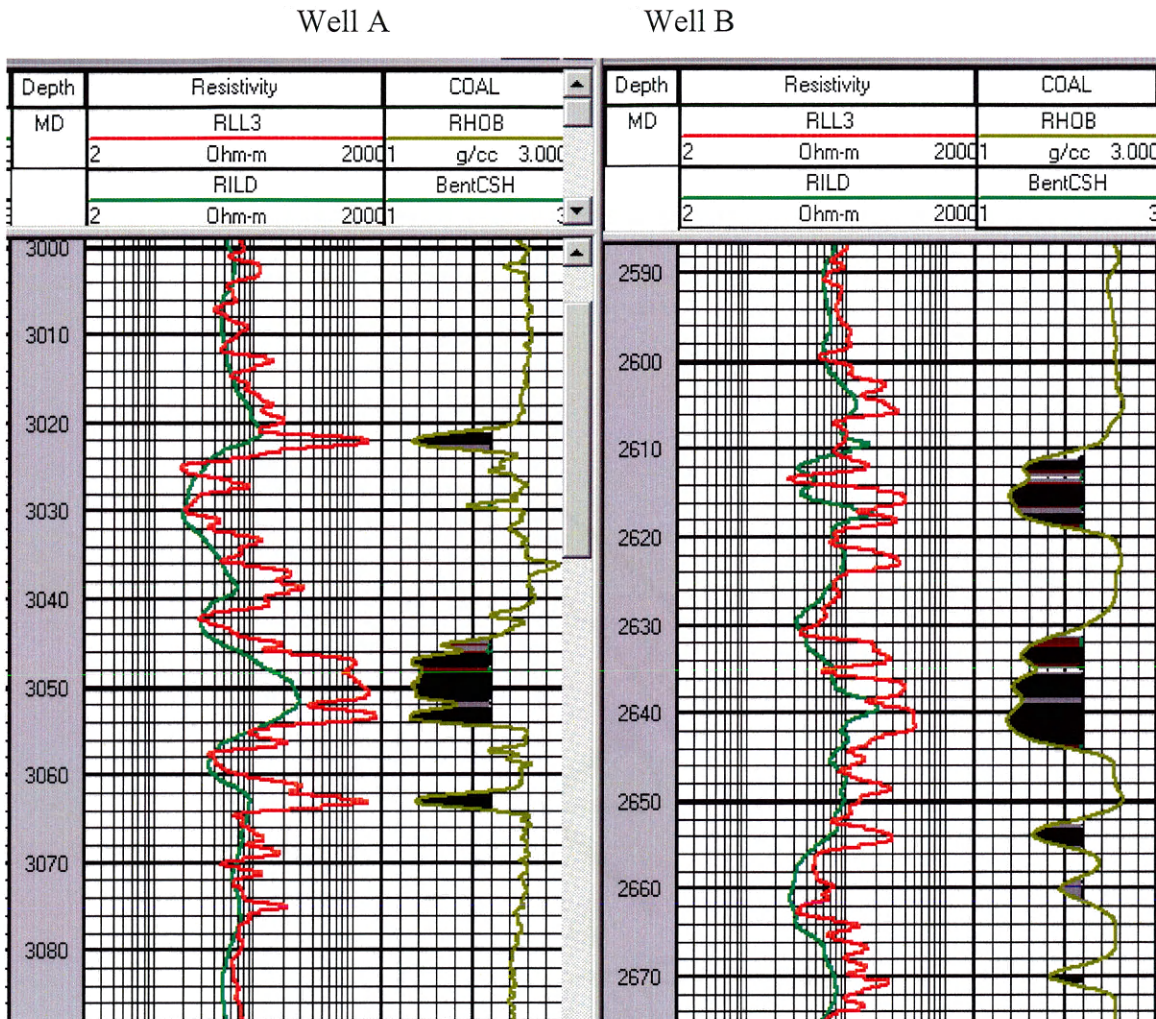
Figure 4-8   Shallow lateral log measurements in wells with different borehole
fluid resistivities

As displayed in Figure 4-8, the shallow lateral logs were recorded in two wells
with different wellbore fluid resistivity. The left set (well A) was measured in a well with
high wellbore fluid resistivity, and the right one (well B) was obtained from a well with
low wellbore fluid resistivity. As a result, the shallow lateral resistivity exceeds 1000
Ohm-m over the high quality coal interval at 3050 feet in well A, while the resistivity
over the corresponding coal interval at 2640 feet in well B is less than 500 Ohm-m.

At first glance the deep induction log (RILD) does not seem to support this interpretation. However, in well A the induction log measures a higher resistivity than in well B because the borehole effect in well A is much smaller than that in well B. The deep induction reads lower than the shallow laterolog (RLL3), because it is mainly affected by the low resistivity water in the cleats, while the RLL3 with its shallow depth of investigation is strongly affected by the high resistivity fluid in the cleats near the wellbore.

In well B the induction log is unreliable, because of the very large borehole effect in the low resistivity horehole fluids. Overall, it has been concluded that the RLL3 is the better tool to indicate the presence of coal and determine coal bed thicknesses. The induction log cannot be used in a qualitative way, while the shallow lateral log has to be corrected for the effect of fluids in the cleat system.

During the history of CBM exploration and development at DWU, two types of wellbore fluids have been used for drilling and completions. During the early stage, the well completion fluid was low salinity water. Its resistivity ranged from approximately 2 Ohm-m to 10 Ohm-m. Later on, for the sake of formation protection, a lower resistivity potassium chloride solution (3 percent KCl) was adopted as the wellbore fluid. The resulting lower borehole fluid resistivity is less than 1 Ohm-m. In response to this change in wellbore fluids, a consistent observation was made that the coal formation resistivity is measured high in older wells, while the coal formation resistivity measured low in newer wells.

4.2.2.2   The effect of ash content

To evaluate the effect of ash content on the conductivity of coal matrix, the ash contents of coal samples were correlated with the shallow lateral log measurements. As indicated in Figure 4-9, the ash content affects the resistivity of all the coal lithologies (from clean coal to carbonaceous shale). As implied by the correlation shown in this

graph, the coal resistivity decreases as the ash content increases. In other words, the coal matrix conductivity is proportional to its ash content.

As Figure 4-9 displays, within high quality coals (less than 30 percent ash content) the coal formation resistivities maintain a high level (approximately 1,000 Ohm-m). As the ash content increases, the formation resistivity declines proportionally. Within lower quality coal lithologies (ashy coal and CSH, 50 percent ash or more), their resistivity diminishes to a level approximately one tenth that of high quality coals.
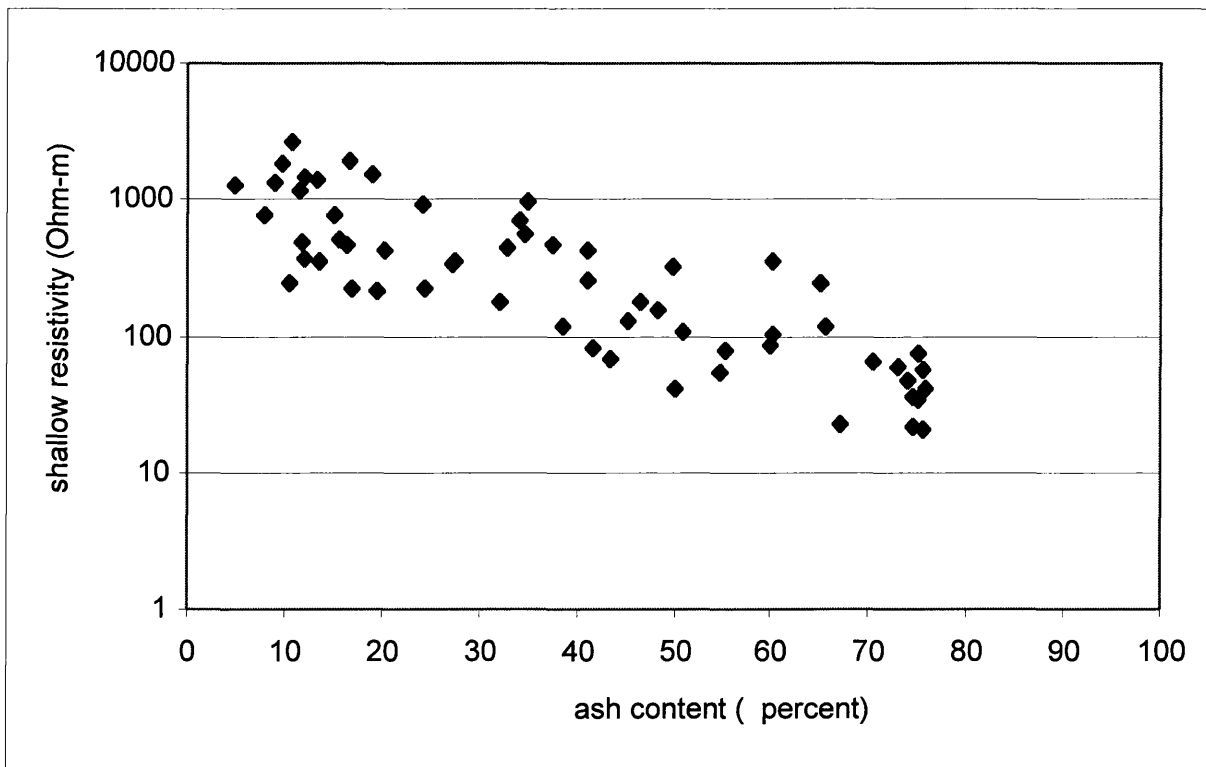
Figure 4-9   Shallow lateral resistivity vs. ash content

4.2.3 Resistivity measurements in different coal lithologies

The preceding section verified that the resistivity of the coal formation is a function of the resistivity of the fluid within the coal cleat system and the ash content of the coal. Subsequently, the resistivity measurement of different coal lithology is specified in this section.

4.2.3.1 Resistivity measurement in high quality coal (clean coal and HGC)

Two major factors associated with high quality coal determine the resistivity: the degree of development of the cleat system and the amount of ash content. In high quality coals, the ash content is minimal and evenly dispersed within the coal matrix. Therefore, the ash content usually makes an insignificant contribution to the coal conductivity. As a result, the resistivity measurement of high quality coal is dominated by the salinity of the fluids within the coal cleat system.

The fluid salinity within the coal cleat system varies from well to well as the result of different wellbore fluids. For the same coal lithology with the same quality, the resistivity measurement can vary significantly if different wellbore fluid is used. Field-wide, the resistivity of borehole fluid varies from approximately 1 Ohm-m to 10 Ohm-m. Correspondingly, the resistivity measurement changes from approximately 100 Ohm-m to 2000 Ohm-m, provided that the borehole is not very washed-out (less than 14 inches).

In substantially enlarged wellbores, the resistivity log of high quality coals can be measured slightly lower than the true value, caused by the enlarged borehole effect. In conclusion, the resistivity measurement of high quality coal remains at high levels under the logging environments at DWU. This observation facilitates the setup of logging cutoffs to identify high quality coals.

4.2.3.2 Log resistivity in ashy coal

In ashy coal (50 percent to 65 percent ash content), the influence of mineral matter on coal resistivity becomes more pronounced, as displayed in Figure 4-10. The

shallow lateral measurement has been appreciably reduced by the combination of enhanced conductivity of the coal matrix and the high salinity of formation fluids.

The shallow lateral resistivity log corresponding to ashy coal beds is displayed by the red curve in the left track. In this well, two seams of ashy coal occur at 3110 feet and 3172 feet, respectively, while a clean coal seam occurs at 3130 feet. The shallow lateral resistivity log over these ashy coal seams varies from 100 Ohm-m to 200 Ohm-m, whereas the shallow resistivity of the clean coal seam exceeds 500 Ohm-m. The significant reduction in resistivity from clean coal to ashy coal is primarily the result of increased ash content, as indicated by the correlation between the ash content and the coal formation resistivity discussed in the preceding section.
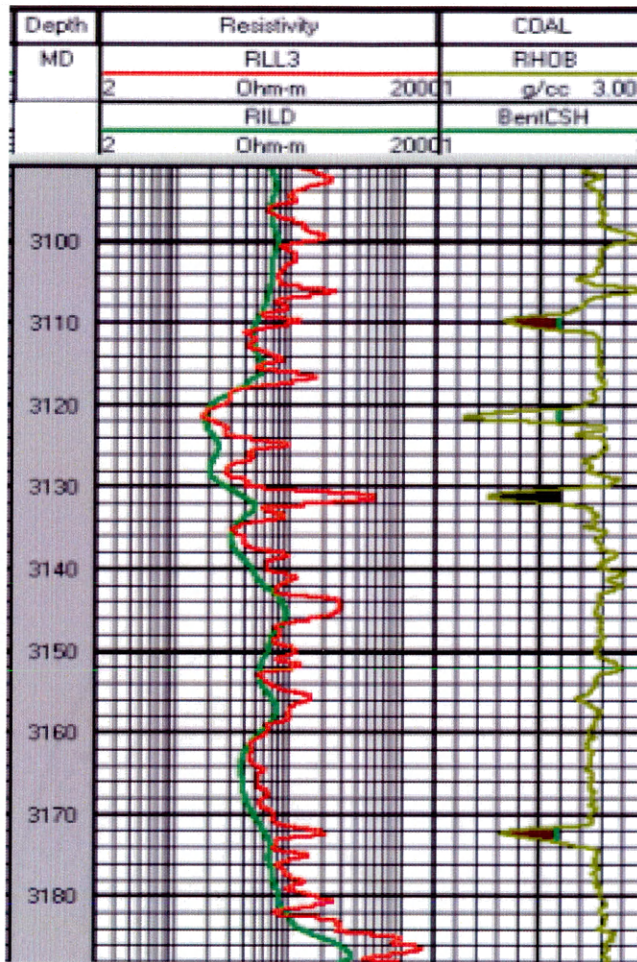
Figure 4-10   Shallow lateral resistivity measurements in ashy coal

4.2.3.3   Log resistivity in carbonaceous shale (CSH)

In carbonaceous shale (65 percent to 76 percent ash), ash content becomes the primary factor determining the formation resistivity. The cleat system and its influences on resistivity have disappeared. The bounded water in the mineral matter becomes the predominant component that determines the conductivity. As a result, the resistivity log of carbonaceous shale, including both CSH and bentonitic CSH, usually diminishes to a very low level.

As displayed in Figure 4-11, the shallow lateral resitivity log (RLL3) for the CSH at 2793 feet only slightly exceeds 22 Ohm-m. It is noteworthy that, within CSH, the lateral variation of resistivity has disappeared. The deep resistivity (RILD), medium induction log resistivity (RILM), and shallow lateral resistivity all converge together, confirming that there is no cleat system, nor permeability, to produce an invaded zone effect.
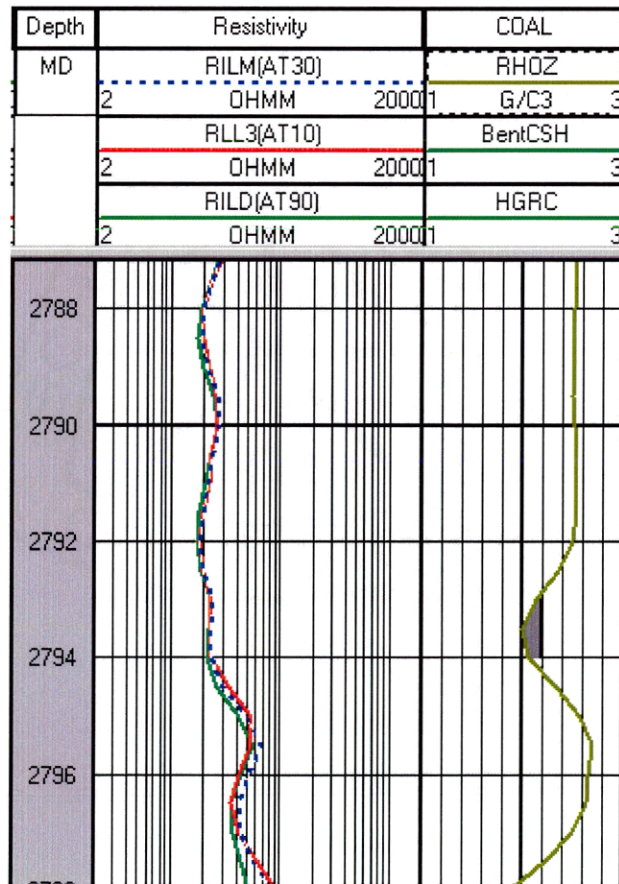
Figure 4-11: Log resistivity of CSH

Figure 4-12 depicts the resistivity measurement of a typical bentonitic CSH that occurrs at 3121 feet. The red curve in the center track represents the shallow lateral log. The direct reading is 18 Ohm-m. To remove the borehole effect, a correction factor of 1.2 was obtained from the correction chart (Figure 4-7). Thus, the corrected shallow lateral measurement is 22 Ohm-m, which is consistent with the resistivity measurement of CSH displayed in Figure 4-11.
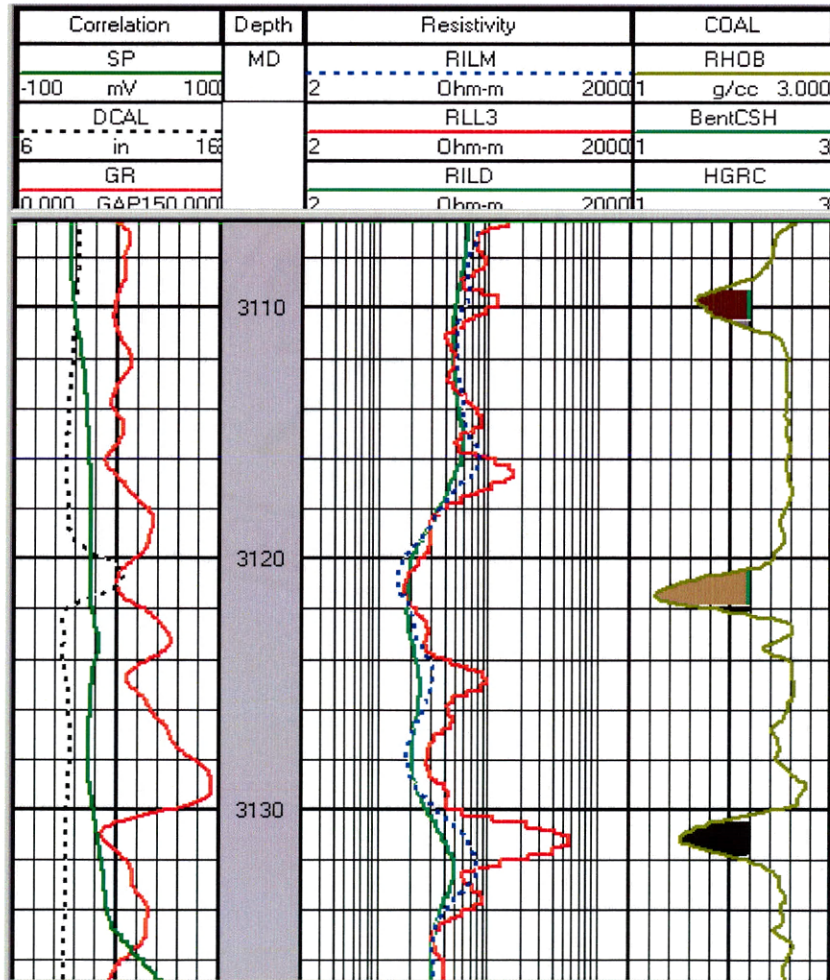
Figure 4-12 Log resistivity of bentonitic CSH

4.3 Gamma ray (GR)

Two major observations have been made through the investigation of coal GR and GR log responses in CBM reservoirs at DWU. GR magnitude in coals at DWU is significantly higher than what the operator originally perceived. This difference has caused clean coal to be underestimated when the GR magnitude of the reference shale formation was applied to coal lithology evaluation. Second, the GR log of a thin coal bed is substantially influenced by the high GR magnitude of the surrounding shale formations. As a result, these thin coal beds are inevitably degraded and incorrectly evaluated as lower quality coals.

4.3.1 Coal GR and GR log

The constituent minerals of ash content in coal are radioactive and the primary GR sources, while the fixed carbon's radioactivity is negligible. Therefore, the GR log in coals has been accepted as an ash indicator.

For coal evaluation using the GR log, the operator used to utilize the GR magnitude of a reference shale formation to represent the GR magnitude of ash content. The GR of this reference shale is 97 API units. To separate clean coal from high gamma-ray coal (HGC), a GR log cutoff of 53 API units, corresponding to 40 percent ash content, was adopted by the operator. Examinations of the relationship between the GR log and measured ash content of coal samples, depicted in Figure 4-13, show that this method can result in significant errors when it is applied to coal lithology evaluation.

As displayed in Figure 4-13, there are a large number of coal samples which exhibit GR above 53 API units, while their ash contents are less than 40 percent. If the 53 API units log cutoff is applied to evaluate coals, all these coal samples with a higher GR log will be wrongly evaluated as lower quality coals. This study indicates that the resultant errors are caused by two factors. First, the GR magnitude of 100 percent ash content of the ash found in coal is significantly higher than that of the reference shale formation.

Second, the thin bed effect of surrounding shale formations on the GR log of thin coal seams obscures the true lower GR level of higher quality coals.
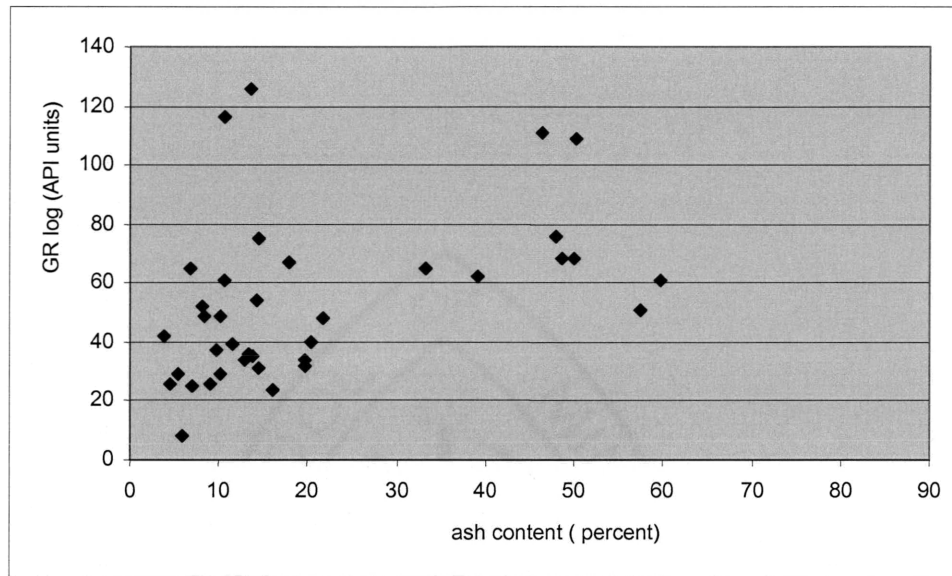
Figure 4-13 GR log of coal beds vs. their ash content

The presence of the higher GR of 100 percent ash content of coals has been substantiated by two observations. First, to get rid of the influence of thin bed effects, thick coal seams were selected for GR examination. The correlation between the GR log and ash content of these thick coal seams shows that the GR magnitude of constituent minerals of ash content is higher than the 97 API units of the reference shale formation. According to the correlation obtained by this study, by substituting 100 percent ash content into Equation 4-2, the GR is predicted to be 143 API units.

$$GR(\log) = 1.238Q_{ash} + 19.2 \qquad\qquad 4.3$$

Where:

$GR(\log)$ = gamma ray log (API units)

$Qash$ = ash content (percent)
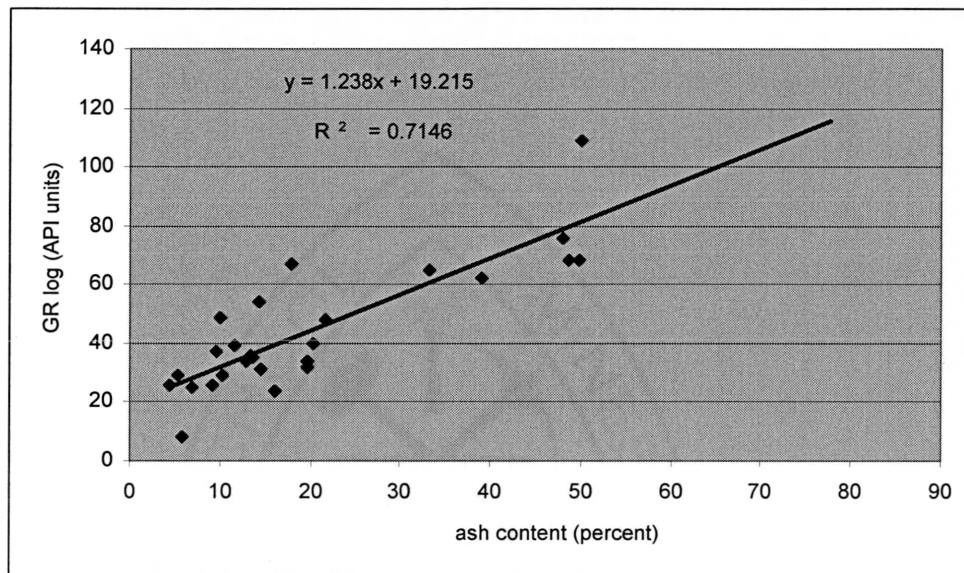
Figure 4-14 Correlation between ash content of GR

Second, the correlation between GR and ash content suggested by Equation 4-3 has been supported by the high GR log responses of the relatively thin beds of surrounding shale formations deposited with Ferron coals. The GR log of these shale formations is close to 150 API units. Therefore, the GR cutoff for clean coal (35 percent maximum ash content), as displayed in Figure 4-14, is 65 API units rather than 53 API units as previously accepted.

4.3.2   Thin bed effect on the gamma ray log

In cases where thin coal beds are interbeded within shale, the gamma ray logs of coal beds are increased to high levels by the presence of high gamma ray shale. This effect is a function of the strata profiles, which represent the relative thickness and position of coal beds and shale formations. Under these situations, the gamma ray log of a thin coal bed can show a "negative reflection" (gamma ray decline), but the GR log magnitude is far higher than its true value. This phenomenon can be observed in Figure 4-15.

As displayed in Figure 4-15, the coal sample at 3130 feet has been determined to be clean coal, and its ash content is 16 percent. However, its GR log (solid red line in the far left track) demonstrates a value of 61 API units. If the original method (53 API units) is applied, this clean coal bed would be interpreted as lower quality coal.
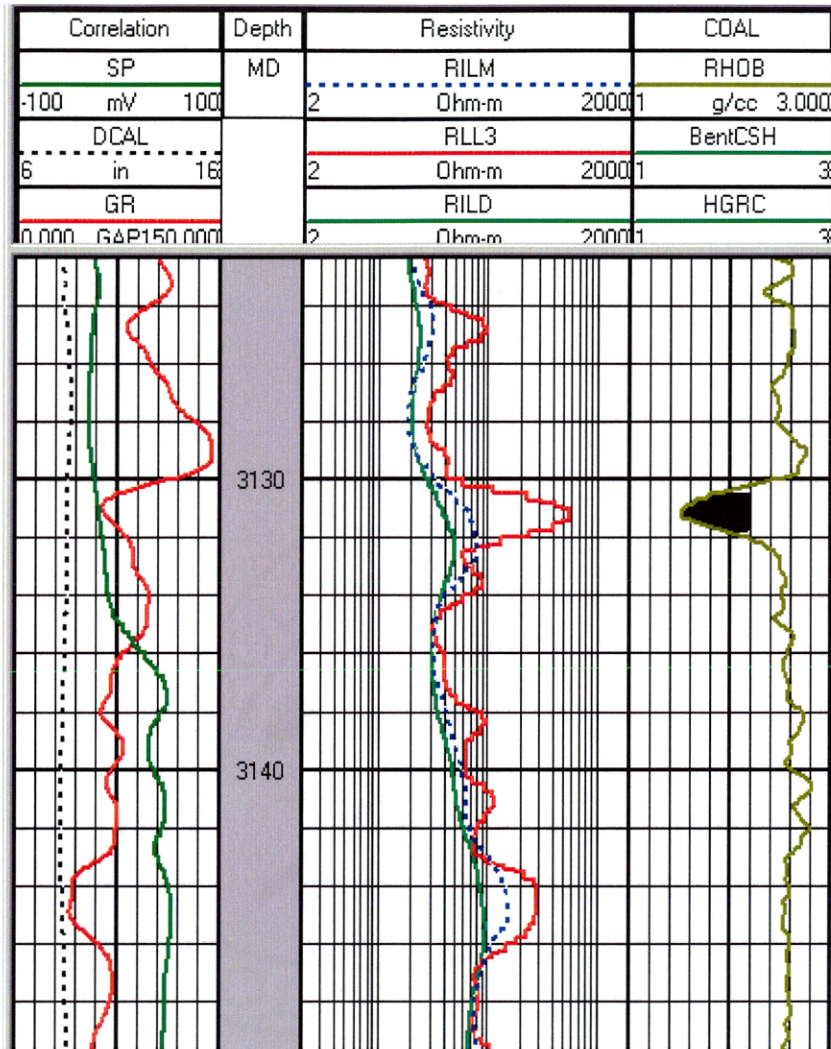
Figure 4-15: Thin bed effect on GR log

CHAPTER 5

LOG CUTOFF SYSTEM

This chapter presents a new log cutoff system to interpret coal lithologies using log data, based on the research of the log responses in the CBM reservoirs at DWU discussed in the previous chapter.

5.1 The fundamentals of the new log cutoff system

A log cutoff system is a methodology to specify one or several log-curve values for the purpose of coal lithology (grade) identification. For example, the previous log cutoff system consisted of two log curves, bulk density and GR. The log cutoffs of the bulk density and GR were 2.0 g/cc and 53 API units, respectively. For a given interval of log, if its bulk density is less than 2.0 g/cc, this interval will be interpreted as coal. Similarly, if the GR log of a portion of the same interval is less than 53 API units, this part of the interval will be interpreted as clean coal.

The investigation into the log responses in the CBM reservoirs at DWU has provided a comprehensive understanding with respect to two aspects: 1) the characteristic log responses of each log parameter within each type of coal lithology; 2) the effect of adverse log environments on the log responses, as well as methods to correct the errors caused by these negative effects of log environments. As a result, these new conclusions laid the foundation for the construction of a new log cutoff system which is more suitable for the coal conditions present at DWU.

The new log cutoff system is composed of two major components, the log parameters and the log environmental checks. The log parameters consist of bulk density, shallow resistivity, deep resistivity, and GR, whereas the log environment checks include caliper log and thickness measurement of each coal seam. After this log cutoff system was programmed in a computer model, the model checks the corresponding log

67

environment for a given coal formation first to determine the credibility of the log parameters, and then to correct the errors as necessary. By doing so, the coal beds are accurately characterized.

5.1.1 Bulk density

The bulk density log is the primary parameter to separate coal from non-coal formations and determine the type of coal lithology. According to the coal bulk density of each type of coal lithology presented in Chapter 3, the log bulk density is used to identify the coal bed and determine the type of lithology. This method can be applied only under a desirable log environment where the coal bulk density can be fully reflected by log bulk density.

Two major adverse log environments that can significantly affect the log bulk density have been commonly reported at DWU; one is the enlarged wellbore and the other is the thin bed effect.

In an enlarged wellbore, the caliper log provides the actual wellbore size and determines the severity of the wellbore washout. If the washout amount is beyond a certain limit, the log bulk density becomes less reliable. In cases where the washout is too large, the log bulk density of a non-coal formation can decline to the level of a coal formation. Under these circumstances, the deep resistivity or the shallow focused resistivity log is used for the discrimination of coals from non-coals, depending on the thickness of the interval.

Within thin coal beds, the coal thickness can be determined by the computer model. Accordingly, the correction method is applied to calculate the reliable bulk density of thin coal beds. Subsequently, the type of coal lithology can be more accurately determined and its gas reserves can be more accurately estimated.

As discussed above, the bulk density part of the new log cutoff system has incorporated the quality control with respect to the enlarged wellbore and thin beds. As a result, errors from adverse log situations are alleviated.

5.1.2 Resistivity

As the research into the resistivity of coals concluded, the resistivity of a coal formation is a function of the resistivity of coal formation fluid, wellbore fluid, coal permeability, ash content, and mineral type of the ash content. Different types of coal lithology exhibit different resistivity magnitudes resulting from the different contributions from each resistivity element.

In quality coals (clean coal and HGC), their shallow resistivity and deep resistivity are determined by the salinity of the coal formation fluid and wellbore water, respectively. Limited amounts of ash content do not significantly contribute to the conductivity of higher quality coals. Therefore, both the deep resistivity and shallow resistivity are very high, compared to lower quality coal. In addition to the resistivities of the coal formation water and wellbore water, the middle resistivity of quality coal is also affected by the extent of the invaded zone resulting from coal matrix permeability.

As ash content increases and coal quality decreases, the resistivity of coal declines. Also, the effect of the coal formation water on resistivity decreases as the result of the diminished cleat system in ashy coal. In ashy coal where the ash content is between 50 and 65 percent, both the shallow resistivity and deep resistivity are reduced substantially.

In carbonaceous shale (CSH), where ash content exceeds 66 percent, the resistivity is predominantly controlled by the ash content. Therefore, the deep resistivity and shallow resistivity converge, and the resistivity is reduced to a low level. In bentonitic carbonaceous shale (bentonitic CSH), the resistivity is reduced to an even lower level as the result of its strong affinity for water.

As discussed above, different types of coal lithology demonstrate different levels of resistivity. Therefore, the boundaries between these coals can be defined by their characteristic resistivity reflected by the log resistivity.

Even though the resistivity log can tolerate a certain amount of wellbore washouts, the caliper log is employed to determine the clearance between the log tool and the wellbore, so either the deep resistivity or the shallow resistivity will be selected.

Additionally, the coal thickness is determined by the computer model for the selection of the shallow resistivity log or the deep resistivity log, dictated by the differences in their resolutions.

5.1.3   GR

The investigation into the coal GR in the CBM reservoirs at DWU revealed two major new observations which affect the GR log cutoff. First, the gamma ray level of the ash content within the coals is appreciably higher than that of the reference shale formation, which had been incorporated into the previous gamma ray log cutoff. Second, the thin bed effect can sustain the GR log of thin coal beds at high levels, resulting in underestimating the coal quality.

As a result of the research into the GR levels in the Ferron coals at DWU, the GR log cutoff for clean coal was increased to 55 API units as a quality check for clean coal under ideal log conditions.

The coal thickness is determined by the computer model for thin bed effect considerations. When the coal bed is confirmed as a thin bed, the corresponding GR log is not applied quantitatively as a log cutoff parameter. Instead, the negative deflection of the GR curve is located for the indication of quality coals.

Compared to the previous log cutoff system, the new log cutoff system exhibits three major advantages.

First, more log parameters have been incorporated into the new system. In addition to the bulk density log and GR log, the shallow resistivity and deep resistivity logs have been incorporated into the new system. It has been shown that the resistivity log can better define the boundary between coal and non-coal formations. Also, resistivity logs are able to accommodate a significant amount of enlarged wellbore.

Second, the caliper log and the interval thickness have been utilized as the means to verify the log environments: enlarged wellbore and thin bed, which are the two major challenging log situations present at DWU. In response, the appropriate log curve is

selected that can tolerate enlarged wellbore. Alternatively, the correction method is selected to alleviate the errors caused by the thin bed effect.

Third, the characteristic log response of each type of coal lithology classified by the new coal lithology system has been established. Therefore, all types of coal lithology can be identified.

The following sections discuss the log cutoff system of each type of coal lithology, as well as the procedures the computer model follows to interpret the coals.

5.2   Clean coal

Step one: Log environment check

(1) Wellbore washout

At DWU all wells are drilled to the top of the Tununk shale formation below the Ferron coal formation where a regular wellbore can be expected. Thus, the averaged GR log of an interval of 20 feet at the bottom of a log set determines the standard bore-hole size. On the basis of this standard bore-hole size, the washout, or the clearance between the log tool and formation face, is calculated from the caliper log.

(2) Thin bed

The computer model uses the bulk density log to determine the thickness of a given formation interval that is to be evaluated. This interval is determined by a bulk density log cutoff of 2.0 g/cc, corresponding to the bottom limit of a coal formation (ashy coal).

Step two: Bulk density correction

If the coal thickness is less than 2.5 feet, the bulk density log is corrected using Equation 5-1.

$$\rho_b(correct) = 0.9221\rho_b(\log) + 0.0685 \qquad\qquad 5.1$$

Where:

ρ_b (correct) = corrected log bulk density, g/cc

ρ_b (log) = log bulk density, g/cc

Step three: Calculate the representative resistivity of quality coal

The computer model calculates the averaged shallow resistivity of all the coal formation intervals which have a log bulk density less than 2.0 g/cc. The largest shallow resistivity is selected as the representative shallow resistivity for this particular well.

Step four: Log cutoffs under different scenarios

(1) In a regular wellbore

if the washout amount is less than 1 inch, and the corrected log bulk density is less than 1.55 g/cc, then it is interpreted as clean coal

(2) In a moderately enlarged wellbore (thick coal)

if the washout amount is between 1 inch and 3 inches, and the log bulk density is less than 1.55 g/cc, and the GR is less than 55 API units, and the shallow resistivity exceeds 66 percent of the representative resistivity, then it is interpreted as clean coal

(3) In a moderately enlarged wellbore (thin coal)

if the coal thickness is less than 2.5 feet, and the washout amount is between 1 inch and 3 inches, and the corrected log bulk density is less than 1.55 g/cc, and the GR demonstrates a negative deflection, and the shallow resistivity exceeds 66 percent of the representative resistivity, then it is interpreted as clean coal

(4) In a seriously enlarged wellbore

    If the washout amount is larger than 3 inches, the log bulk density will be substantially affected. Therefore, no clean coal is interpreted. This prospective coal interval is evaluated by the lower quality coal cutoffs.

5.3   High gamma-ray coal (HGC)

Step one: Log environment check

(1) Wellbore washout

    At DWU all wells are drilled to the top of the Tununk shale formation below the Ferron coal formation where a regular wellbore can be expected. Thus, the averaged GR log of an interval of 20 feet at the bottom of a log set determines the standard bore-hole size. On the basis of this standard bore-hole size, the washout, or the clearance between the log tool and formation face, is calculated from the caliper log.

(2) Thin bed

    The computer model uses the bulk density log to determine the thickness of a given formation interval that is to be evaluated. This interval is determined by a bulk density log cutoff of 2.0 g/cc, corresponding to the bottom limit of a coal formation (ashy coal).

Step two: Bulk density correction

    If the coal thickness is less than 2.5 feet, the bulk density log is corrected using Equation 5-1.

$$\rho_b(correct) = 0.9221\rho_b(\log) + 0.0685 \qquad\qquad 5.1$$

Where:

ρ_b (correct) = corrected log bulk density, g/cc

ρ_b (log) = log bulk density, g/cc

Step three: Calculate the representative resistivity of quality coal

The computer model calculates the averaged shallow resistivity of all the coal formation intervals, which have a log bulk density less than 2.0 g/cc. The largest shallow resistivity is selected as the representative shallow resistivity for this particular well.

Step four: Log cutoffs under different scenarios

(1) In a regular wellbore

if the washout amount is less than 1 inch, and the corrected log bulk density is less than 1.75 g/cc, then it is interpreted as HGC

(2) In a moderately enlarged wellbore (thick coal)

if the washout amount is between 1 inch and 3 inches, and the log bulk density is less than 1.75 g/cc, and the shallow resistivity exceeds 66 percent of the representative resistivity, then it is interpreted as HGC

(3) In a moderately enlarged wellbore (thin coal)

if the coal thickness is less than 2.5 feet, and the washout amount is between 1 inch and 3 inches, and the corrected log bulk density is less than 1.75 g/cc, and the shallow resistivity exceeds 66 percent of the representative resistivity, then it is interpreted as HGC

(4) In a seriously enlarged wellbore

if the log bulk density is less than 1.75 g/cc, and the shallow resistivity (when the washout amount is larger than 3 inches), or the deep resistivity (when the washout

74

is larger than 5 inches) exceeds 66 percent of the corresponding representative resistivity, then it is interpreted as HGC.

5.4 Ashy coal

Step one: Log environment check

(1) Wellbore washout

At DWU all wells are drilled to the top of the Tununk shale formation where a regular wellbore can be expected. Thus, the averaged GR log of an interval of 20 feet at the bottom of a log set determines the standard bore-hole size. On the basis of this standard bore-hole size, the washout, or the clearance between the log tool and formation face, is calculated from the caliper log.

(2) Thin bed

The computer model uses the bulk density log to determine the thickness of a given formation interval that is to be evaluated. This interval is determined by a bulk density log cutoff of 2.0 g/cc, corresponding to the bottom limit of a coal formation (ashy coal).

Step two: Bulk density correction

If the coal thickness is less than 2.5 feet, the bulk density log is corrected using Equation 5-1.

$$\rho_b(correct) = 0.9221\rho_b(\log) + 0.0685 \qquad\qquad 5.1$$

Where:

ρ_b (correct) = corrected log bulk density, g/cc

ρ_b (log) = log bulk density, g/cc

Step three: Calculate the representative resistivity of quality coal

The computer model calculates the averaged shallow resistivity of all the coal formation intervals which have a log bulk density less than 2.0 g/cc. The largest shallow resistivity is selected as the representative shallow resistivity for this particular well.

Step four: Log cutoffs under different scenarios

(1) In a regular wellbore

if the washout amount is less than 1 inch, and the corrected log bulk density is less than 2.0 g/cc then, it is interpreted as ashy coal

(2) In a moderately enlarged wellbore (thick coal)

if the washout amount is between 1 inch and 3 inches, and the log bulk density is less than 2.0 g/cc, and the shallow resistivity exceeds 40 percent of the representative resistivity, then it is interpreted as ashy coal

(3) In a moderately enlarged wellbore (thin coal)

if the coal thickness is less than 2.5 feet, and the washout amount is between 1 inch and 3 inches, and the corrected log bulk density is less than 2.0 g/cc, and the shallow resistivity exceeds 40 percent of the representative resistivity, then it is interpreted as ashy coal

(4) In a seriously enlarged wellbore

if the washout amount is larger than 3 inches, and the log bulk density is less than 2.0 g/cc, and the shallow resistivity exceeds 40 percent of the representative resistivity, then, it is interpreted as ashy coal.

5.5 CSH

Log cutoffs under different scenarios

(1) In a regular wellbore and moderately enlarged wellbore

if the washout amount is less than 4 inches, shallow resistivity exceeds 30 Ohm-m, and the log bulk density is less than 2.2 g/cc, then it is interpreted as CSH

(2) In a seriously enlarged wellbore

if the washout amount is larger than 4 inches, deep resistivity exceeds 30 Ohm-m, and the log bulk density is less than 2.2 g/cc, then it is interpreted as CSH.

5.6 Bentonitic CSH

Log cutoffs under different scenarios

(1) In a regular wellbore and moderately enlarged wellbore

if the washout amount is less than 4 inches, shallow resistivity is less than 30 Ohm-m, and the log bulk density is less than 2.2 g/cc, then it is interpreted as bentonitic CSH

(2) In a seriously enlarged wellbore

if the washout amount is larger than 4 inches, deep resistivity is less than 30 Ohm-m, and the log bulk density is less than 2.2 g/cc, then it is interpreted as bentonitic CSH.

CHAPTER 6

GAS DESORPTION, GAS ADSORPTION, AND GAS CONTENT

This chapter presents the observations with respect to gas desorption, adsorption characteristics, and the resultant method for calculating gas content.

6.1 Gas desorption

The gas desorption tests performed on coal samples obtained from 23 core holes have provided information on three critical reservoir properties: 1) gas content; 2) gas diffusion behavior, and 3) gas composition.

6.1.1 Gas desorption test

The gas desorption test is a standard method measuring the gas content, gas diffusion behavior, and gas composition. This measurement involves cutting fresh core samples at the well-site and putting them into desorption canisters of known volume as soon as the core samples are retrieved to the surface. These canisters are placed in water baths where ambient temperature is regulated to the CBM reservoir temperature. Subsequently, the desorbed gas is measured as a function of time, temperature, and pressure. Based on the condition of temperature and pressure when the measurement is recorded, the desorbed gas volumes are corrected to the standard pressure and temperature.

The gas content measurements are carried out at the well-site until the end of the coring operation, then the canisters are transferred to the laboratory for further measurement. In the case of the adsorption tests performed on the Ferron coal samples at DWU, the duration of the gas desorption measurement lasts two months. In addition to the total desorbed gas measurements, gas chromatography analyses are performed periodically to measure the constituent components of the natural gas. The major

components measured in the Ferron coal at DWU consist of methane, ethane, propane, i-butane, n-butane, i-pentane, n-pentane, and carbon dioxide. Details of the gas composition will be discussed in the subsection of gas composition.

After the termination of canister measurements, the residual gas volume is measured. The measurement of residual gas entails sealing each coal sample in a gas-tight mill and crushing it for approximately 30 seconds. The gas-tight mill crushes a 100-gram sample to less then 200 mesh particle size. The released gas is then vented into a burette system for volumetric measurement. Meanwhile, the barometric pressure and ambient temperature are recorded for volume corrections to standard pressure and temperature.

The recorded testing data are utilized for the evaluation of gas content, gas diffusion behavior, and gas composition, which are elaborated in the following sections.

6.1.2 Gas content

Gas content of a given coal sample is the summation of the canister desorbed gas content, residual gas content, and the lost gas. While the canister desorbed gas and residual gas are direct measurements of gas contents, the lost gas is estimated using the US Bureau of Mines (USBM) technique.

To estimate the lost gas content, the canister desorbed gas is plotted versus the square root of desorption time. As displayed in Figure 6-1, the best fit straight line at the early stage of the desorption test is extrapolated to time zero when the core sample was cut and lifted off the bottom of the hole. The negative intersection on the vertical coordinate is deemed as the total lost gas.

In the case illustrated in Figure 6-1, the lost gas volume is 0.991 standard liters, the total canister measured gas volume is 11.914 standard liters, and the total measured desorbed gas volume is 12.905 standard liters, which is equivalent to 305.3 scf/ton.

6.1.3 Gas composition

Gas composition analysis measures the hydrocarbon and non-hydrocarbon components constituting the natural gas produced from CBM reservoirs. The measured components include methane, ethane, propane, i-butane, n-butane, i-pentane, and n-pentane. The non-hydrocarbon component primarily refers to carbon dioxide (CO_2). Other impure substances such as nitrogen and hydrogen sulfide that are common for conventional gas reservoirs are negligible at DWU. In this section, the concentration of gas components, as well as the variation of component concentrations, are discussed as functions of desorption time.
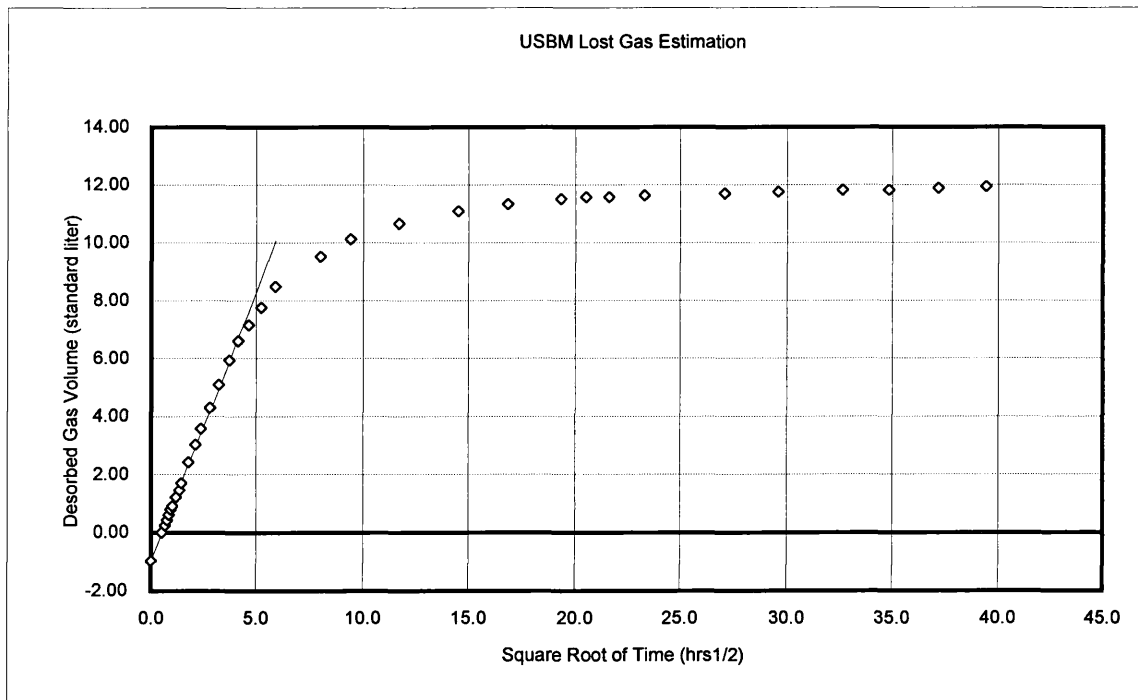
Figure 6-1 USMB lost gas estimation

The chromatography test indicates that the methane concentration varies from 70 percent to 90 percent, while the ethane concentration varies from 3 percent to 22 percent in tested coal samples of Ferron coal at DWU. The combined concentrations of propane through decane are constantly less than 2 percent. The CO_2 concentration varies from 2 percent to 19 percent.

During the process of desorption tests, concentrations of each gas component, both the hydrocarbons and non-hydrocarbons, change to various degrees. Figure 6-2 demonstrates the characteristic concentration variations of measured gas species.

During the gas desorption process it was observed that the core samples share similar behavior in concentration changes of each gas species. Methane concentration steadily decreases, while such other hydrocarbon components as ethane, propane, and butane increase in concentration. The concentration of carbon dioxide decreases during the life of the desorption test.

Gas Species (mol. %) vs Cumulative Gas (%)
Sample: 4 Depth: 2808.3-09.3 ft.
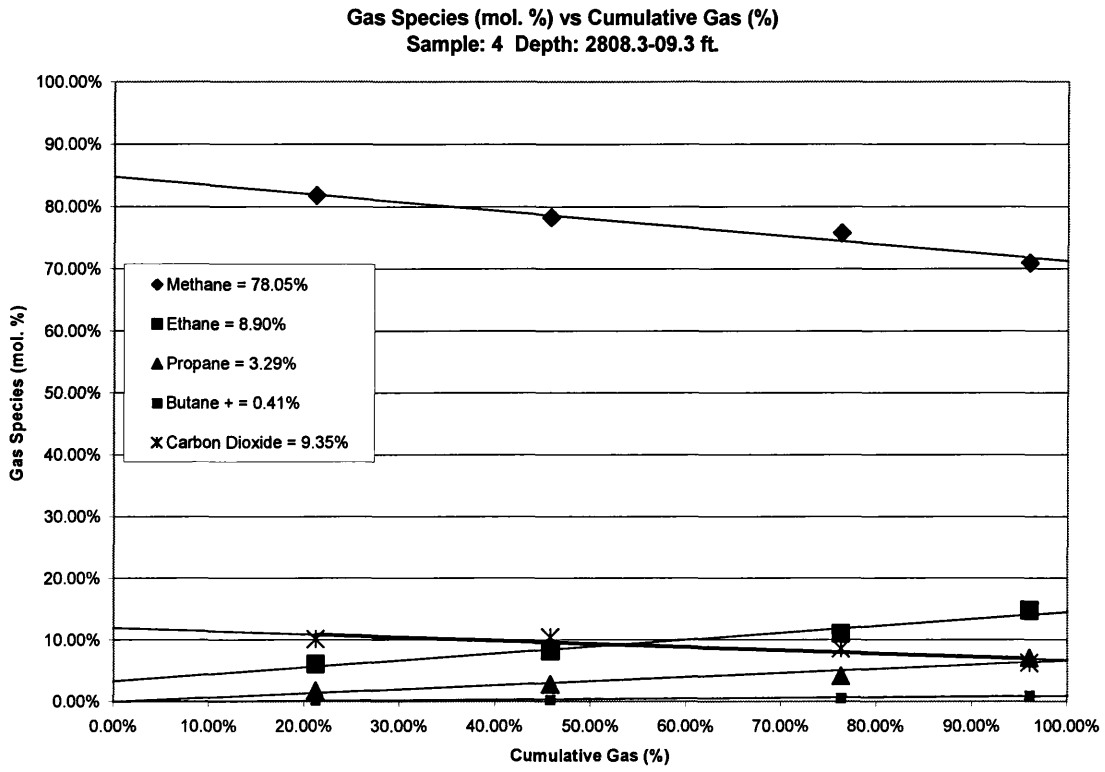
Figure 6-2   Gas species (mol percent) vs. cumulative gas volume (percent).
The concentrations of the gas components in the rectangle are
the equilibrium total concentrations under standard conditions

According to the testing results shown in Figure 6-2, methane concentration
declined from approximately 85 mol percent at the beginning to approximately 72 mol
percent at the end. Carbon dioxide decreased from approximately 12 mol percent to
approximately 7 mol percent. Ethane increased from approximately 4 mol percent to
approximately 14 mol percent; propane constantly increased from trace amounts to
approximately 7 mol percent. The increment in butane is perceptible, even though it is
minimal.

82

6.1.4 Gas diffusivity behavior

The sorption time is defined as the time required to desorb 63 percent of the canister measured gas. The sorption time is indicative of the diffusion behavior of gas desorption from a given coal sample. In other words, it reflects how quickly the adsorbed natural gas gets desorbed from the free surface of the coal matrix and transported within the conduits – the cleat system. Therefore, sorption time is an important coal reservoir parameter that is indicative of the producing capacity of a given CBM reservoir.

Figure 6-3 displays a typical correlation between cumulative desorbed gas volume and elapsed desorption time. In this case, the total measured gas volume is 4.612 standard liters. Sixty-three percent of this total gas volume is 2.91 standard liters. According to the correlation between cumulative desorbed gas and elapsed time, the sorption time is approximately 78 hours.
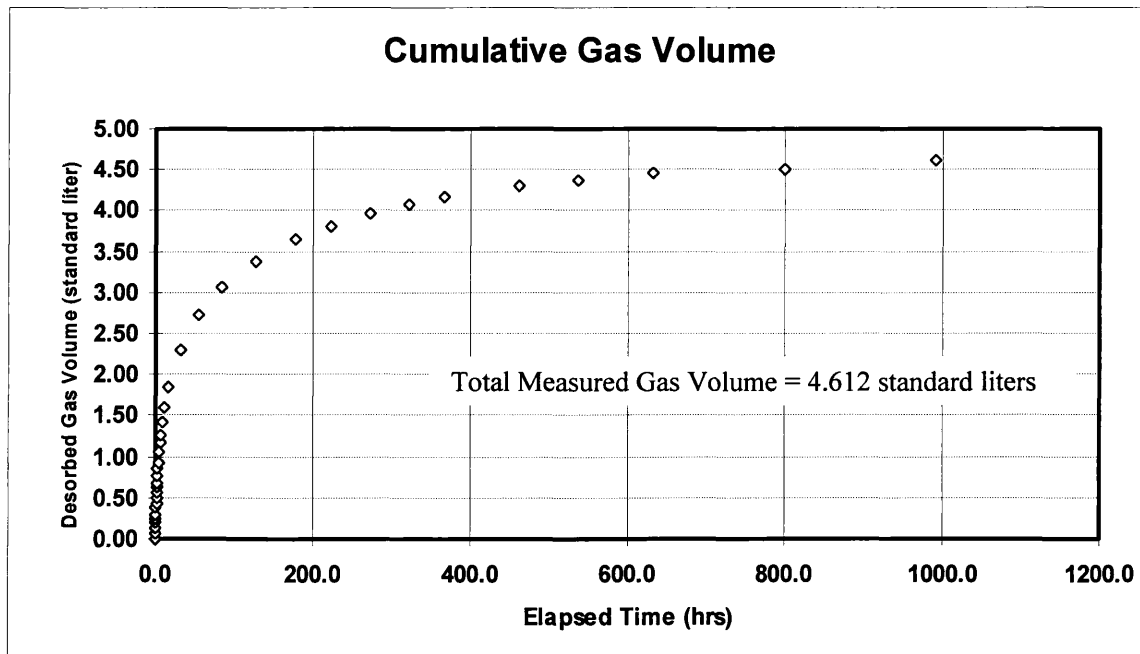
Figure 6-3   Cumulative gas volume vs. desorption time

The sorption time of more than 100 coal samples covers a broad range, from as short as 10 hours to more than 100 hours. Compared to the same rank of coal occurring in the San Juan basin (Bell, 1986), the sorption times of Ferron coals are shorter.

6.2 Gas adsorption

The gas adsorption test reveals two critical properties of CBM reservoirs: 1) gas storage capacities under different pressures at a given reservoir temperature, and 2) the ultimate gas recovery at a specific producing pressure. In addition to the gas adsorption characteristics of the Ferron coals at DWU, this section discusses the observed deviation between the gas content predicted from the Langmuir Equation and the actual gas content in lower quality coal formations.

6.2.1 Gas adsorption test

Gas adsorption tests measure the gas storage capacity of coal as a function of pressure at a fixed reservoir temperature. As indicated in the previous section, the produced natural gas primarily consists of methane, ethane, and carbon dioxide. Thus, the gas adsorption tests have been performed with methane, ethane, and carbon dioxide.

To prepare the coal samples for the adsorption tests, coal samples need to be ground to pass a 20-mesh screen. To equilibrate the moisture content of coal samples, the samples are subjected to 97 percent humidity at reservoir temperature, under 30 mm hg pressure for approximately 20 days.

To obtain the correlation between the cumulative adsorbed gas volume and pressure, pressure is gradually increased from 50 psig to a level that is above the highest known reservoir pressure throughout the unit. Therefore, the maximum testing pressure is usually no more than 1500 psig.

Table 6-1 through Table 6-3 displays the adsorption test results performed with methane, ethane, and carbon dioxide, on the basis of raw coal, which contains the in-situ moisture and ash content.

As indicated in these tables, under the same testing conditions the same coal sample demonstrates different gas adsorption capacities for different gas species. Under the same situation, the gas capacity for carbon dioxide is substantially higher than that for hydrocarbon gases (methane and ethane).

Methane Adsorption Isotherm

Phillips Petroleum   **Well: DW 24-561**
Sample: 2   **Depth: 2558.3-59.3**
Raw Basis

Sample Weight = 112.82 g	Ash Content = 14.61 percent
	EQ. Moisture Content = 2.16
Particle Size = < 20 Mesh	percent
Temperature = 98.0°F (36.7°C)	

Methane Adsorption

Pressure		Gas Content (Raw Basis)	
(psia)	(MPa)	(scf/ton)	(scc/gm)
53	0.37	41.3	1.29
104	0.72	72.9	2.27
202	1.39	122.3	3.81
348	2.40	180.2	5.61
506	3.49	220.6	6.87
806	5.56	280.0	8.72
1,208	8.33	329.5	10.26
1,607	11.08	373.0	11.62
2,062	14.22	403.6	12.57

Table 6-1   Methane adsorption isotherm

Ethane Adsorption Isotherm

Phillips Petroleum

Sample: 2

Raw Basis

Well: DW 24-561

Depth: 2558.3-59.3

Sample Weight = 112.82 g Particle Size = < 20 Mesh Temperature = 98.0°F (36.7°C)	Ash Content = 14.61 percent EQ. Moisture Content = 2.16 percent

Ethane Adsorption

Pressure		Gas Content (Raw Basis)	
(psia)	(MPa)	(scf/ton)	(scc/gm)
20	0.14	56.6	1.76
42	0.29	115.0	3.58
83	0.57	191.0	5.95
148	1.02	248.4	7.74
201	1.39	298.8	9.31
258	1.78	328.5	10.23
316	2.18	355.3	11.07
368	2.54	368.4	11.48
440	3.03	384.5	11.98

Table 6-2   Ethane adsorption isotherm

Carbon Dioxide Adsorption Isotherm

Phillips Petroleum   **Well: DW 24-561**

Sample: 2   **Depth: 2558.3-59.3**

Raw Basis

Sample Weight = 112.82 g	Ash Content = 14.61 percent
	EQ. Moisture Content = 2.16
Particle Size = < 20 Mesh	percent
Temperature = 98.0°F (36.7°C)	

Carbon Dioxide Adsorption

Pressure		Gas Content (Raw Basis)	
(psia)	(MPa)	(scf/ton)	(scc/gm)
29	0.20	46.6	1.45
50	0.34	92.6	2.88
92	0.63	165.4	5.15
148	1.02	233.7	7.28
223	1.54	303.6	9.46
298	2.05	358.2	11.16
401	2.76	414.2	12.90
505	3.48	462.0	14.39
642	4.43	505.7	15.75

Table 6-3   Carbon dioxide adsorption isotherm

6.2.2   Adsorption Langmuir Equation for each gas species

Adsorbed gas volume is a function of pressure at which the adsorption process reaches equilibrium. This relation is usually expressed by the Langmuir Equation. The Langmuir Equation is determined by two parameters: Langmuir volume and Langmuir

87

pressure. The Langmuir volume represents the maximum gas volume that can be adsorbed in a given amount of coal samples at an extremely high pressure, which is usually less than 10,000 psig. The Langmuir pressure corresponds to the pressure at which half the Langmuir volume can be adsorbed.

The general Langmuir Equation is represented as:

$$V = VL \frac{P}{PL + P}$$
6.1

Where:

VL = Langmuir volume, sfc/ton

PL = Langmuir pressure, psig

V = gas content, scf/ton

P = pressure, psig

In general, high Langmuir volume implies high gas content, while high Langmuir pressure corresponds to less curvature in the isotherm curves, or less ultimate gas recovery. Therefore, when a specific Langmuir Equation is established for a particular coal sample, this Langmuir Equation could be used to estimate the gas content of coal. This technique is commonly termed as the "indirect method" for calculating gas contents.

As indicated by the gas adsorption isotherm characteristics discussed in the preceding subsection, different gas species demonstrate different gas adsorption behaviors. Therefore, for a given coal sample, each gas species dictates different Langmuir Equations. Figure 6-4 through Figure 6-6 displays the typical gas adsorption behavior and the resultant Langmuir Equation of methane, ethane, and carbon dioxide. As indicted by the Langmuir volumes of each gas species, the gas capacity for carbon dioxide is appreciably higher than that for hydrocarbon gases, for the same coal sample.
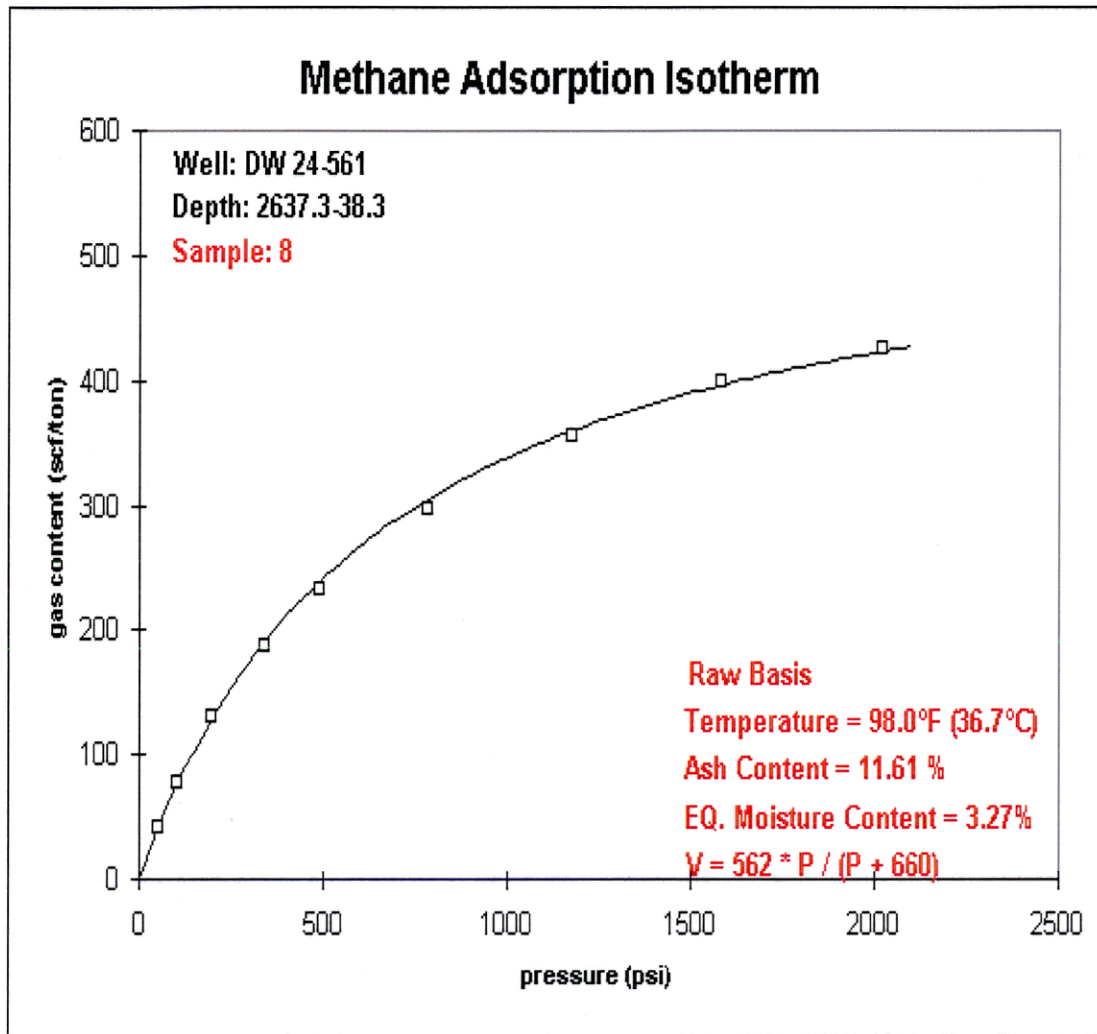
Figure 6-4   Methane adsorption isotherm

Langmuir Coefficients		V = 562 * P / (P + 660)	
PL		VL (Raw Basis)	
(psia)	(MPa)	(scf/ton)	(scc/gm)
660	4.55	562	17.5

Table 6-4   Langmuir Equation and Langmuir coefficients for methane
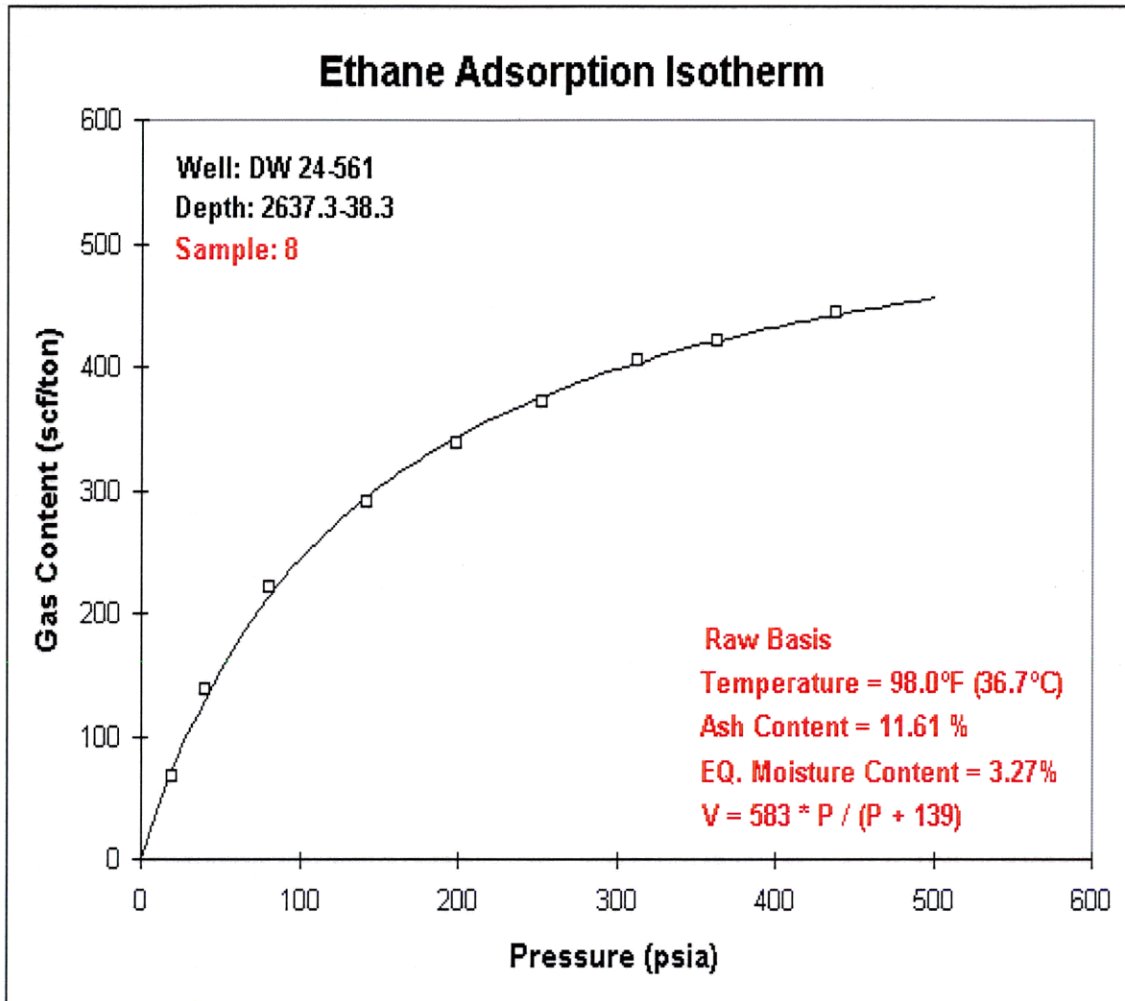
Figure 6-5   Ethane adsorption isotherm

Langmuir Coefficients		$V = 583 * P / (P + 139)$	
PL		VL (Raw Basis)	
(psia)	(MPa)	(scf/ton)	(scc/gm)
139	0.96	583	18.2

Table 6-5   Langmuir Equation and Langmuir coefficients for ethane
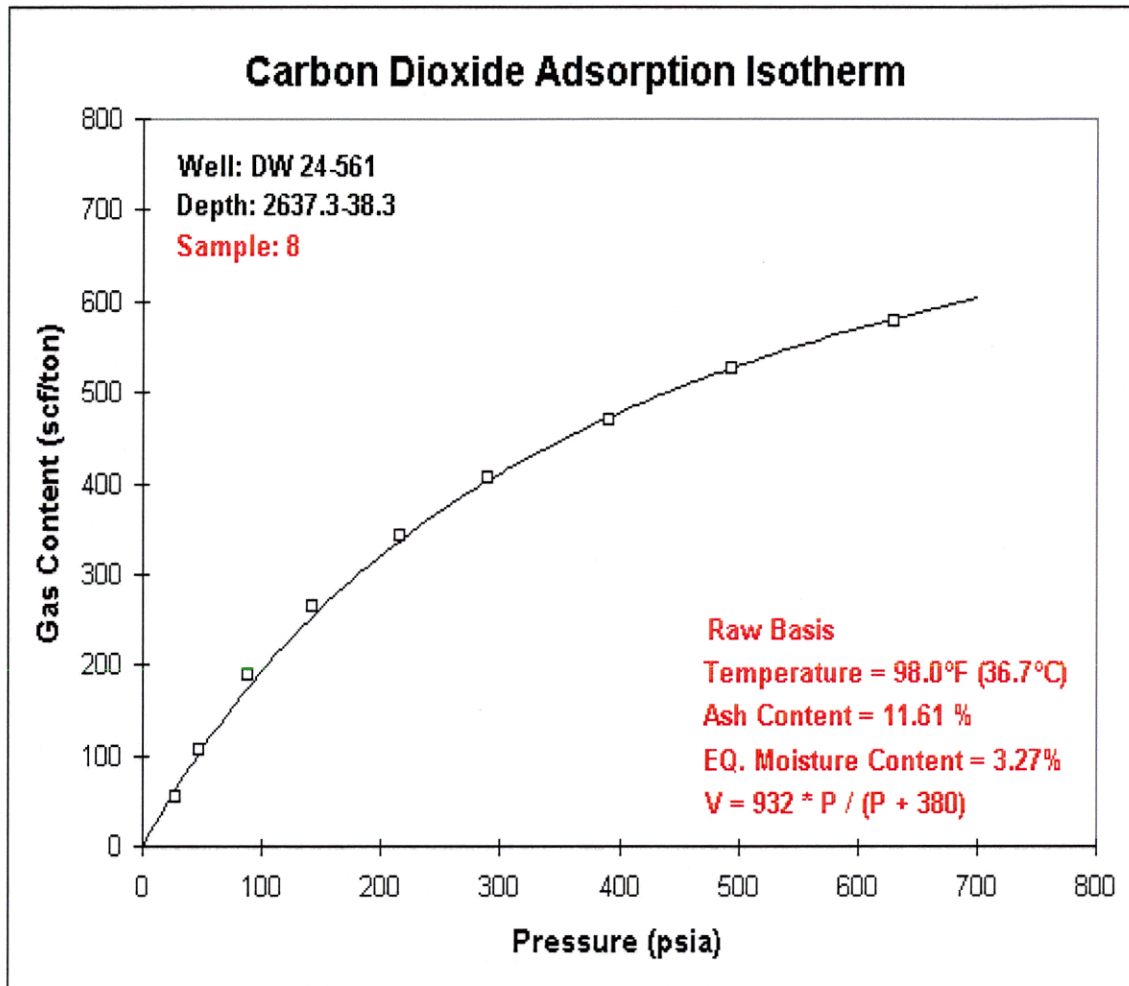
Figure 6-6   Carbon dioxide adsorption isotherm

Langmuir Coefficients		V = 932 * P / (P + 380)	
PL		VL (Raw Basis)	
(psia)	(MPa)	(scf/ton)	(scc/gm)
380	2.62	932	29.0

Table 6-6   Langmuir Equation and Langmuir coefficients for carbon dioxide

6.2.3 Extended Langmuir Equation

The Extended Langmuir Equation is formulated by each individual Langmuir Equation of each of the gas species which compose a given gas sample. Therefore, the Extended Langmuir Equation represents the gas adsorption behavior of this particular gas sample. To construct an Extended Langmuir Equation, the Langmuir volume is derived from the combination of the Langmuir volume of each gas species. In a similar way, the Langmuir pressure can be calculated from that of each gas species. To establish a particular Extended Langmuir Equation for a given coal sample, the composition of desorbed gas, as well as the Langmuir Equation of each gas species, has to be known.

The Langmuir coefficients (Langmuir pressure and Langmuir volume) of the given coal samples in the preceding figures are provided below.

Langmuir coefficients:

Methane: VL = 562 scf/ton, PL = 660 psia

Ethane: VL = 583 scf/ton, PL = 139 psia

Carbon dioxide: VL = 932 scf/ton , PL = 380 psia

Composition of desorbed gas:

Methane: 78 mol percent

Ethane: 14 mol percent

Carbon dioxide: 8 mol percent

Therefore, the Extended Langmuir coefficients are:

PL = PL(CH4) * 0.78 + PL(C2H6) * 0.14 + PL(CO2) * 0.08 = 565 psia

VL = VL(CH4) * 0.78 + VL(C2H4) * 0.14 + VL(CO2) * 0.08 = 595 scf/ton

Therefore, the Extended Langmuir Equation for this given coal sample is:

$$V = 595 \frac{P}{P + 565}$$
6.2

6.2.4 Deviation related to the Extended Langmuir Equation

The Langmuir Equation is a powerful tool to estimate gas contents on a dry, ash free basis under a given reservoir pressure. With the knowledge of gas content on a dry ash free basis the in-situ gas content can be calculated by its ash content. Therefore, the Extended Langmuir Equation has been widely known as the "indirect method" of calculating gas contents.

However, through the comparison between the gas content predicted by the Langmuir Equation and the desorbed gas contents measured on 3 core holes, this study observed that the desorbed gas contents deviate from the prediction of the Langmuir Equation as ash content increases. This observation indicates that the increased ash content can compromise the validity of the Extended Langmuir Equation regarding its prediction for gas contents.

As depicted in Figure 6-7 through Figure 6-9, the deviation starts at an ash content of approximately 30 percent. As the ash content increases, the desorbed gas content decreases proportionally, and the deviation becomes more pronounced. When the ash content exceeds 66 percent, corresponding to carbonaceous shale, that deviation reaches its zenith.

There can be some disagreement about the mechanisms behind this observed deviation. It might be the result of incomplete gas desorption from high ash coals, or the high ash content and the substantially reduced permeability prevent complete gas desorption.

No matter what reasons and mechanisms are behind this deviation, this observation indicates that increased ash content proportionally decreases the expected gas

contents under reservoir conditions. Therefore, when the Extended Langmuir Equation is used to predict the gas content of lower quality coals, a significant amount of inaccuracy may be introduced. According to the testing results in the three core holes, a deviation of approximately 50 percent was observed.
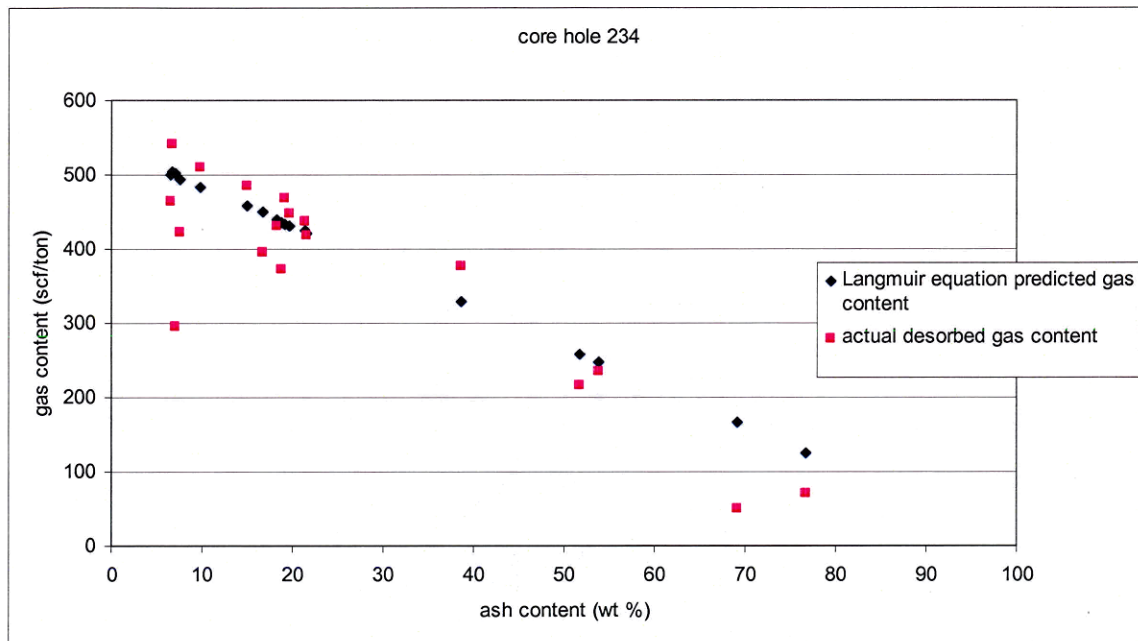
Figure 6-7   Langmuir Equation predicted gas content vs. actual gas content
in core hole 234
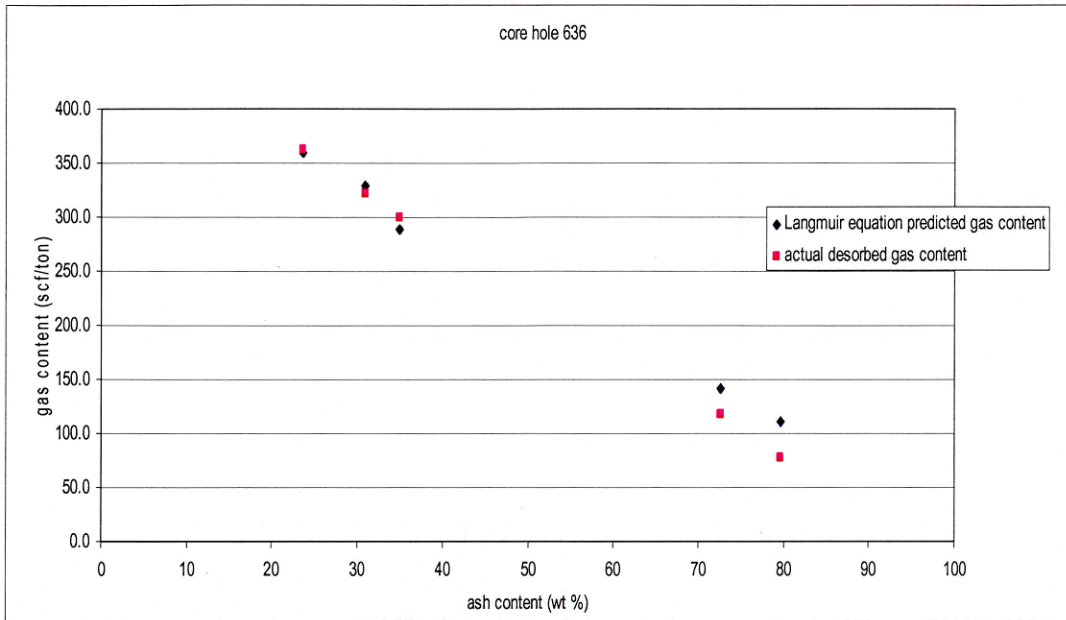
Figure 6-8   Langmuir Equation predicted gas content vs. actual gas content
in core hole 636
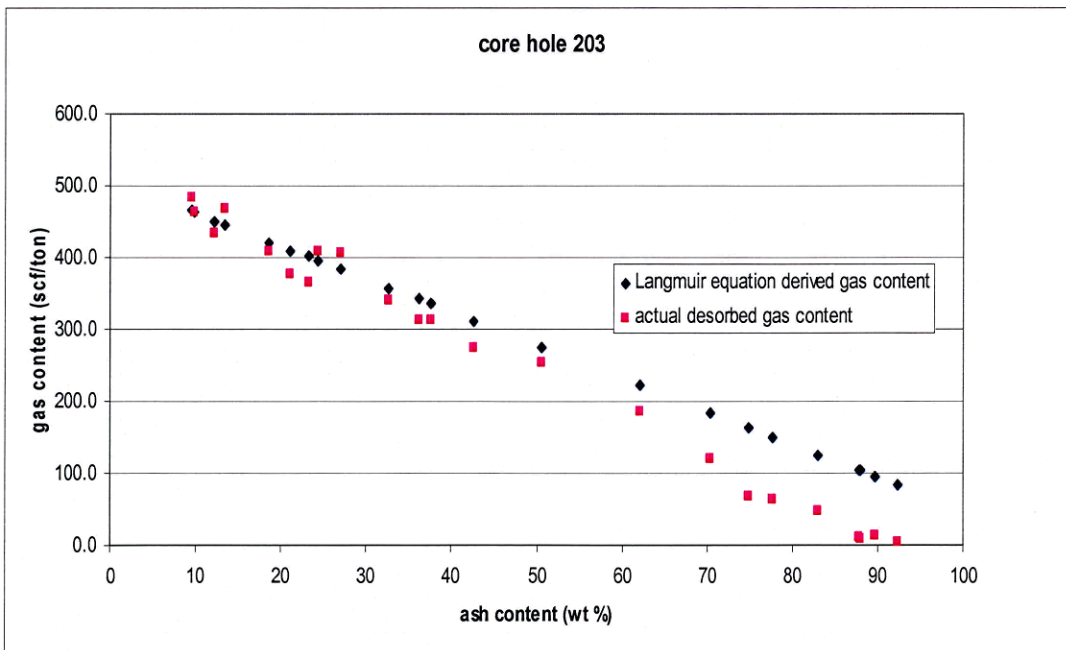
Figure 6-9   Langmuir Equation predicted gas content vs. actual gas content
in core hole 203

6.3 Gas content calculation

This section addresses the gas content calculation method which was incorporated into the new CBM computer model. For this purpose, there are two widely used methods: the direct method and the indirect method. The direct method is established on the basis of gas desorption characteristics, while the indirect method is determined by gas adsorption behavior. Usually, one of these two methods is selected depending on the particular project situations. The investigation into these two methods has revealed that simple application of these methods can result in significant inaccuracies in gas content calculations. In response, this research has devised a new method based on the direct method, which can more accurately compute the gas contents.

6.3.1   The direct method

Since useful core holes have been drilled at DWU before and during this research, and a large number of coal samples have been tested for gas content measurements, the direct method using the gas desorption tests have been used. To apply this method to estimate the gas content of a given coal bed, the field-wide average gas content for a particular type of coal lithology was utilized as the representative gas content of this given type of lithology. For example, if a coal interval was determined to be clean coal, the representative clean coal gas content was applied to this coal interval. The investigation into the gas desorption characteristics on a large number of coal samples reveals that this method can result in significant errors.

Figure 6-19 displays the relationship between the desorbed gas content and the corresponding ash content of all the coal samples retrieved from 7 core holes. Generally speaking, the desorbed gas content is inversely proportional to the corresponding ash content, that is, desorbed gas content decreases as ash content increases. However, the correlation between desorbed gas content and ash content for quality coals (ash content less than 50 percent) is not strong enough to be used for gas content calculating purposes. In other words, for coals possessing the same ash content, their desorbed gas contents are

not the same, or even close. For example, for clean coals concentrated on the left end of the horizontal coordinate, the desorbed gas content varies from less than 250 scf/ton to more than 800 scf/ton. If the averaged gas content is applied to represent the rest of the gas content, significant errors are introduced.
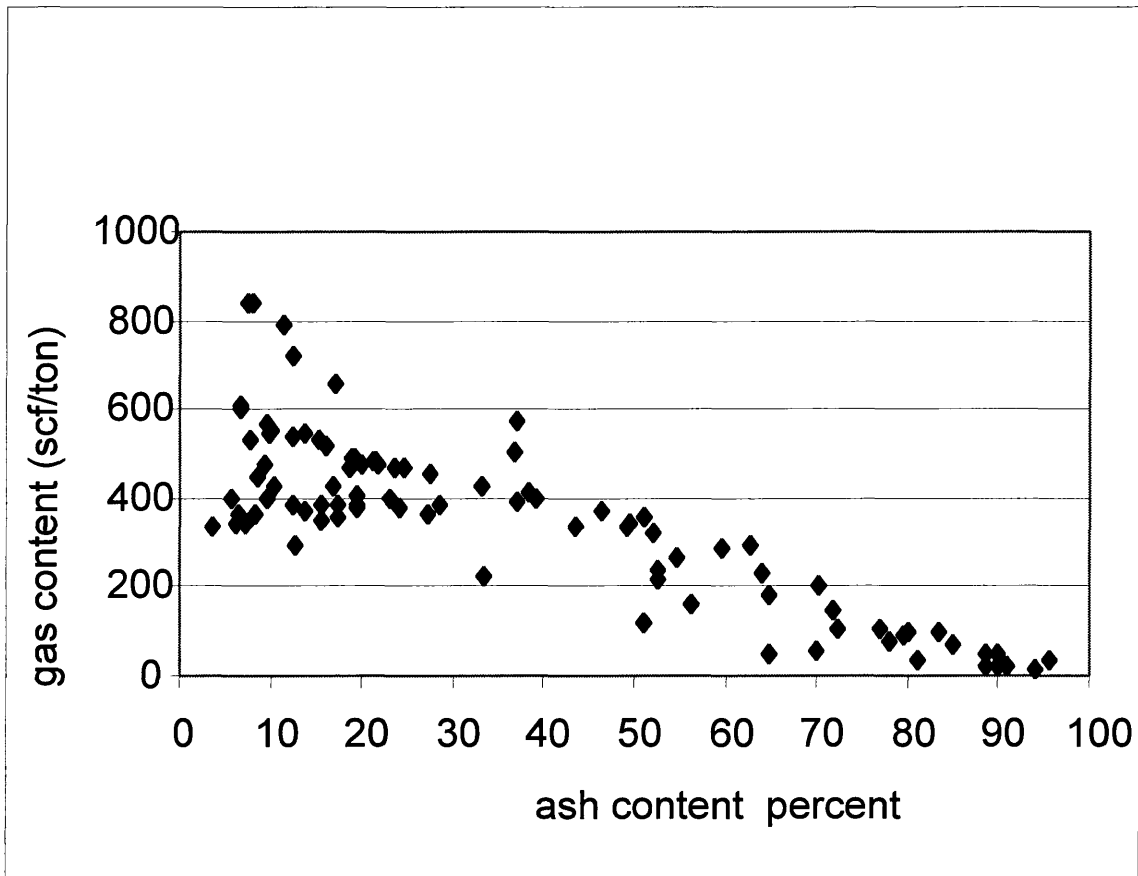
Figure 6-10 Desorbed gas content vs. ash content

6.3.2 The indirect method

The indirect method entails the establishment of the representative Extended Langmuir Equation, which is the averaged result of all the individual Langmuir

Equations obtained from each coal sample. Analogous to the direct method, the applicability of the representative Extended Langmuir Equation depends on the deviations between the representative Extended Langmuir Equation and individual Langmuir Equations. In other words, if the individual Langmuir Equations share the same Langmuir coefficients, the representative Extended Langmuir Equation would be reliable. Otherwise, the representative Extended Langmuir Equation would lead to significant errors in gas content calculations.

According to the discussion in Section 6-2, the individual Extended Langmuir Equation is determined by the gas adsorption characteristics of a given coal sample. Therefore, only gases with similar gas adsorption behavior can yield similar Extended Langmuir Equations. As indicated in Figure 6-11, which features the gas adsorption behaviors of the coal samples from different core holes, the adsorption characteristics of these core holes are not uniform. For example, at a pressure of 1000 psia (typical reservoir pressure at DWU), adsorbed gas content in core hole 149 is 460 scf/ton, while the adsorbed gas content in core hole 203 is 800 scf/ton. The substantial differences in adsorbed gas contents among core samples do not support the establishment of the representative Extended Langmuir Equation.
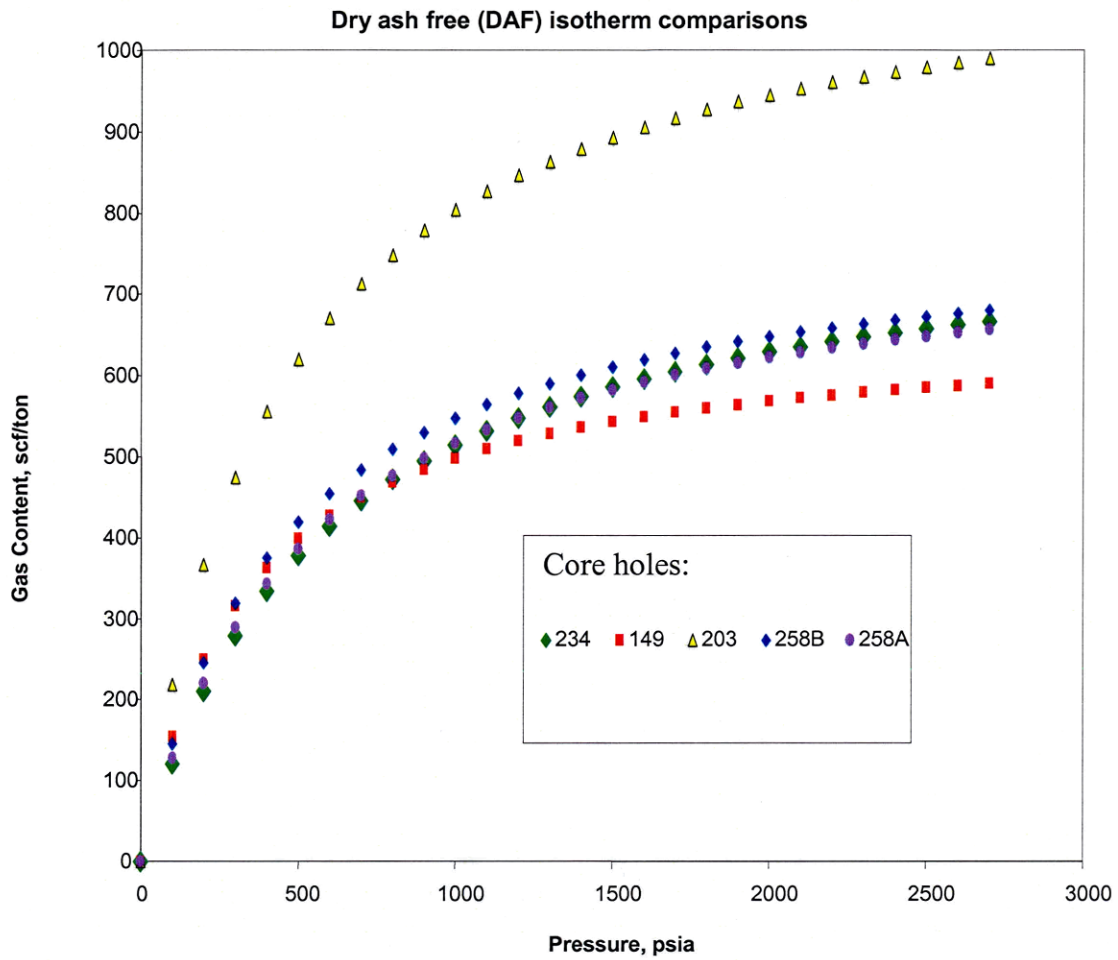
Figure 6-11   Adsorbed gas content vs. pressure

6.3.3   The new method

A new method has been devised on the basis of two factors. First, this study has observed that for a given core hole the desorbed gas content is strongly correlated with the corresponding ash content. Second, at the time this study was completed, 23 core holes had been drilled throughout the CBM unit.

As indicated in Figure 6-12 through Figure 6-18, the desorbed gas content can be closely correlated with the corresponding ash content. This strong correlation between gas content and ash content in individual core holes is substantiated by the high regression coefficients, which vary from 0.83 to 0.99. This observation suggests that, for a given CBM well, the ash content can accurately reflect the corresponding gas content.

Based on the observations discussed above, the new method for calculating gas content has been established, which consists of the following steps:

- Obtain a representative ash content of clean coals
- Define the clean coal gas content of each core hole
- Generate a contour map of gas content based on the existing core hole data
- From the gas content contour map, assign each well location a clean coal gas content
- Calculate the gas content vertical distribution for each coal zone in each well
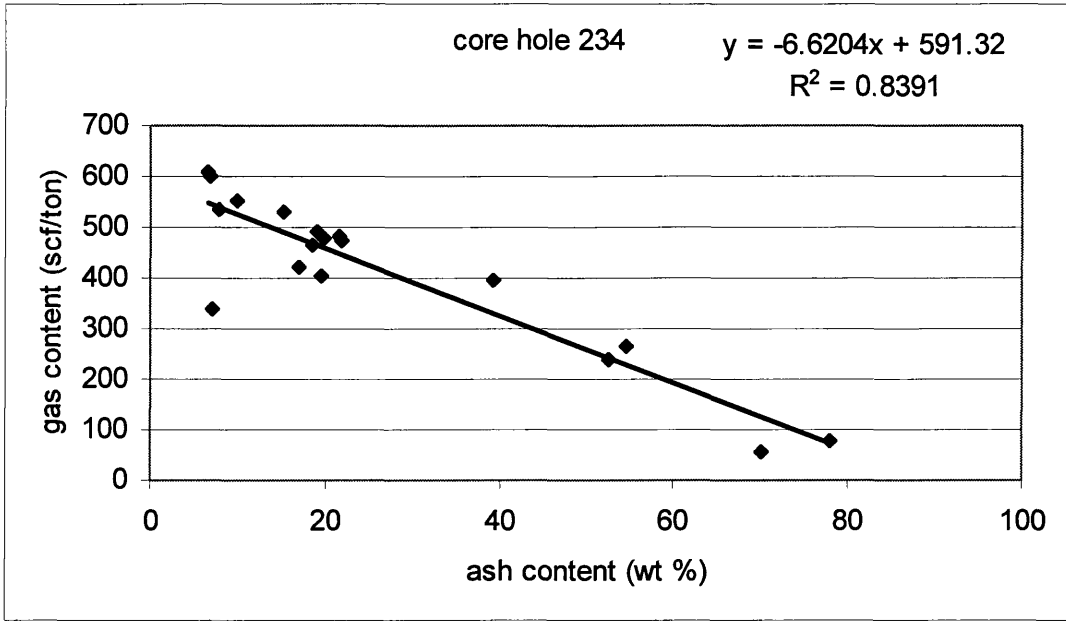
Figure 6-12 Desorbed gas content vs. ash content in core hole 234
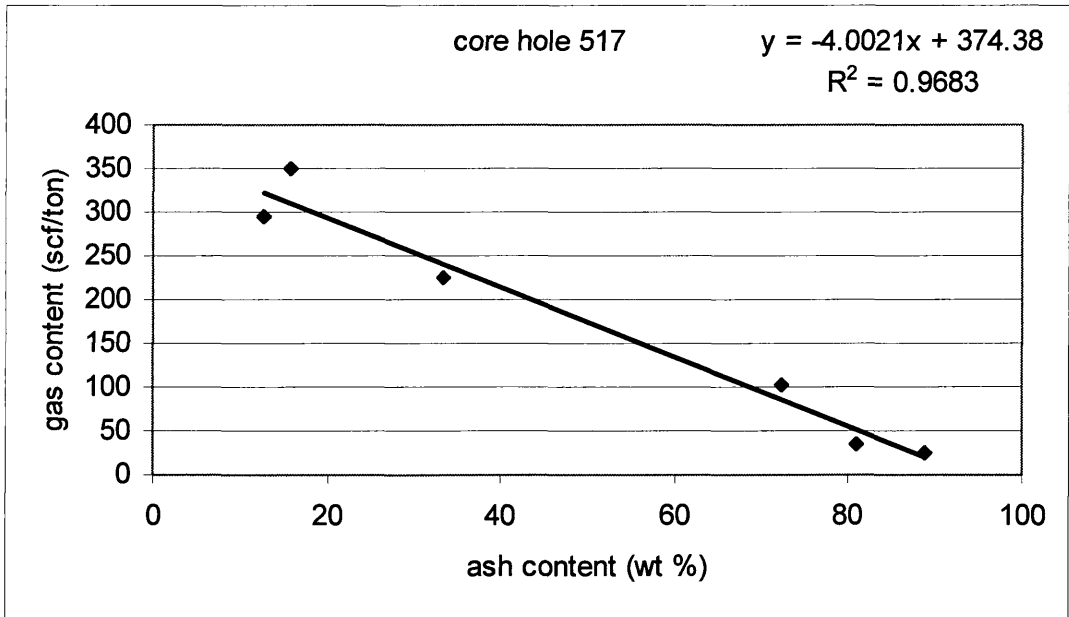
Figure 6-13 Desorbed gas content vs. ash content in core hole 517

101
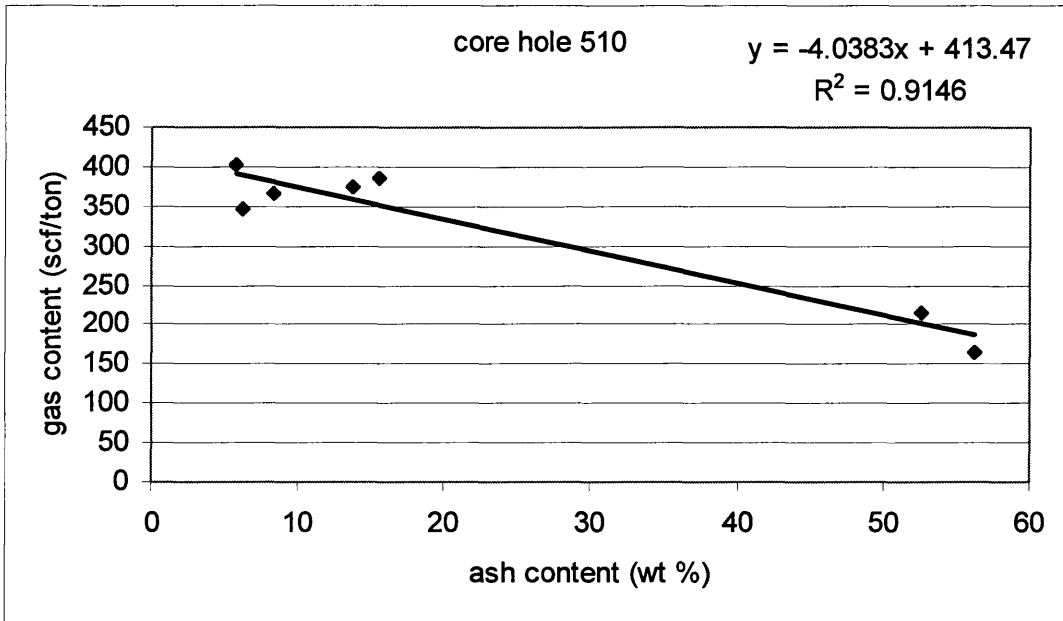
Figure 6-14   Desorbed gas content vs. ash content in core hole 510
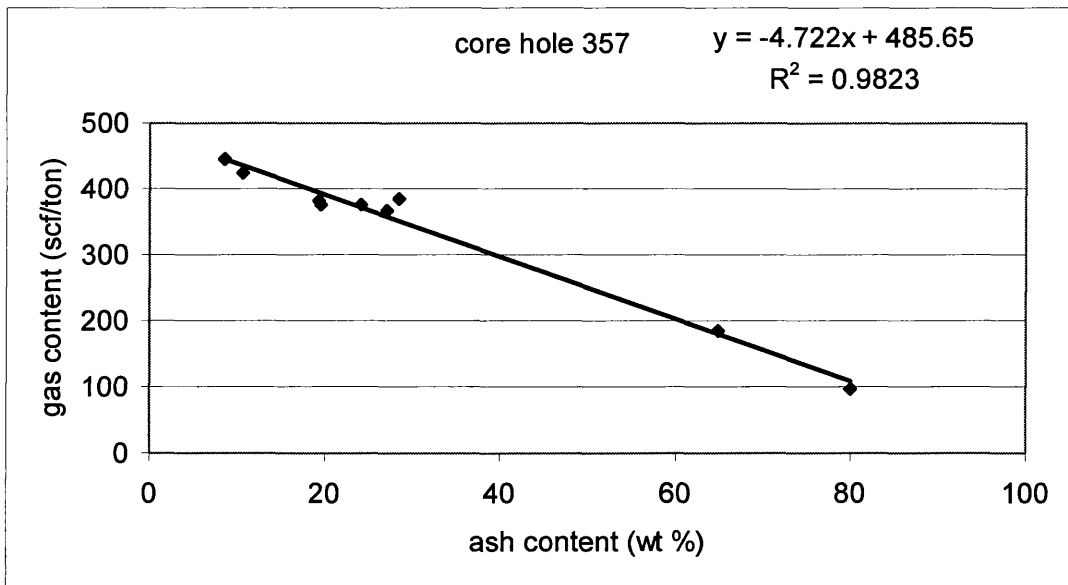
Figure 6-15   Desorbed gas content vs. ash content in core hole 357
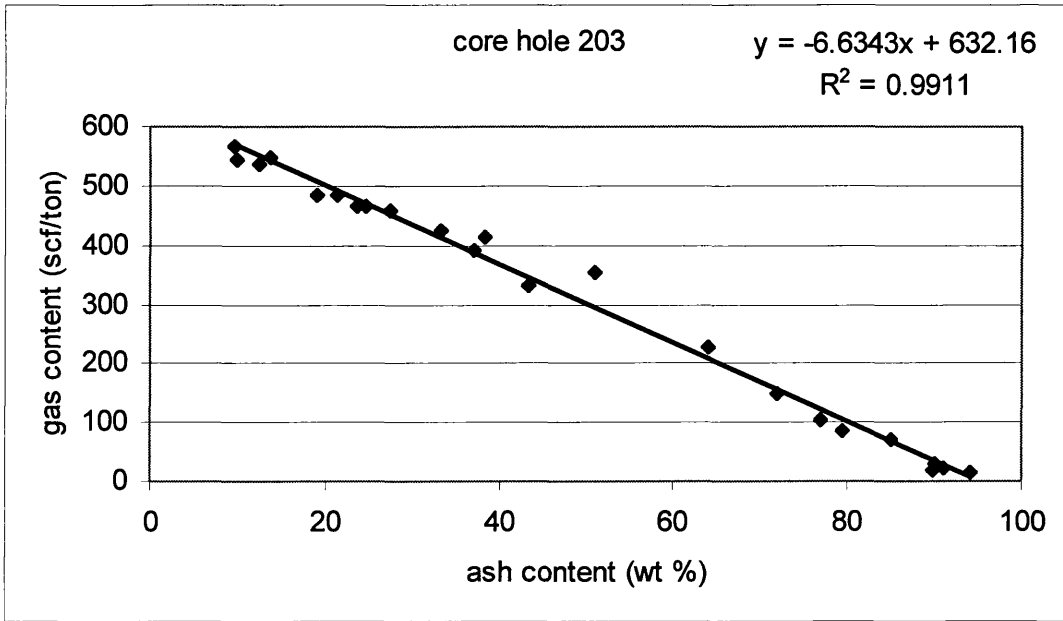
Figure 6-16   Desorbed gas content vs. ash content in core hole 203
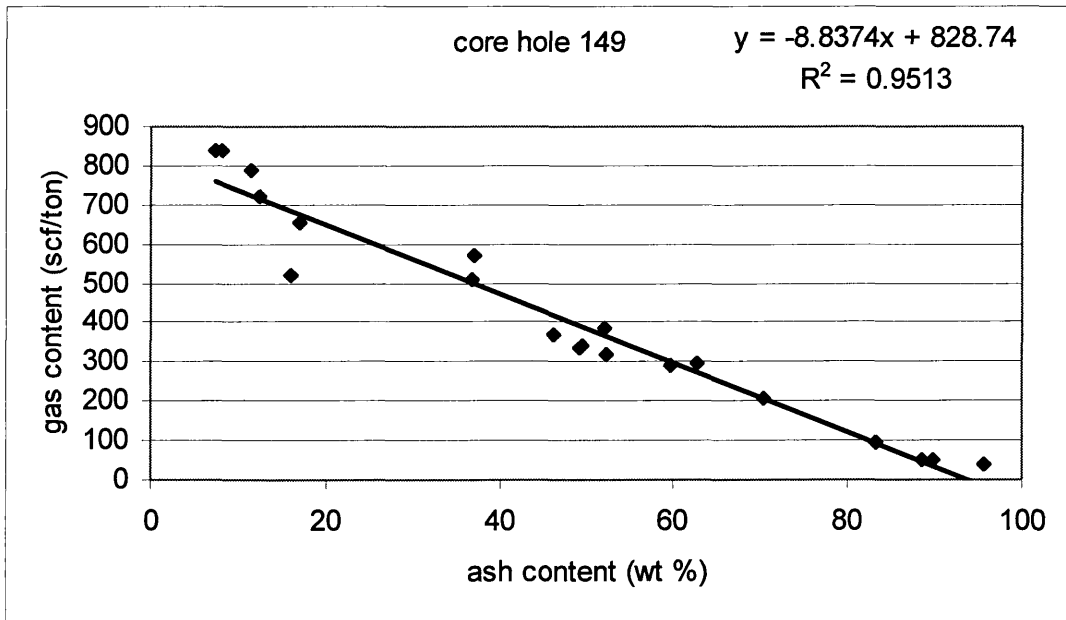
Figure 6-17   Desorbed gas content vs. ash content in core hole 149

103
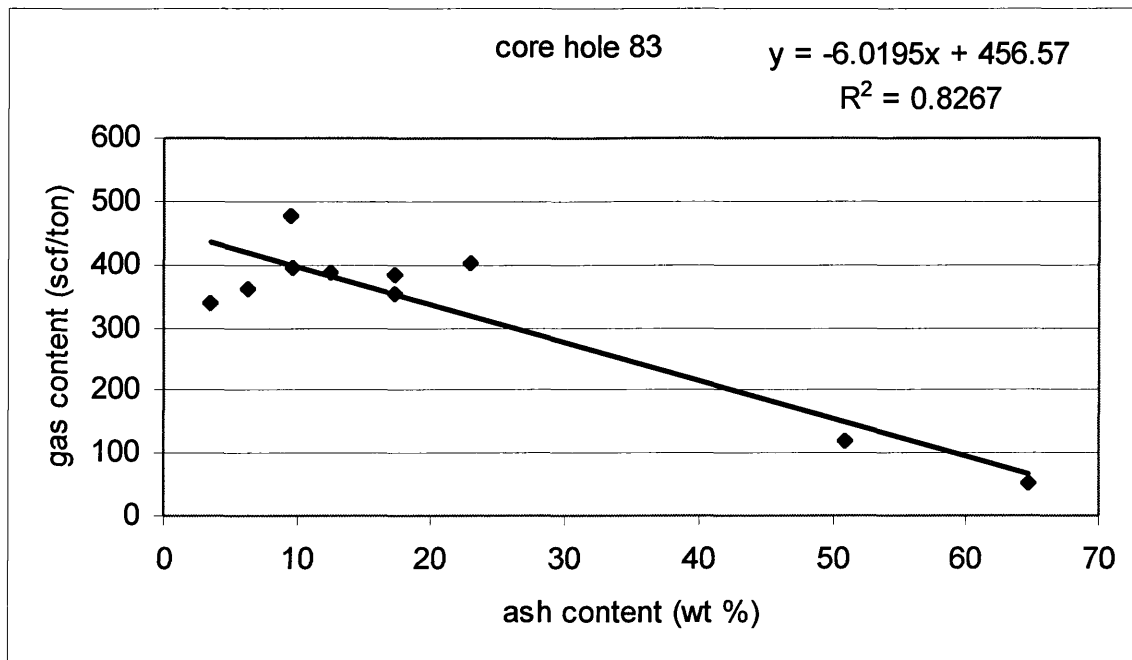
Figure 6-18 Desorbed gas content vs. ash content in core hole 83

Procedures for calculating the gas content distribution in each well:

Step 1: Obtain a representative ash content of clean coals

As displayed in Figure 6-19, the existing clean coal samples exhibit an ash content variation from 6 percent to 35 percent. The averaged ash content is 16 percent. This averaged ash content is defined as the reference ash content, to which the ash content of a given coal interval will be compared for the gas content calculation.

Step 2: Define the clean coal gas content of each core hole

The clean coal ash content of each core hole was calculated by averaging the gas contents of all the clean coal samples.

104

Step 3: Generate a contour map of gas content (Figure 6-20) based on the existing core hole data.

The gas content contour map was generated on the basis of gas content data from 23 core holes.

Step 4: From the gas content contour map, assign each well location a clean coal gas content.

The gas content contoured map assigns a gas content for each well location for the clean coal with the reference ash content.

Step 5: Calculate the gas content vertical distribution for each coal zone in each well.

The computer model automatically selects the assigned clean coal gas content to a given well and calculates the gas content based on the ash content of a given coal interval. Figure 6-21 displays the new CBM computer model generated gas content curves (in-situ gas content) in one example well.
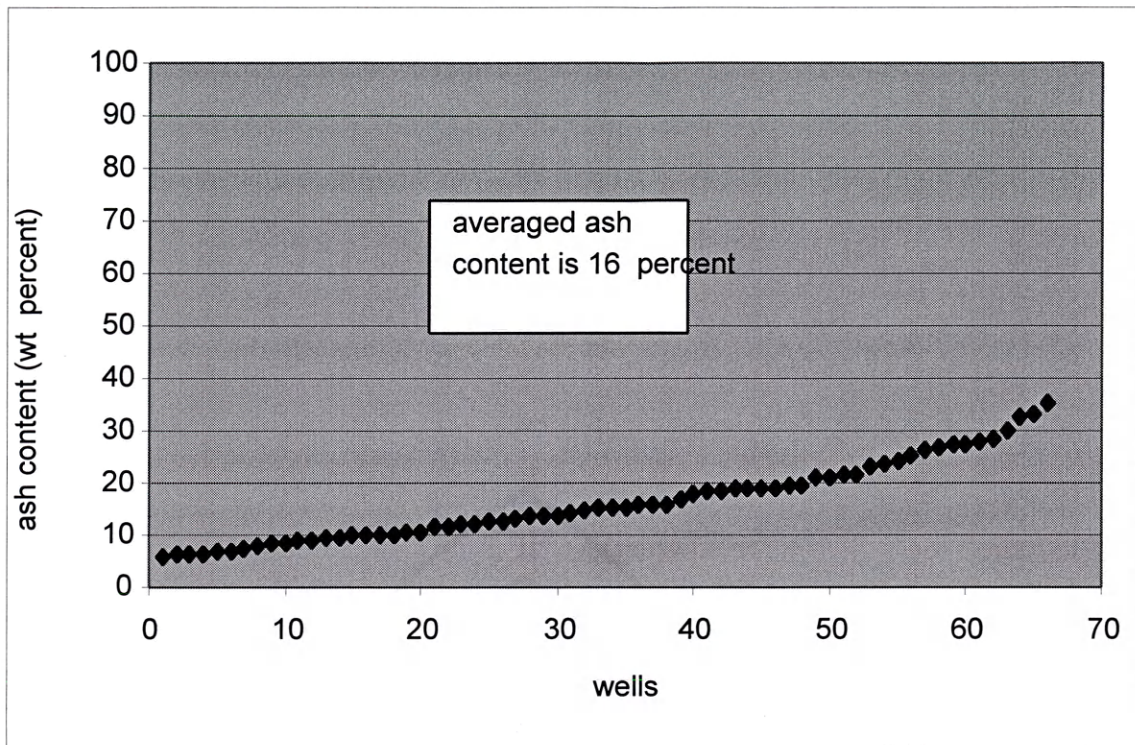
Figure 6-19: Ash content distribution in clean coal samples
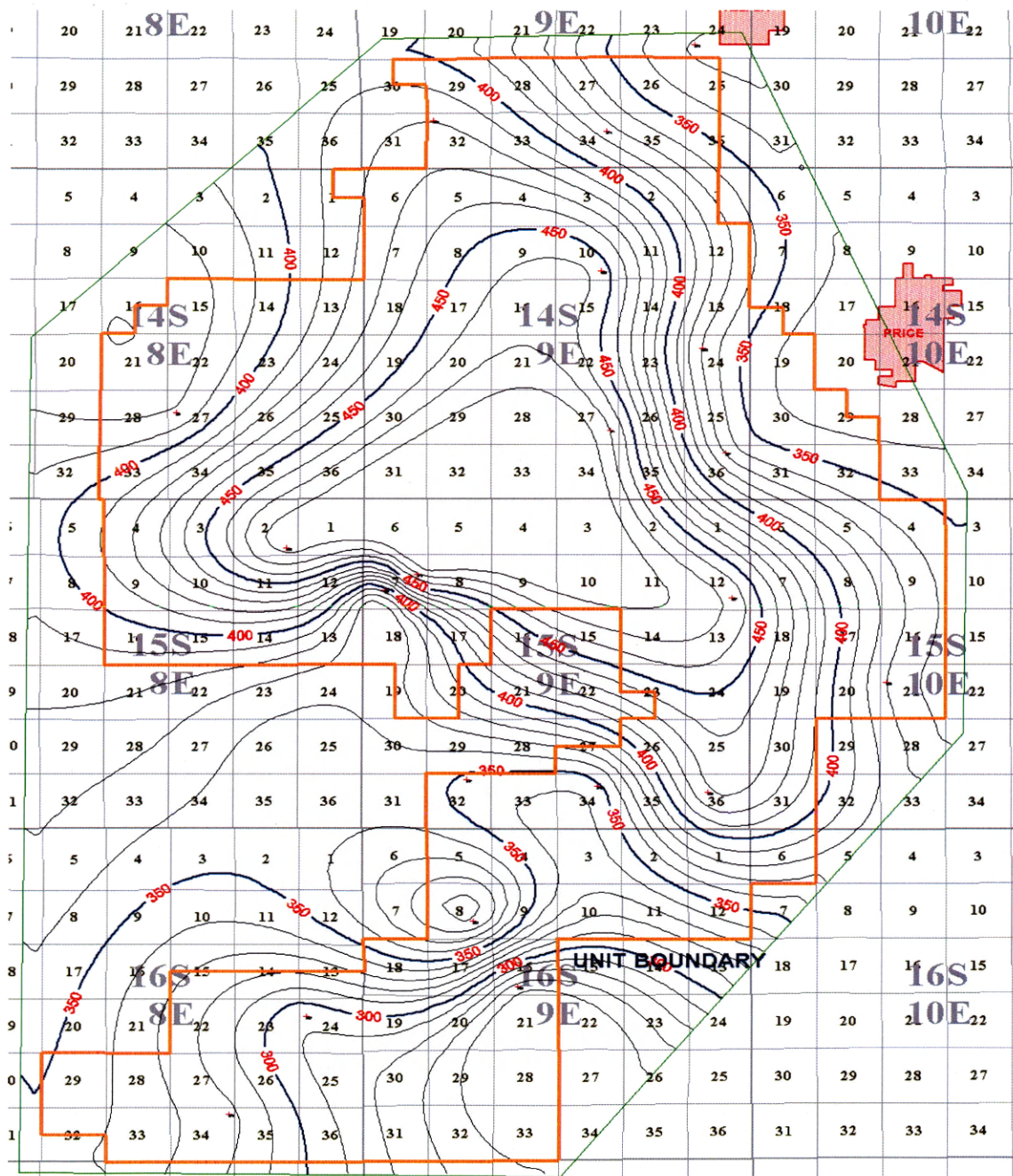
Figure 6-20: Gas content contour based on the existing 23 core holes. The units of the gas content contour lines which are labeled by the numerical number in red are scf/ton.
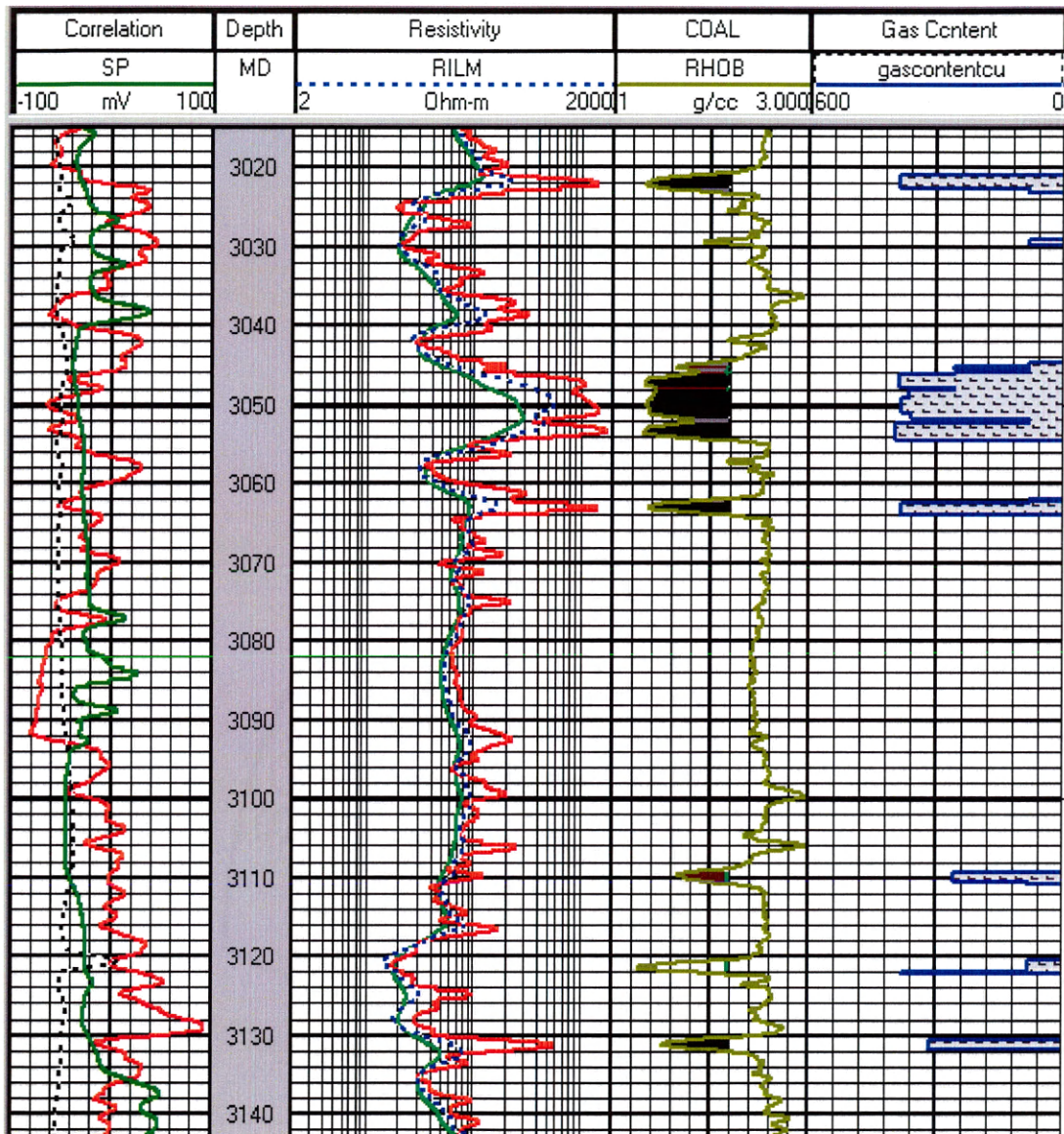
Figure 6-21   Gas content vertical distribution example. The unit of the gas content curve is scf/ton.

CHAPTER 7

MODEL CONSTRUCTION

This chapter presents four major programming tasks required for the construction of the new CBM computer model: 1) input curves management, 2) coal lithology identification, 3) gas-in-place calculation, and 4) representative petrophysical properties and coal bed specifications.

7.1 Input curves management

This part of the model specifies the input curves and processes individual curves for the purpose of coal lithology identificaion.

7.1.1 Input curves

The input curve set comprises bulk density, gamma ray, resistivity, and caliper. During a decade span of exploration and development at DWU, a large amount of log data has been recorded from more than 460 wells. Even though the log parameters measured in all the wells can be classified into four major categories (bulk density, gamma ray, resistivity, and caliper), different logging companies have adopted different curve names (mnemonic names). Therefore, in order to make the model more capable of accommodating all the existing log curves, all the possible log curve names have to be specified.

Log parameter	Mnemonic (curve name)
Gamma ray	GR, GR-MAIN, EHGR, HGR
Bulk density	RHOB, RHOB-MAIN, RHOZ, RHO8
Resistivity	DEEP-RT, SHALLOW-RT, AHT10, AO10, SGRD, RILL3, DFL, RHOZ, ROX8
Caliper	CALI, DCAL, HCAL, CALIPER

Table 7-1:   Input curves

7.1.2   Individual curve processing

The individual curve processing entails such work as curve normalization, curve correction for thin bed effect, and boundary resistivity calculation. By doing so, the input curves are made acceptable for coal identification purposes.

7.1.2.1 Bulk density

(1) Select the high resolution curve

In most cases, both the high resolution curve and the normal resolution curve are input into the model. To achieve more accuracy, a function is programmed to pick the high resolution curve.

(2) Correct bulk density for thin-bed effect

Functions are programmed to measure the thickness of each coal seam. Then the empirical equation is used to correct the thin-bed effects.

(3) Reconstruct the bulk density curve

All the log data are recorded as a curve because of the combined effects of both the tool's resolution and changes of lithologies. However, the true densities of coals are relatively distinctive and constant for most of the intervals. Therefore, a rectangular

curve is a better reflection of the true bulk density. Functions are programmed to convert the existing wiggling curves into rectangular curves.

7.1.2.2 Resistivity curves

(1) Calculate the array of "boundary resistivity"

An array of "boundary resistivity" was generated by the shallow resistivity curve to identify the thin bed carbonaceous shale interbed within thick coal seams. Functions are programmed to pick each local minimum and maximum value, and use the following empirical equation to calculate the "boundary resistivity." This array of "boundary resistivity" is used to define the boundaries between coals and carbonaceous shales (as well as non-coal formations).

$$R(boundary) = 1.8 \frac{R\max + R\min}{R\max\, R\min} \qquad\qquad 7.1$$

Where:

R(boundary) = the resistivity log at the boundary between the coal and non-coal formation

Rmax = the maximum resistivity log

Rmin = the minimum resistivity log

(3) Calculate the average clean coal resistivity

Functions were programmed to pick the thickest coal seam and average its shallow resistivity. This value represents the shallow resistivity of clean coal in any given well.

7.1.2.3 Gamma ray

(1) Identify the negative deflections

Functions are programmed to identify the local minimums and maximums. Then, the negative deflections are determined as the signal of coal quality improving, and the middle points between the minimums and maximums are used to define the boundary between strata.

(2) Normalization

Gamma ray logs cover a large aerial extent. Therefore, gamma ray log shift is inevitable. To perform a gamma ray normalization, part of the wide spread and stable marine shale on top of the Ferron is selected as the reference strata. The following formula is employed for the gamma ray normalization purpose.

GR(normalized) = GR(log) – GR (log at shale) + GR (reference)   7.2

Where:

GR(normalized) = the normalized GR log

GR (log) = GR log readings

GR (log at shale) = the GR log at the reference shale

GR (reference) = the reference GR log

7.1.2.4 Caliper

(1) Calculate washout

To calculate the amount of washout, a competent sand formation near the bottom of the well is selected as the reference, where the regular bore hole diameter is very close to the bit size.

7.2 Coal lithology identification

This part of the model uses the new log cutoff system to classify the coal lithologies.

Step 1. Verify the available input curves

A complete input curve set includes bulk density, gamma ray, shallow resistivity, deep resistivity, and caliper. Some of the wells had fewer input curves than a complete set. In these cases, adjusted log cutoff systems are selected accordingly.

Step 2. Program the log cutoff system to classify coal lithologies (grades)

According to the availability of input curves, as well as the log environments determined by the washout and coal thickness, the appropriate log cutoff system was selected to classify the coal lithologies (grades).

7.3 Gas-in-place calculation

The programming task for this part of the model consists of ash content determination, gas content calculation, and gas-in-place computation.

7.3.1 Calculate the ash contents

Step 1. Verify the amount of washouts

Step 2. Calculate the ash content using the corrected bulk density log if the bore hole is regular (washout is less than 1.5 inches)

Step 3. Determine the ash content if the wellbore is irregular (washout is larger than 1.5 inches)

113

In these cases, the average ash contents are assigned to each classified coal lithologies.

     Clean coal: 18 percent

     HGC: 43 percent

     Ashy coal: 58 percent

     Carbonaceous shale: 71 percent

7.3.2   Gas content

Step 1. Obtain the clean coal gas content from the field-wide contour map of clean coal gas content

Step 2.   Calculate the gas contents according to the ash content

7.3.3   Original gas-in-place

Original gas-in-place (OGIP)

Step 1. The following equation was programmed to calculate the gas-in-place using the gas content, coal thickness, and drainage area of 160 acres

$$OGIP = 1800 \times H(coal) \times A \times GC \hspace{3cm} 7.3$$

Where:

    OGIP = original gas-in-place, SCF

    GC = gas content, scf/ton

    $H(coal)$ = coal thickness, feet

    A = the drainage area, acres

    1800 = constant, standard cubic feet per ton

Step 2. The gas-in-place of each coal seam is summed to arrive at the total gas-in-place for a given well

7.4 Representative petrophysical properties and coal bed specifications

To calculate the representative petrophysical parameters of a given well, the thickest clean coal bed is selected by the model. Subsequently, the representative values of each log parameter for these clean coal seams are calculated. The petrophysical parameters include bulk density, GR, shallow resistivity, middle resistivity, and deep resistivity.

This part of the model also calculates the specific details of each individual coal bed, such as the thickness, burial depth, coal grade, gas content, and gas-in-place.

CHAPTER 8

APPLICATIONS OF THE NEW CBM COMPUTER MODEL

The new CBM computer model has been accepted by the operator as a working tool to evaluate the CBM reservoirs at DWU for individual wells and for field-wide applications. This chapter discusses the modeling results of 460 CBM wells and a field-wide CBM reservoir evaluation conducted on the basis of the new modeling results.

8.1 Modeling results

The modeling results of 460 CBM wells can be displayed in three formats: numerical, graphical, and field-wide mapping.

8.1.1 Numerical outputs

The outputs are classified into three categories: coal lithologies, CBM reservoir properties, and coal stratigraphic configuration.

Coal lithologies:

- Individual clean coal seams and their thickness
- Individual HGC seams and their thickness
- Individual ashy coal seams and their thickness
- Individual carbonaceous shale seams and their thickness
- Individual bentonitic carbonaceous shale seams and their thickness
- Total clean coal seams and their thickness for each well
- Total HGC seams and their thickness
- Total ashy coal seams and their thickness
- Total carbonaceous shale seams and their thickness

- Total bentonitic carbonaceous shale seams and their thickness

CBM reservoir properties:

- Ash content vertical distribution
- Gas content vertical distribution
- Gas-in-place of individual coal seams
- Total gas-in-place of a given well
- Residual gas content of individual coal seams
- Maximum gas reserves of individual coal seams
- Total maximum gas reserves of a given well

Coal stratigraphic configuration:

- Total number of coal seams
- Composition of individual coal seams (percentage of different coals)
- Thickness of individual coal seams
- Burial depth of individual coal seams

8.1.2 Graphical outputs

As illustrated in the example graph, any output parameter of the modeling results can be depicted in a bitmap format (Figure 8-1).

8.1.3 Field-wide mapping

Any output parameter of the modeling results can be mapped on a field-wide basis (Figure 8-2). The example map portrays the total clean coal thickness distribution at DWU.
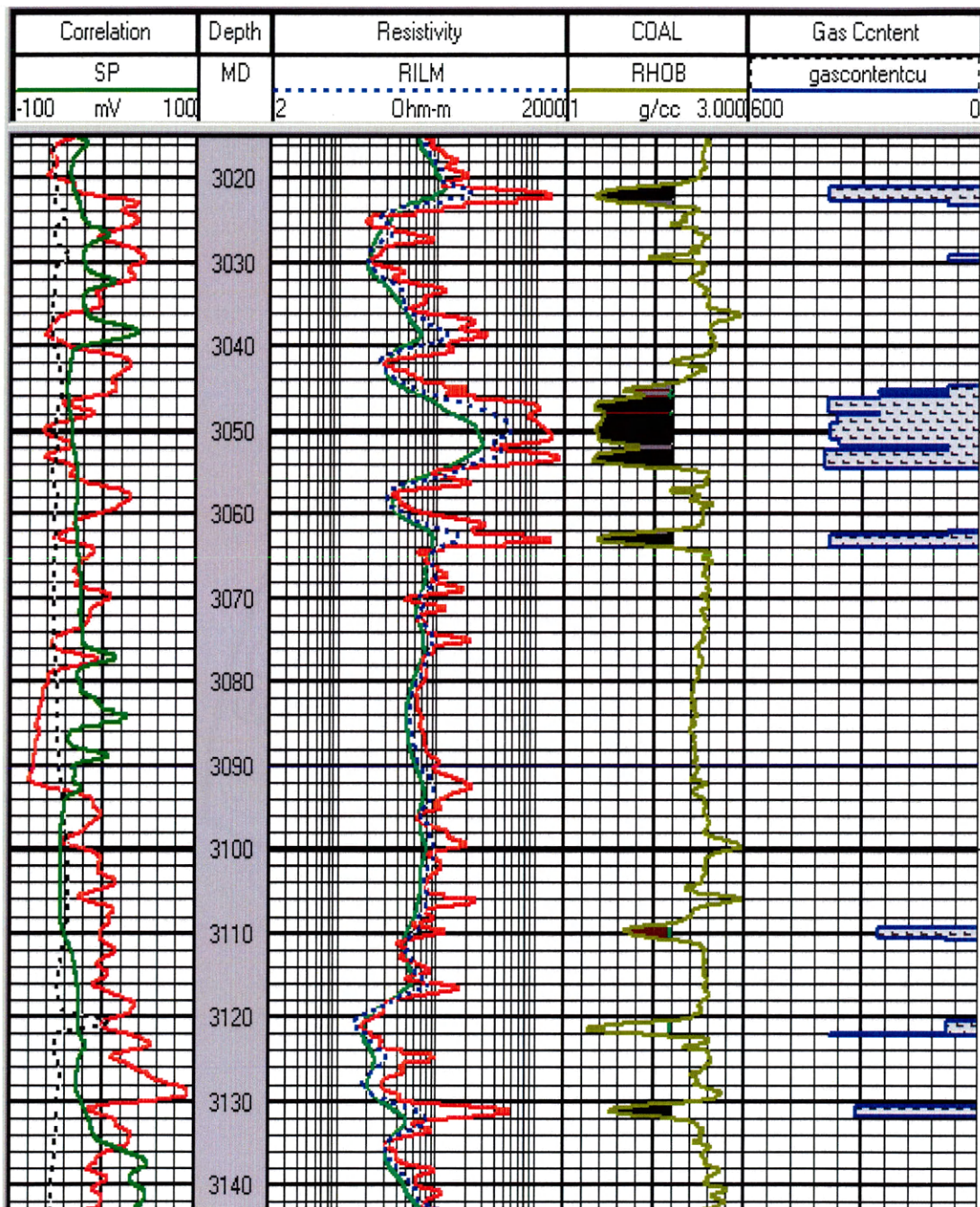
Figure 8-1 Model interpreted coal lithologies and gas contents. The units of the gas content curve on the far right-hand side are standard cubic feet per ton (scf/ton).

118
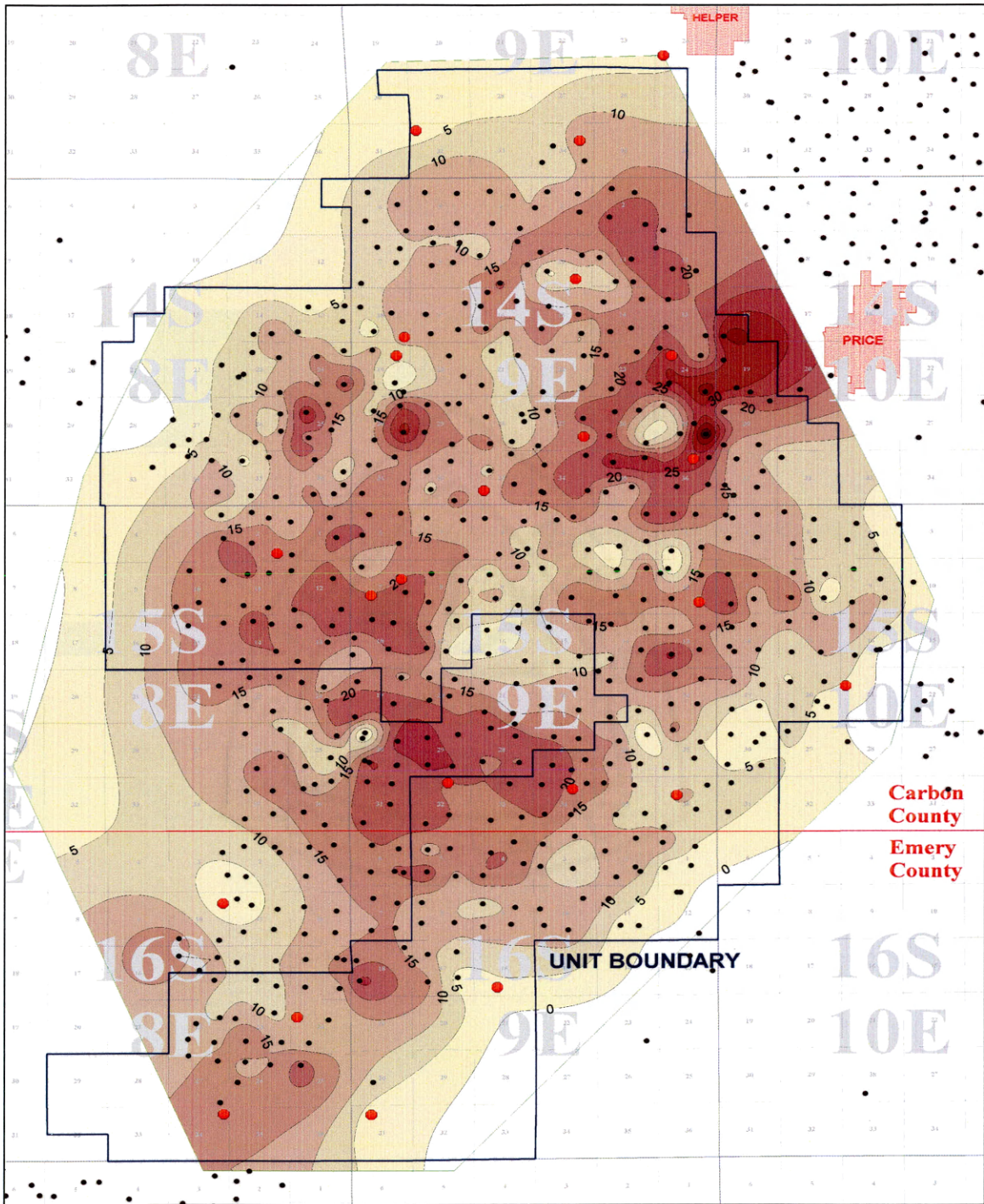
Figure 8-2   Clean coal distribution at DWU. The coal thickness is representd by the
numerical number and color, and the map is scaled in sections and townships.

8.2   The comparison between the new model and previous methods

Figure 8-3 and Figure 8-4 illustrate the lithology interpretions of the new model and that of the previous method for the same core hole. This example clearly shows that the new CBM model is able to accommodate such hostile log situations as thin-bed effects, enlarged wellbore, and high GR environment, while the old method yields significant inaccuracies.

Thin-bed effect:

Among the six major coal seams occurring in this well (core hole), there are two thin coals present at 3021 feet and 3131 feet, respectively. According to the proximate analysis results, these two coal seams are clean coals. When the new model was used to process the log data, the model checked the coal thickness and performed the density correction for thin-bed effects. As a result, these two coal beds were interpreted as clean coal that is colored in black by the new model, whereas the old method interpreted them as high gamma ray coal (HGC).

Enlarged wellbore effect:

According to the core description, there is a streak of bentonitic carbonaceous shale at 3121 feet, which is brown colored. The new model checked the wellbore size and determined the enlarged wellbore. Subsequently, the new model consulted the resistivity log and identified it as a bentonitic carbonaceous shale. In this case, because of the enlarged wellbore effect, the bulk density log was reduced to the level of clean coal. As a result, the old method incorrectly interpreted it as clean coal.

High GR influence:

Within the thick coal bed between 3046 feet and 3054 feet, a thin HGC is interbeded between clean coals. Because of the high GR of ash, the surrounding clean coals were mistakenly interpreted as HGC by the old method.

To compare the applicabilities of the new model and the old method, two major comparisons have been performed. The first one involves five representative coreholes, and the second one exhibits the effects of enlarged wellbores. Table 8-1 lists the coal lithologies interpreted by different methods in the coreholes, and Figure 8-3 depicts that in severely enlarged wellbores the new model is capable of yielding reliable interpretations.

As indicated in Table 8-1, both the clean coal and HGC evaluated by the new model are consistent with the core description with respect to the thickness and the coal lithologies, while the old method consistently overestimates HGC and underestimates clean coal. This discrepancy is the result of the incorrect GR cutoff associated with the old method. As pointed out in Chapter 4, the correct GR level of the ash within Ferron coal is signicantly higher than what was previously perceived and accepted by the old method.

This table also displays that the new model is capable of evaluating ashy coal and bentonitic CSH, while the old method was not able to do so. This difference is the result of the investigation into the logging responses in CBM reservoirs at DWU. The unique logging features assocated with ashy coal and bentonitic CSH lie in the effects of ash content on the coal matrix conductivity.

Corehole #	Clean coal			HGC			Ashy coal			CSH			Bentonitic CSH		
	core	new	old	core	new	old	core	new	old	core	new	old	core	new	old
510	11.5	11.2	7.2	1.7	1.4	7.1	0.0	0.0	n/a	3.5	3.1	2.4	3.1	2.7	n/a
517	6.4	7.1	3.9	2.1	0.8	3.1	0.0	0.8	n/a	1.5	4.0	0.6	0.0	0.0	n/a
561	11.6	11.8	5.9	2.0	2.1	6.4	1.3	0.0	n/a	1.1	1.7	1.9	1.4	0.0	n/a
234	20.9	20.5	16.5	1.9	2.0	4.0	1.5	1.5	n/a	5.2	5.0	4.5	1.0	2.6	n/a
37	22.5	21.0	16.0	3.8	3.5	12.5	0.0	0.0	n/a	4.5	10.0	0.0	0.0	0.0	n/a

Table 8-1   Interpreted coal lighologies in feet by the new and old method in core holes

As depicted in Figure 8-5, well A is a corehole and well B is the offset well which shares the same coal seams with well A. The core hole was drilled with a drilling mud and created a regular wellbore, while the offset well was drilled with air and a significantly enlarged wellbore was formed. Within the interval of 3058 feet to 3082 feet in well B, the wellbore was enlarged from the bit size of 8 inches to 13.6 inches. As a result, the bulk density log within this interval has been significantly altered from the true value. Based on the erroneous bulk density log, the old method interprets the entire interval as coal. Because the new model incorporated the resistivity parameter the low resistivity in the upper part prevents this part of the interval from being interpreted as coal, even though the bulk density log suggests so. As a result, the new model accuratedly distinguishes the coal at the bottom of the interval from the CSH occur at the top. Except for core holes, the majority of wells at DWU were drilled with air where significant enlarged wellbores have been observed. The new model uses the resistivity curve and is capable of accommodating this unfavorable logging condition.
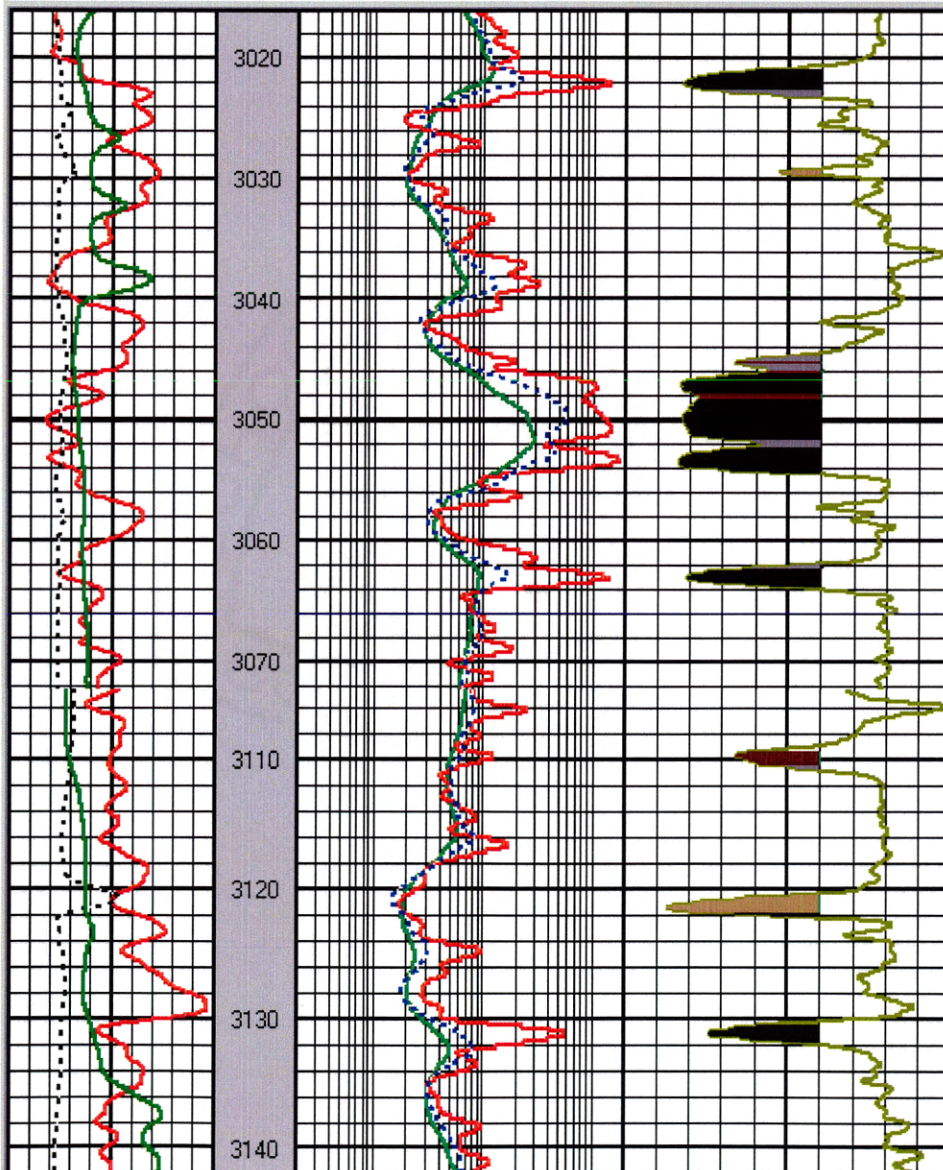
Figure 8-3:   The new model interpreted coal lithologies
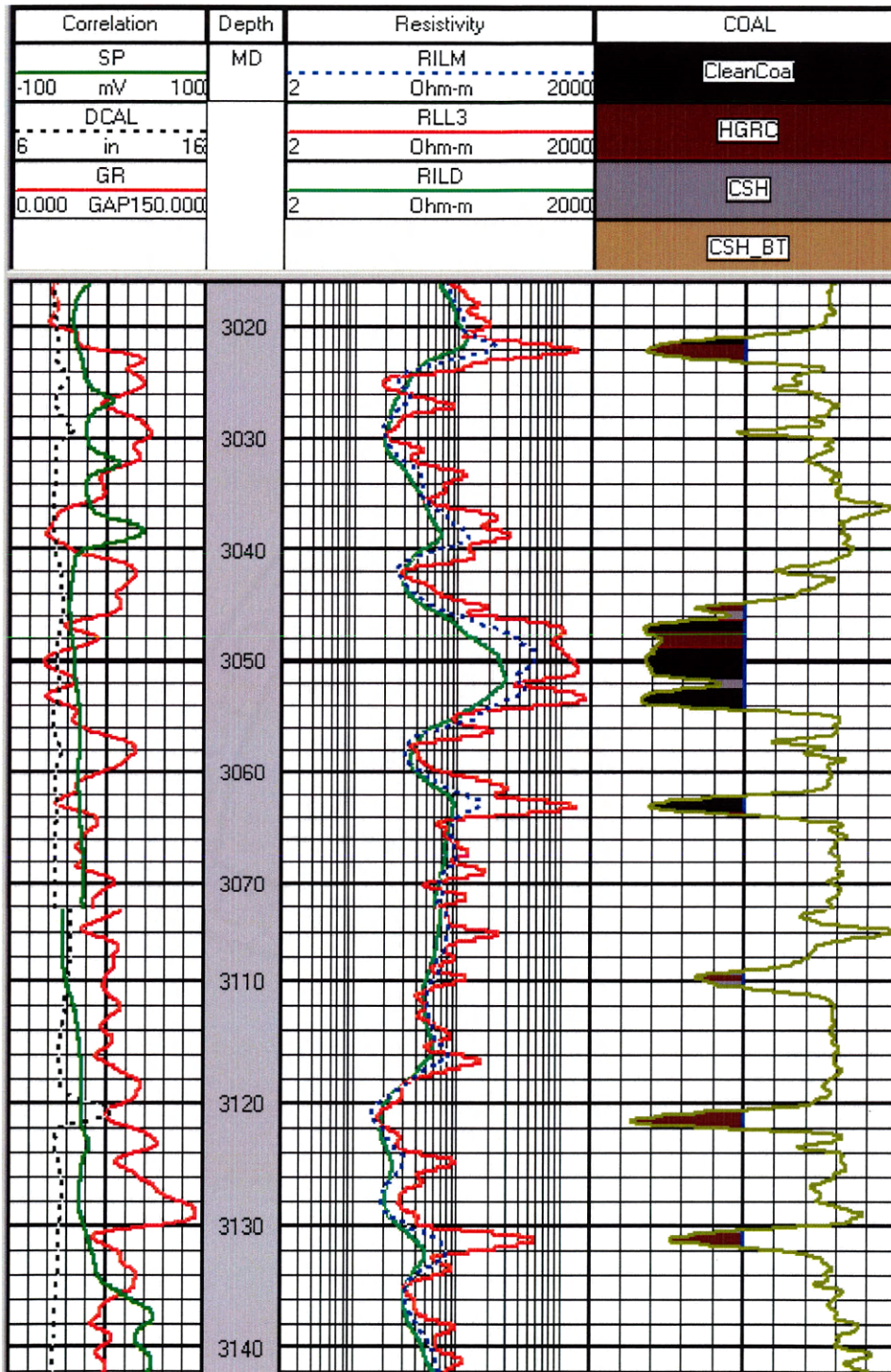
Figure 8-4: The previous method interpreted coal lithologies
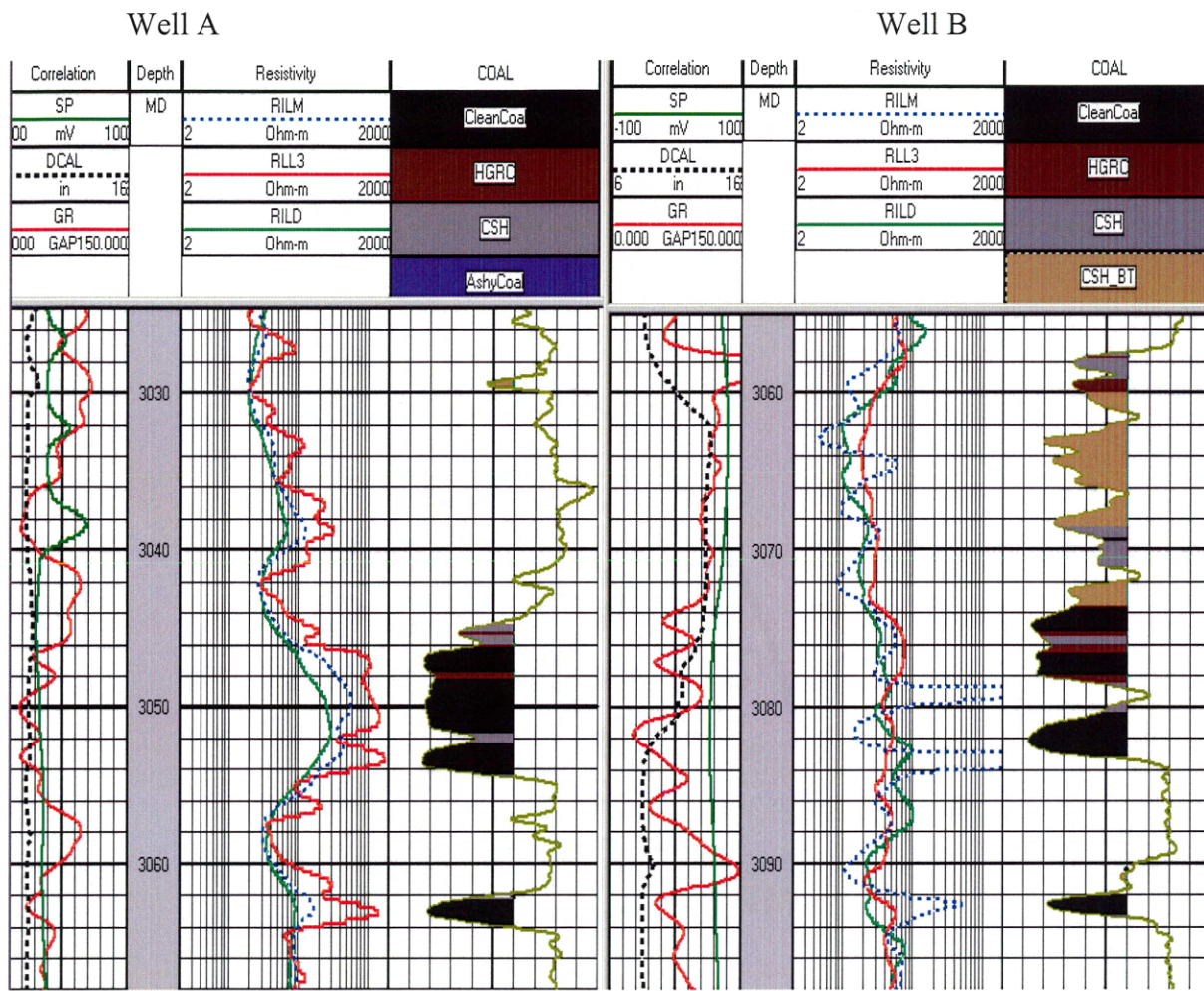
Figure 8-5   Application of the new model in enlarged wellbore

8.3 Applications

The new modeling technique and results have facilitated better individual well completion designs and field-wide CBM reservoir evaluation.

8.2.1 Applications in individual wells

After a well has been drilled and logged, the model provides sufficient information to facilitate the subsequent operational practices.

First, the casing design can be optimized by the modeling results. For example, the burial depth of the basal coal seam can justify the casing setting depth. This casing design may avoid unnecessary casing length that is usually determined by local commonly accepted operational practices.

Second, the perforating intervals can be better selected with the help of the new modeling results. For instance, the model predicts coal properties of a given coal bed (thickness, ash content, gas content, gas-in-place, and maximum gas reserves) better than the old method.

8.2.2 Applications in field-wide reservoir evaluations

Subsequent to the development of the new CBM computer model, the modeling results have been utilized to perform an intensive study into the parameters controlling well performances. The results of this investigation produced many new and significant observations with respect to gas production from coals, gas production from sands, water production behavior, remaining gas-in-place, and the producibility of the remaining gas-in-place. These new observations provided fundamental insights into better understanding of reservoir characterization, well performances, and optimal operational practices.

The results and observations of this evaluation for the operator helps answer four significant CBM questions: 1) what are the controlling factors of gas production from coals? 2) How much do gas-charged sands contribute to gas production? 3) Where does the water come from? 4) Where are the remaining gas reserves located and how can they

be produced? According to the agreement with the operator, this part of the research work is proprietary and belongs to the operator. Therefore, no more details can be released here.

CHAPTER 9

CONCLUSIONS AND RECOMMENDATIONS

As a result of this research, many new and significant observations have been made with respect to the coal lithology, petrophysical log responses in CBM reservoirs, and gas desorption/adsorption characteristics. These new observations have resulted in the development of a new CBM computer model and the enhancement of the reliability of a new model to interpret the reservoir properties in terms of coal lithology, coal thickness, gas content, and gas-in-place. This chapter provides conclusions made from this study and recommendations for future work.

9.1   Conclusions

(1)   There is a wider variety of coal lithologies present at DWU than originally perceived. As a result of this research, a new coal lithology system has been established to more adequately represent CBM reservoirs; furthermore, for the first time, each coal lithology has been quantitatively defined by two representative parameters: bulk density and ash content. This new coal lithology system consists of clean coal, high gamma-ray coal, ashy coal, carbonaceous shale, and bentonitic carbonaceous shale. The establishment of this new coal lithology system has laid the foundation for any CBM reservoir evaluations at DWU, as well as other CBM basins.

(2)   The investigation into petrophysical log responses in the CBM reservoir has revealed petrophysical properties of coal lithologies, corresponding log responses, and effects of adverse log environments on log responses. The result of this investigation has facilitated the development of the new dynamic log cutoff system which can more accurately identify the coal lithologies.

- Bulk density:

  Proximate Analysis results suggest that the coal bulk density is a strong function of ash content. This correlation is reflected by Equation 4.1.

- Resistivity:

  This research observed that five major factors determine the resistivities distribution from the near-wellbore formation to the non-invaded zone of CBM reservoirs at DWU: (1) the resistivity of coal formation fluid (Rw); (2) the resistivity of logging fluid in the wellbore (Rmf); (3) the permeability of coals; (4) the ash content, and (5) the mineral type of ash content.

- Gamma ray (GR):

  This research concluded that the GR magnitude of the lower quality coals at DWU is significantly higher than that of the reference shale formation selected by the operator. This discrepancy has caused the underestimation of clean coal when the GR magnitude of the reference shale formation was applied to the coal lithology evaluation. A correlation generated by this research indicates that the GR of ash within Ferron coals at DWU is approximately 150 API units.

- Thin-bed effect on bulk density log

  The presence of a large number of thin coal seams negatively affects the reliability of the bulk density log, and the bulk density log inevitably reads too high. To characterize and overcome this discrepancy, a correlation has been developed to correct the bulk density log.

- Enlarged wellbore effect on bulk density log

  The reliability of the bulk density log can be significantly affected by the presence of an enlarged wellbore, which is commonly reported at DWU. The comparison between the density log and its corresponding core samples indicated that a significant density log error would be introduced when the washout is more than 1.5 inches. A washout amount of 4 inches or more can render the bulk density log

useless. Based on this observation, the new dynamic log cutoff system has incorporated the washout amount as a quality check to avoid misinterpretation of coal lithologies in enlarged wellbores.

(3)   The investigation into the gas desorption/adsorption characteristics revealed that high ash contents impose a negative effect on gas desorption capability. Therefore, a deviation was observed between the actual desorbed gas content and the predicted gas content by the Extended Langmuir Equation. This deviation became significant when ash content reaches approximately 30 percent and increases proportionally with ash content. As a result of these new observations associated with gas adsorption/desorption behaviors, a new method was developed to calculate gas content and gas-in-place based on a corrected Extended Langmuir Equation.

(4)   Based on the new observations associated with coal lithologies present at DWU, petrophysical log responses in the CBM reservoir, and gas desorption/adsorption behavior, a new dynamic log cutoff system and gas content calculation method were developed to interpret coal lithologies and calculate gas-in-place, respectively. For applications of individual well and field-wide projects, a new CBM computer model has been developed on the basis of this new log cutoff system and gas content calculation method.

(5)   The new CBM model has been accepted by the operator as a working tool to evaluate CBM reservoirs at DWU for individual well completion design and field-wide reservoir evaluation.

9.2   Recommendations

(1)   The new methodology for coal lithology classification, petrophysical log response in CBM reservoirs, gas desorption/adsorption characteristics, and the programming routines can be applied to other CBM plays. For the CBM

reservoirs located in the Rocky Mountain areas where many coal occurrences share the same rank and similar depositional environment, the new CBM computer model may be applicable.

(2)   The observations related to the resistivity distribution from near-wellbore to the non-invaded zone indicate that, for a given CBM reservoir where the formation fluid and well completion fluid do not vary, the development of the cleat system can be reflected by this resistivity distribution. Therefore, further investigations should be pursued into a method to characterize the development of the cleat system using the resistivity log, such as a dual laterolog/micro resistivity combination.

(3)   The field-wide CBM reservoir evaluation performed by this new model has revealed many new observations with respect to gas production from coals, gas production from sands, water production behavior, remaining gas-in-place, and the producibility of the remaining gas-in-place. These observations should be used to improve the current operations, such as hydraulic fracturing, horizontal drilling programs, and re-stimulaiton plans. Similar useful and improved results should be expected for other CBM fields in other basins.

NOMENCLATURE

A	=	the drainage area, acres
Ashy coal	=	ash content between 50% and 66%
b	=	Langmuir constant
BCSH	=	bentonitic carbonaceous shale ash content 66% and 76%
CSH	=	carbonaceous shale, ash content 66% to 76%
Clean coal	=	ash content less than 35%
D	=	diffusion coefficient, cm^2/min
GC	=	gas content, scf/ton
H(coal)	=	coal thickness, feet
HGC	=	high gamma ray coal, ash content between 35% and 50%
r	=	characteristic diffusion length, cm
R(boundary)	=	boundary resistivity, Ohm-m
R(max)	=	the maximum resistivity, Ohm-m
R(min)	=	the minimum resistivity, Ohm-m
OGIP	=	original gas-in-place, scf
P	=	pressure, psia
ρ e	=	electron density
ρ b	=	bulk density, g/cc
ρ b(coal)	=	coal bulk density, g/cc
ρ b(log)	=	log bulk density, g/cc
Q	=	heat of sorption, Jouls per thousand moles (J/Kmol)
Qash	=	ash content, wt %
R	=	universal gas constant
T	=	temperature, K
V	=	adsorption capacity, scf/ton

VL   =   Langmuir volume, scf/ton

Z   =   molecular weight

REFERENCES

Arri, L.E., 1992, Modeling coalbed methane production with binary gas sorption, SPE Paper 24363, SPE Rocky Mountain Regional Meeting, Casper, Wyoming, p.459-472

Bates, R.L., 1987, Glossary of geology, 3rd Edition: Alexandria, Virginia, American Geological Institute, p. 788

Bell, G.J., 1986, Hysteresis of Methane/Coal Sorption Isotherms, SPE 15454, SPE 61st Annual Technical Conference and Exhibition, New Orleans, Louisiana

Clayton J.L., 1993, Composition of Crude Oils Generated from Coals and Coaly Organic Matter in Shales, AAPG Special Publication, p. 185-201

Close, J.C., 1989, Significance and determination of gas content data as related to coalbed methane reservoir evaluation and production implication, Proceedings of 1989 Coalbed Methance Symposium, p. 735-742

Durand, B. and Paratte, M., 1983, Oil potential of coals: a geochemical approach, in Brooks, J., Petroleum geochemistry and exploration of Europe: Oxford, Blackwell, p. 255-265

Ellis, D., 1988, Mineral logging parameters—Nuclear and acoustic, The Technical Review, p. 38-52

Ettinger, I., 1966, Natural Factors Influencing Coal Sorption Properties 1, Petrography and the Sorption Properties of Coals, Fuel, Vol. 45, p. 267-275

Hobbs, D.W., 1967, The formation of tension joints in sedimentary rocks: An explanation, Geological Magazine, vol. 104, p. 550-556

Hobbs, B. E., 1976, An outline of structural geology: New York, John Wiley & Sons, p. 571

Hunt, J. M., 1979, Petroleum geochemistry and geology, San Francisco, W.H. Freeman and Co., p. 617

Johnston, D. J., 1990, Thoroughly Evaluate Coalbeds with Geochemical logging data: Oil and Gas Journal, vol. 78, p. 45-49

Johnston, D. J., and Scholes, P.L., 1991, Predicting cleats in coal seams from mineral and maceral composition with wireline logs, Rocky Mountain Association of Geologists Guidebook, p. 123-136

Joubert, J. I., 1973, Sorption of Methane in Moist Coal, Fuel, vol. 52, p. 181-185

Joubert, J. I.M Grein, C. T., and Bienstock, D., 1974, Effect of Moisture on the Methane Capacity of American Coals, Fuel, Vol. 53, p. 186-191

Kim, A.G., and Douglas, L.J., 1972, Hydrocarbon gases produced in a simulated swamp environment, U.S. Bureau of Mines Report of Investigations 7690, p. 15

Kim, A. G., 1977, Estimating the methane content of bituminous coalbeds from adsorption data, U.S. Bureau of Mines Report of Investigations 8245, p. 22

Kolesar, J. E., 1990, Fractured core analysis interpretation, logging, and use of natural and induced fractures in core. American Association of Petroleum Geologists Methods in Exploration Series no.8, p. 88

Levine, J.R.M., 1987, Influence of coal composition on the generation and retention of coalbed natural gas, Proceedings of the 1987 Coalbed Methane Symposium, Tuscaloosa, Alabama, p.15-18

Levine, J.R.M., 1992, Influence of coal composition on coalseam reservoir quality: a review, Symposium on Coalbed Methane Research and Development in Australia, p. 20-22

Littke, R., 1993, Migration of Oil and Gas in Coals, AAPG Special Publication, p. 219-236

Mavor, M.J., and Close, J.C., 1989, Western Cretaceous Coal Seam Project Evaluation of the Hamilton #3 Well Operated by Mesa Operating Limited Partership: GRI Topical Report No. GRI 90/0040

Mavor, M.J., 1990, Formation evaluation of exploration coalbed methane wells: presented at the International Technical Meeting jointly hosted by the Petroleum Society of CIM and the Society of Petroleum Engineers, Calgary, Canada, p.1-6

Mullen, M., 1988, Log evaluation in wells drilled for coalbed methane, Rocky Mountain Association of Geologists Guidebook, p. 113-124

Poe, S., 1987, Density gradient centrifugation on 100 mesh coal: Proceedings of the 4th Annual Meeting of the Society for Organic Petrology, San Francisco, California, p. 62

Rice, D.D., 1981, Generation, accumulation, and resource potential of biogenic gas: AAPG Bulletin, v. 65, p. 5-25

Rice, D.D., and Claypool, G.E., 1981, Controls, habitat, and resource potential of ancient bacterial gas, Editions Technip, p. 91-118

Ruppel, T.C., 1972, Adsorption of Methane/Ethane Mixtures on Dry Coal at Elevated Pressure, Fuel, vol. 53, 152-162

Sawyer, J.T., and Horner, D.M., 1987, Using reservoir simulation and field data to define mechanisms controlling coalbed methane production, Proceedings of the 1987 Coalbed Methane Symposium, Tuscaloosa, Alabama, p. 295-307

Seldon, R.F., 1934, The occurrence of Gases in Coals, Report no. 3233, U.S. Bureau of Mines, p.14-34

Schopf, J.M., 1956, A definition of coal: Economic Geology, vol. 51, p.521-527

Tissot, B.P., 1984, Recent advances in petroleum geochemistry applied to hydrocarbon exploration: AAPG Bulletin, v. 68, p. 545-563

Tremain, C.M., 1983, Coalbed methane desorption data: Colorado Geological Survey Open-file Report 81-4, p. 514

Van der sommen, J., 1978, The significance of sorption studies for practical coal mining, Solid Fuel Chemistry, vol. 12, p. 107-113

Woese, C.R., Kandler, O., 1990, Towards a natural system of organisms, proceedings of the National Academy of Science (U.S.A.), vol. 87, p.4576-4579

Yang, R.T., 1985, Adsorption of gases on coals and heat treated coals at elevated temperature and pressure, adsorption from hydrogen and methane as single gases, Fuel, vol. 64, p. 616-620

Yee, D., Arri, L.E., 1991, Binary gas sorption on coal and its influence on produced gas composition, paper number 19752, Geological Society of America, vol. 23, p. 11-16

Zhang, Y.G., and Chen, H.J., 1985, Concept on the generation and accumulation of biogenic gas: Journal of Petroleum Technology, Society of Petroleum Engineers, vol.8, p.405-422

APPENDIX

THE SOURCE CODE OF THE NEW CBM ANALYSIS MODEL

Compiler: Microsoft Visual C++ 6.0

```
// CBM_Drunkards Wash Unit

//#include "windows.h"
#include "PrizmAPI.h"
#include <math.h>
#include <string.h>
#include <tchar.h>
#include <stdlib.h>

int DefineInputOutput();
int MyInitialize();
int InitialCalculation();
int RunCalculation();
void LUdcmp();
void LUbksB();

//Globals...

//input data curve array
double *gr;
double *rhob;
double *cali;
double *res;
double *GRcshA;

//others
double *thicknessDA;
double *NGRA;

double *rintDA;
double *rhobDA;
double *cshDA;
double *cgrDA;
double *crhobDA;

//coal lithology array
double *cleancoalA;
double *HGRA;
double *HASHA;
double *BENTCSHA;
double *CSHA;


double* Washouts;
double* GRcoalA;
double* RILDnm;


float LUa[11][11];              //Array
int   LUn = 0;                  //Matrix Dimension Number
float LUb[11];                  //Input Meaurements/Output Volume
float LUvv[11];                 //Pivot Point
int   LUindx[11];               //Index Data
//Endpoints
double P1D = 0.0;
double P1U = 0.0;
double P2D = 0.0;
double P2U = 0.0;
double P3D = 0.0;
double P3U = 0.0;
double P4D = 0.0;
double P4U = 0.0;
```

```
//Saved (last) Endoints for Zoned Parameters...
double P1Dlst = 0.0;
double P1Ulst = 0.0;
double P2Dlst = 0.0;
double P2Ulst = 0.0;
double P3Dlst = 0.0;
double P3Ulst = 0.0;
double P4Dlst = 0.0;
double P4Ulst = 0.0;

void ParseCommandLine( LPSTR lpszString , char** filename , BOOL* isregister );

// Remove leading and trailing space from a non-CString string.
void ZapSpaces( LPTSTR lpszString )
{
        TCHAR ch;
        int nPosStart = 0;
        int nOriginalEnd, nPosEnd;

        // Find starting position
        ch = lpszString[nPosStart];
        while( (ch != '\0') && isspace(ch) )
        {
                nPosStart++;
                ch = lpszString[nPosStart];
        }

        if ( ch == '\0' )
        {
                lpszString[0] = '\0';
        }
        else
        {
                // Find ending position
                nOriginalEnd = nPosEnd = strlen(lpszString) - 1;
                while ( isspace(lpszString[nPosEnd]) )
                        nPosEnd--;

        // if the start is different from the original start, extract the middle.
                if ( nPosStart != 0 )
                {
                        int nLength = nPosEnd - nPosStart + 1;
                        memmove(lpszString, &lpszString[nPosStart], nLength*sizeof(TCHAR) );
                        lpszString[nLength] = '\0';
                }
                else if ( nPosEnd != nOriginalEnd )
                        lpszString[nPosEnd+1] = '\0';
        }
}

void WriteMessage( LPCTSTR msg )
{
        MessageBox( HWND_DESKTOP, msg, "DW Message", MB_OK );
}


int WINAPI WinMain(
                HINSTANCE hInstance,  // handle to current instance
                HINSTANCE hPrevInstance,  // handle to previous instance
                LPSTR lpCmdLine,      // pointer to command line
                int nCmdShow          // show state of window
                )
```

```
{
        int result = 13;
        LPTSTR filename;
    BOOL isregister;

    ParseCommandLine( lpCmdLine , &filename , &isregister );

        if ( isregister )
        {
    PDK_Initialize();
    PDK_DefineModelName ( "Thickness; RHOB" );                    //1
                result = DefineInputOutput();
                if ( result == 0 )
                  result = PDK_SaveCurvesParams( filename );
                PDK_ShutDown();
}
        else
        {
    PDK_Initialize();
    DefineInputOutput();

    result = PDK_LoadData( filename );

    if ( result == 0 )
    {
                    InitialCalculation();

        RunCalculation();

                    result = PDK_SaveData( filename );
                    if ( result != 0 )
                            WriteMessage( "Saving Data Failed" );
        }
                else
                    WriteMessage( "Loading Data Failed" );

            PDK_ShutDown();
        }
        return result;
}

int DefineInputOutput()
{
    //Define Input Parameters
    PDK_DefineParameter(PRIZM_SDK_REQUIRED_INPUT, "GRshl", "API", "Gamma Ray Shale", 100.0);
    PDK_DefineParameter(PRIZM_SDK_REQUIRED_INPUT, "GRcln", "API", "Gamma Ray Clean", 20.0);
    PDK_DefineParameter(PRIZM_SDK_REQUIRED_INPUT, "RhoM", "GM/CC", "Bulk Density Matrix", 2.68);
    PDK_DefineParameter(PRIZM_SDK_REQUIRED_INPUT, "RhoF", "GM/CC", "Bulk Density Fluid", 1.0);
    PDK_DefineParameter(PRIZM_SDK_REQUIRED_INPUT, "Rw", "OHMM", "Formation Water Resistivity ", 0.04);
    PDK_DefineParameter(PRIZM_SDK_REQUIRED_INPUT, "RwBnd", "OHMM", "Bound Water Resistivity", 0.15);
    PDK_DefineParameter(PRIZM_SDK_REQUIRED_INPUT, "Rshl", "OHMM", "Resistivity shale", 5.0);
    PDK_DefineParameter(PRIZM_SDK_REQUIRED_INPUT, "a", "", "Archie 'a'", 1.0);
    PDK_DefineParameter(PRIZM_SDK_REQUIRED_INPUT, "m", "", "Archie 'm'", 2.0);
    //4Mineral
    PDK_DefineParameter(PRIZM_SDK_REQUIRED_INPUT, "P1Den", "gm/cc", "P1 (LS) Den", 2.71);
    PDK_DefineParameter(PRIZM_SDK_REQUIRED_INPUT, "P2Den", "gm/cc", "P2 (SS) Den", 2.65);
    PDK_DefineParameter(PRIZM_SDK_REQUIRED_INPUT, "P3Den", "gm/cc", "P3 (DM) Den", 2.85);
    PDK_DefineParameter(PRIZM_SDK_REQUIRED_INPUT, "P4Den", "gm/cc", "P4 (SHL) Den", 2.95);
    PDK_DefineParameter(PRIZM_SDK_REQUIRED_INPUT, "P1Uma", "gm/cc", "P1 (LS) Uma", 13.77);
    PDK_DefineParameter(PRIZM_SDK_REQUIRED_INPUT, "P2Uma", "gm/cc", "P2 (SS) Uma", 4.88);
    PDK_DefineParameter(PRIZM_SDK_REQUIRED_INPUT, "P3Uma", "gm/cc", "P3 (DM) Uma", 9.0);
    PDK_DefineParameter(PRIZM_SDK_REQUIRED_INPUT, "P4Uma", "gm/cc", "P4 (SHL) Uma", 10.0);
```

```
//gascontent
PDK_DefineParameter(PRIZM_SDK_REQUIRED_INPUT, "GasContent", "gm/cc", "P4 (SHL) Uma", 0.0);

//Define Input Curves
PDK_DefineCurve(PRIZM_SDK_OPTIONAL_INPUT, "RHOB", "GM/CC", "Bulk Density");//RHOB
    PDK_DefineCurve(PRIZM_SDK_OPTIONAL_INPUT, "RHOZ", "GM/CC", "Bulk Density");
    PDK_DefineCurve(PRIZM_SDK_OPTIONAL_INPUT, "RHOB_MAIN", "G/C3", "Density");
    PDK_DefineCurve(PRIZM_SDK_OPTIONAL_INPUT, "RHO8", "API", "Gamma Ray");

    PDK_DefineCurve(PRIZM_SDK_OPTIONAL_INPUT, "RHOB2", "G/C3", "Density");//DW
    PDK_DefineCurve(PRIZM_SDK_OPTIONAL_INPUT, "RHOB3", "API", "Gamma Ray");//DW

PDK_DefineCurve(PRIZM_SDK_OPTIONAL_INPUT, "GR", "API", "Gamma Ray"); //GR
    PDK_DefineCurve(PRIZM_SDK_OPTIONAL_INPUT, "GR_MAIN", "API", "Gamma Ray");

    PDK_DefineCurve(PRIZM_SDK_OPTIONAL_INPUT, "GR2", "API", "Gamma Ray");
    PDK_DefineCurve(PRIZM_SDK_OPTIONAL_INPUT, "GR3", "API", "Gamma Ray");//DW
    PDK_DefineCurve(PRIZM_SDK_OPTIONAL_INPUT, "CGR", "API", "Gamma Ray");
    PDK_DefineCurve(PRIZM_SDK_OPTIONAL_INPUT, "EHGR", "API", "Gamma Ray");
    PDK_DefineCurve(PRIZM_SDK_OPTIONAL_INPUT, "HGR", "API", "Gamma Ray");//DW

    PDK_DefineCurve(PRIZM_SDK_OPTIONAL_INPUT, "RLL3", "OHMM", "Resistivity"); //RLL3
PDK_DefineCurve(PRIZM_SDK_OPTIONAL_INPUT, "SHALLOW_RT", "V/V", "Neutron Porosity");
PDK_DefineCurve(PRIZM_SDK_OPTIONAL_INPUT, "AO30", "OHMM", "Resistivity");
PDK_DefineCurve(PRIZM_SDK_OPTIONAL_INPUT, "AHT30", "B/E", "PhotoElectic");
    PDK_DefineCurve(PRIZM_SDK_OPTIONAL_INPUT, "AT30", "OHMM", "Resistivity"); //1
PDK_DefineCurve(PRIZM_SDK_OPTIONAL_INPUT, "SGRD", "API", "Gamma Ray");
    PDK_DefineCurve(PRIZM_SDK_OPTIONAL_INPUT, "SFLU", "OHMM", "Resistivity"); //1
PDK_DefineCurve(PRIZM_SDK_OPTIONAL_INPUT, "DFL", "API", "Gamma Ray");

PDK_DefineCurve(PRIZM_SDK_OPTIONAL_INPUT, "AHO30", "V/V", "Neutron Porosity");
PDK_DefineCurve(PRIZM_SDK_OPTIONAL_INPUT, "AHF30", "OHMM", "Resistivity");
PDK_DefineCurve(PRIZM_SDK_OPTIONAL_INPUT, "AF30", "B/E", "PhotoElectic");
    PDK_DefineCurve(PRIZM_SDK_OPTIONAL_INPUT, "LL3", "OHMM", "Resistivity"); //1
PDK_DefineCurve(PRIZM_SDK_OPTIONAL_INPUT, "RSHAL", "API", "Gamma Ray");
    PDK_DefineCurve(PRIZM_SDK_OPTIONAL_INPUT, "RXOZ", "OHMM", "Resistivity"); //1
PDK_DefineCurve(PRIZM_SDK_OPTIONAL_INPUT, "RXO8", "API", "Gamma Ray"); //DW

    PDK_DefineCurve(PRIZM_SDK_OPTIONAL_INPUT, "CALI", "OHMM", "Resistivity");//CALI
PDK_DefineCurve(PRIZM_SDK_OPTIONAL_INPUT, "DCAL", "B/E", "PhotoElectic");
    PDK_DefineCurve(PRIZM_SDK_OPTIONAL_INPUT, "HCAL", "OHMM", "Resistivity"); //1
PDK_DefineCurve(PRIZM_SDK_OPTIONAL_INPUT, "CALI_MAIN", "API", "Gamma Ray");

    PDK_DefineCurve(PRIZM_SDK_OPTIONAL_INPUT, "CALI_1", "B/E", "PhotoElectic");
    PDK_DefineCurve(PRIZM_SDK_OPTIONAL_INPUT, "CALIPER", "OHMM", "Resistivity"); //DW

    PDK_DefineCurve(PRIZM_SDK_OPTIONAL_INPUT, "DPHI", "V/V", "Density Porosity");
    PDK_DefineCurve(PRIZM_SDK_OPTIONAL_INPUT, "NPHI", "V/V", "Neutron Porosity");
PDK_DefineCurve(PRIZM_SDK_OPTIONAL_INPUT, "RT", "OHMM", "Resistivity");
PDK_DefineCurve(PRIZM_SDK_OPTIONAL_INPUT, "PEF", "B/E", "PhotoElectic");

    PDK_DefineCurve(PRIZM_SDK_OPTIONAL_INPUT, "HMRS", "B/E", "PhotoElectic");

    PDK_DefineCurve(PRIZM_SDK_OPTIONAL_INPUT, "DPSS", "V/V", "Density Porosity");
    PDK_DefineCurve(PRIZM_SDK_OPTIONAL_INPUT, "NPSS", "V/V", "Neutron Porosity");
PDK_DefineCurve(PRIZM_SDK_OPTIONAL_INPUT, "CNPOR", "OHMM", "Resistivity");
PDK_DefineCurve(PRIZM_SDK_OPTIONAL_INPUT, "DPOR", "B/E", "PhotoElectic");

    PDK_DefineCurve(PRIZM_SDK_OPTIONAL_INPUT, "RILD", "B/E", "PhotoElectic");
```

```
//Define Output Curves
    PDK_DefineCurve(PRIZM_SDK_OUTPUT, "CoalTh", "API", "coalthickness"); //2
    PDK_DefineCurve(PRIZM_SDK_OUTPUT, "HGRCTh", "API", "coalthickness"); //2
    PDK_DefineCurve(PRIZM_SDK_OUTPUT, "AshyCTh", "API", "coalthickness"); //2
    PDK_DefineCurve(PRIZM_SDK_OUTPUT, "CSHTh", "API", "coalthickness"); //2
    PDK_DefineCurve(PRIZM_SDK_OUTPUT, "BCSHTh", "API", "coalthickness"); //2

PDK_DefineCurve(PRIZM_SDK_OUTPUT, "PHIDout", "V/V", "Density Porosity");
PDK_DefineCurve(PRIZM_SDK_OUTPUT, "PHIA", "V/V", "Apparent Porosity");
PDK_DefineCurve(PRIZM_SDK_OUTPUT, "PHIE", "V/V", "Effective Porosity");
PDK_DefineCurve(PRIZM_SDK_OUTPUT, "Vshl", "", "Shale Volume");
PDK_DefineCurve(PRIZM_SDK_OUTPUT, "RoDW", "OHMM", "Water Bearing Resistivity");
PDK_DefineCurve(PRIZM_SDK_OUTPUT, "SwA", "V/V", "SW Archie");
PDK_DefineCurve(PRIZM_SDK_OUTPUT, "SwT", "V/V", "SW Total");
PDK_DefineCurve(PRIZM_SDK_OUTPUT, "SwE", "V/V", "SW Effective");
PDK_DefineCurve(PRIZM_SDK_OUTPUT, "BVW", "V/V", "Bulk Volume Water");
PDK_DefineCurve(PRIZM_SDK_OUTPUT, "SwMS", "V/V", "Modified Simandoux Water Saturation");
PDK_DefineCurve(PRIZM_SDK_OUTPUT, "SwI", "V/V", "Indonesian Water Suration");
    PDK_DefineCurve(PRIZM_SDK_OUTPUT, "Thickness", "FEET", "Thickness"); //1
    PDK_DefineCurve(PRIZM_SDK_OUTPUT, "Rint", "OHMM", "Interface resistivity"); //1
    PDK_DefineCurve(PRIZM_SDK_OUTPUT, "CRHOB", "GM/CC", "Corrected RHOB"); //2
    PDK_DefineCurve(PRIZM_SDK_OUTPUT, "CRHOBcsh", "GM/CC", "Corrected RHOB"); //2
    PDK_DefineCurve(PRIZM_SDK_OUTPUT, "CCGR", "API", "Corrected GR"); //2
    PDK_DefineCurve(PRIZM_SDK_OUTPUT, "CCRHOB", "GM/CC", "Corrected RHOB"); //2
    PDK_DefineCurve(PRIZM_SDK_OUTPUT, "CleanCoal", "GM/CC", "coal"); //2
    PDK_DefineCurve(PRIZM_SDK_OUTPUT, "HGRC", "GM/CC", "Corrected RHOB"); //2
    PDK_DefineCurve(PRIZM_SDK_OUTPUT, "Hash", "API", "Corrected GR"); //2
    PDK_DefineCurve(PRIZM_SDK_OUTPUT, "csh", "GM/CC", "Corrected RHOB"); //2
    PDK_DefineCurve(PRIZM_SDK_OUTPUT, "BentCSH", "GM/CC", "coal"); //2
    PDK_DefineCurve(PRIZM_SDK_OUTPUT, "NGR", "API", "GR_RAY"); //2
    PDK_DefineCurve(PRIZM_SDK_OUTPUT, "ashcontent", "API", "ashcontent"); //2
    PDK_DefineCurve(PRIZM_SDK_OUTPUT, "DPORO", "API", "ashcontent"); //2


    PDK_DefineCurve(PRIZM_SDK_OUTPUT, "GRcsh", "API", "coalthickness"); //2

    PDK_DefineCurve(PRIZM_SDK_OUTPUT, "Washout", "API", "coalthickness"); //2
    PDK_DefineCurve(PRIZM_SDK_OUTPUT, "GRcoal", "API", "coalthickness"); //2

    PDK_DefineCurve(PRIZM_SDK_OUTPUT, "coal1", "API", "ashcontent"); //2
    PDK_DefineCurve(PRIZM_SDK_OUTPUT, "topdepth1", "API", "coalthickness"); //2
    PDK_DefineCurve(PRIZM_SDK_OUTPUT, "coal percent1", "API", "coalthickness"); //2

    PDK_DefineCurve(PRIZM_SDK_OUTPUT, "coal2", "API", "ashcontent"); //2
    PDK_DefineCurve(PRIZM_SDK_OUTPUT, "topdepth2", "API", "coalthickness"); //2
    PDK_DefineCurve(PRIZM_SDK_OUTPUT, "coal percent2", "API", "coalthickness"); //2

    PDK_DefineCurve(PRIZM_SDK_OUTPUT, "coal3", "API", "ashcontent"); //2
    PDK_DefineCurve(PRIZM_SDK_OUTPUT, "topdepth3", "API", "coalthickness"); //2
    PDK_DefineCurve(PRIZM_SDK_OUTPUT, "coal percent3", "API", "coalthickness"); //2

    PDK_DefineCurve(PRIZM_SDK_OUTPUT, "coal4", "API", "ashcontent"); //2
    PDK_DefineCurve(PRIZM_SDK_OUTPUT, "topdepth4", "API", "coalthickness"); //2
    PDK_DefineCurve(PRIZM_SDK_OUTPUT, "coal percent4", "API", "coalthickness"); //2

    PDK_DefineCurve(PRIZM_SDK_OUTPUT, "coal5", "API", "ashcontent"); //2
    PDK_DefineCurve(PRIZM_SDK_OUTPUT, "topdepth5", "API", "coalthickness"); //2
    PDK_DefineCurve(PRIZM_SDK_OUTPUT, "coal percent5", "API", "coalthickness"); //2

    PDK_DefineCurve(PRIZM_SDK_OUTPUT, "coal6", "API", "ashcontent"); //2
    PDK_DefineCurve(PRIZM_SDK_OUTPUT, "topdepth6", "API", "coalthickness"); //2
    PDK_DefineCurve(PRIZM_SDK_OUTPUT, "coal percent6", "API", "coalthickness"); //2
```

```
PDK_DefineCurve(PRIZM_SDK_OUTPUT, "coal7", "API", "ashcontent");  //2
PDK_DefineCurve(PRIZM_SDK_OUTPUT, "topdepth7", "API", "coalthickness");  //2
PDK_DefineCurve(PRIZM_SDK_OUTPUT, "coal percent7", "API", "coalthickness");  //2

PDK_DefineCurve(PRIZM_SDK_OUTPUT, "coal8", "API", "ashcontent");  //2
PDK_DefineCurve(PRIZM_SDK_OUTPUT, "topdepth8", "API", "coalthickness");  //2
PDK_DefineCurve(PRIZM_SDK_OUTPUT, "coal percent8", "API", "coalthickness");  //2

PDK_DefineCurve(PRIZM_SDK_OUTPUT, "cleancoal1", "API", "coalthickness");  //2
PDK_DefineCurve(PRIZM_SDK_OUTPUT, "HGRC1", "API", "coalthickness");  //2

PDK_DefineCurve(PRIZM_SDK_OUTPUT, "cleancoal2", "API", "coalthickness");  //2
PDK_DefineCurve(PRIZM_SDK_OUTPUT, "HGRC2", "API", "coalthickness");  //2

PDK_DefineCurve(PRIZM_SDK_OUTPUT, "cleancoal3", "API", "coalthickness");  //2
PDK_DefineCurve(PRIZM_SDK_OUTPUT, "HGRC3", "API", "coalthickness");  //2

PDK_DefineCurve(PRIZM_SDK_OUTPUT, "cleancoal4", "API", "coalthickness");  //2
PDK_DefineCurve(PRIZM_SDK_OUTPUT, "HGRC4", "API", "coalthickness");  //2

PDK_DefineCurve(PRIZM_SDK_OUTPUT, "cleancoal5", "API", "coalthickness");  //2
PDK_DefineCurve(PRIZM_SDK_OUTPUT, "HGRC5", "API", "coalthickness");  //2

PDK_DefineCurve(PRIZM_SDK_OUTPUT, "cleancoal6", "API", "coalthickness");  //2
PDK_DefineCurve(PRIZM_SDK_OUTPUT, "HGRC6", "API", "coalthickness");  //2

PDK_DefineCurve(PRIZM_SDK_OUTPUT, "cleancoal7", "API", "coalthickness");  //2
PDK_DefineCurve(PRIZM_SDK_OUTPUT, "HGRC7", "API", "coalthickness");  //2

PDK_DefineCurve(PRIZM_SDK_OUTPUT, "cleancoal8", "API", "coalthickness");  //2
PDK_DefineCurve(PRIZM_SDK_OUTPUT, "HGRC8", "API", "coalthickness");  //2

PDK_DefineCurve(PRIZM_SDK_OUTPUT, "GIP", "API", "coalthickness");  //2
PDK_DefineCurve(PRIZM_SDK_OUTPUT, "GIPcleancoal", "API", "coal");  //2
PDK_DefineCurve(PRIZM_SDK_OUTPUT, "GIPhgrc", "API", "coalthickness");  //2
PDK_DefineCurve(PRIZM_SDK_OUTPUT, "GIPashycoal", "API", "coalthickness");  //2
PDK_DefineCurve(PRIZM_SDK_OUTPUT, "GIPshales", "API", "coalthickness");  //2

PDK_DefineCurve(PRIZM_SDK_OUTPUT, "CO2", "API", "CO2");  //2

PDK_DefineCurve(PRIZM_SDK_OUTPUT, "sandgas", "API", "CO2");  //2
PDK_DefineCurve(PRIZM_SDK_OUTPUT, "GIPsandgas", "API", "CO2");  //2
PDK_DefineCurve(PRIZM_SDK_OUTPUT, "SW", "API", "CO2");  //2

PDK_DefineCurve(PRIZM_SDK_OUTPUT, "sand", "API", "CO2");  //2
PDK_DefineCurve(PRIZM_SDK_OUTPUT, "sandphih", "API", "CO2");  //2

PDK_DefineCurve(PRIZM_SDK_OUTPUT, "RILDavg", "API", "CO2");  //2

PDK_DefineCurve(PRIZM_SDK_OUTPUT, "gascontentcurve", "scf/ton", "gascontentcurve");  //

PDK_DefineCurve(PRIZM_SDK_OUTPUT, "TGIPclean", "API", "CO2");  //2
PDK_DefineCurve(PRIZM_SDK_OUTPUT, "TGIPhgr", "API", "CO2");  //2
PDK_DefineCurve(PRIZM_SDK_OUTPUT, "TGIPashy", "API", "CO2");  //2
PDK_DefineCurve(PRIZM_SDK_OUTPUT, "TGIPcsh", "API", "CO2");  //2
PDK_DefineCurve(PRIZM_SDK_OUTPUT, "TGIPbcsh", "API", "CO2");  //2
PDK_DefineCurve(PRIZM_SDK_OUTPUT, "TGIP", "API", "CO2");  //2

PDK_DefineCurve(PRIZM_SDK_OUTPUT, "CleanCoalGR", "API", "CO2");  //2
PDK_DefineCurve(PRIZM_SDK_OUTPUT, "CleanCoalRILD", "API", "CO2");  //2
PDK_DefineCurve(PRIZM_SDK_OUTPUT, "CleanCoalPHIN", "API", "CO2");  //2
```

```
//4Mineral
PDK_DefineCurve(PRIZM_SDK_OUTPUT, "P1", "V/V", "Volumn Limestone");
PDK_DefineCurve(PRIZM_SDK_OUTPUT, "P2", "V/V", "Volumn Quartz");
PDK_DefineCurve(PRIZM_SDK_OUTPUT, "P3", "V/V", "Volumn Dolomite");
PDK_DefineCurve(PRIZM_SDK_OUTPUT, "P4", "V/V", "Volumn Shale");
PDK_DefineCurve(PRIZM_SDK_OUTPUT, "P1dsp", "V/V", "Display Limestone");
PDK_DefineCurve(PRIZM_SDK_OUTPUT, "P2dsp", "V/V", "Display Quartz");
PDK_DefineCurve(PRIZM_SDK_OUTPUT, "P3dsp", "V/V", "Display Dolomite");
PDK_DefineCurve(PRIZM_SDK_OUTPUT, "P4dsp", "V/V", "Display Shale");
PDK_DefineCurve(PRIZM_SDK_OUTPUT, "UMA", "", "Apparent Photoelectric Factor");
PDK_DefineCurve(PRIZM_SDK_OUTPUT, "DGA", "GM/CC", "Apparent Grain Density");

        return 0;
}

int MyInitialize()
{
        return 0;
}

int InitialCalculation()
{
        // None for this model.
        return 0;
}

int RunCalculation()
{
   //Declare input parameters
   double GRcln, GRshl, RhoM, RhoF, Rw, RwBnd, Rshl, a, m, GasContent;

   //Declare input parameter indices
   int lngGRcln, lngGRshl, lngRhoM, lngRhoF, lngRw, lngRwBnd, lngRshl, lnga, lngm, lngGasContent;

   //Declare Input Curve values
   double GR, RHOB, DPHI, RT, NPHI, PEF, RLL3, GR_MAIN, RHOZ, RHOB_MAIN;  //1
   double SHALLOW_RT, AO30, AHT30, AT30, SGRD, CALI, DCAL, HCAL, CALI_MAIN, SFLU, DFL, RHO8;

        double RHOB2, RHOB3;//DW
        double CGR, EHGR, HGR, GR2, GR3;
        double AHO30, AHF30, AF30, LL3, RSHAL, RXOZ, RXO8, HMRS;
        double CALI_1, CALIPER;
        double DPSS, NPSS, DPOR, CNPOR, RILD;

   //Declare Input Curve indices
   int lngGR, lngRHOB, lngDPHI, lngRT, lngNPHI, lngPEF, lngRLL3,lngGR_MAIN;  //1
   int lngRHOZ, lngRHOB_MAIN, lngSHALLOW_RT, lngAO30, lngAHT30, lngAT30, lngSGRD;
        int lngCALI, lngDCAL, lngHCAL, lngCALI_MAIN, lngSFLU, lngDFL, lngRHO8, lngHMRS;

        int lngRHOB2, lngRHOB3;//DW
        int lngCGR, lngEHGR, lngHGR, lngGR2, lngGR3;
        int lngAHO30, lngAHF30, lngAF30, lngLL3, lngRSHAL, lngRXOZ, lngRXO8;
        int lngCALI_1, lngCALIPER;
        int lngDPSS, lngNPSS, lngDPOR, lngCNPOR, lngRILD;

   //Declare Output Curve values
   double PHIDout, PHIA, PHIE, Vshl, RoDW, SwE, SwA, SwT, BVW, SwMS, SwI, Y;
   double P1, P2, P3, P4, P1dsp, P2dsp, P3dsp, P4dsp, UMA, DGA, Thickness, Rint, CRHOB, CRHOBcsh;  //3
   double CCGR, CCRHOB, CleanCoal, HGRC, Hash, csh, BentCSH, NGR, ashcontent;
        double GRcsh;
        double CoalTh, HGRCTh, AshyCTh, CSHTh, BCSHTh;
        double Washout;
```

```
double coal1, topdepth1, coal percent1;
double coal2, topdepth2, coal percent2;
double coal3, topdepth3, coal percent3;
double coal4, topdepth4, coal percent4;
double coal5, topdepth5, coal percent5;
double coal6, topdepth6, coal percent6;
double coal7, topdepth7, coal percent7;
double coal8, topdepth8, coal percent8;
double cleancoal1, HGRC1;
double cleancoal2, HGRC2;
double cleancoal3, HGRC3;
double cleancoal4, HGRC4;
double cleancoal5, HGRC5;
double cleancoal6, HGRC6;
double cleancoal7, HGRC7;
double cleancoal8, HGRC8;

double GIP, GIPcleancoal, GIPhgrc, GIPashycoal, GIPshales;

double CO2=0, DPORO, sandgas=0, GIPsandgas=0, SW;

double sand=0;
double sandphih=0;

double RILDavg;

double TGIPclean=0, TGIPhgr=0, TGIPashy=0, TGIPcsh=0, TGIPbcsh=0, TGIP=0, gascontentcurve;

double CleanCoalGR=100, CleanCoalRILD=0, CleanCoalPHIN=0;


//Declare Output Curve indices...
int lngPHIDout, lngPHIA, lngPHIE, lngVshl, lngRoDW, lngSwE, lngSwA, lngSwT, lngBVW, lngSwMS, lngSwI;
int lngP1, lngP2, lngP3, lngP4, lngP1dsp, lngP2dsp, lngP3dsp, lngP4dsp, lngUMA, lngDGA, lngThickness;//4
    int lngRint, lngCRHOB, lngCRHOBcsh, lngCCGR, lngCCRHOB, lngCleanCoal, lngHGRC, lngHash, lngcsh, lngBentCSH;
    int lngNGR, lngashcontent, lngGRcsh;
    int lngCoalTh, lngHGRCTh, lngAshyCTh, lngCSHTh, lngBCSHTh;
    int lngWashout, lngGRcoal;
    int lngcoal1, lngtopdepth1, lngcoal percent1;
    int lngcoal2, lngtopdepth2, lngcoal percent2;
    int lngcoal3, lngtopdepth3, lngcoal percent3;
    int lngcoal4, lngtopdepth4, lngcoal percent4;
    int lngcoal5, lngtopdepth5, lngcoal percent5;
    int lngcoal6, lngtopdepth6, lngcoal percent6;
    int lngcoal7, lngtopdepth7, lngcoal percent7;
    int lngcoal8, lngtopdepth8, lngcoal percent8;
    int lngcleancoal1, lngHGRC1;
    int lngcleancoal2, lngHGRC2;
    int lngcleancoal3, lngHGRC3;
    int lngcleancoal4, lngHGRC4;
    int lngcleancoal5, lngHGRC5;
    int lngcleancoal6, lngHGRC6;
    int lngcleancoal7, lngHGRC7;
    int lngcleancoal8, lngHGRC8;

    int lngGIP, lngGIPcleancoal, lngGIPhgrc, lngGIPashycoal, lngGIPshales;

    int lngCO2, lngDPORO, lngsandgas, lngGIPsandgas, lngSW;

    int lngsand, lngsandphih, lngRILDavg;

    int lngTGIPclean, lngTGIPhgr, lngTGIPashy, lngTGIPcsh, lngTGIPbcsh, lngTGIP, lnggascontentcurve;
```

```
        int lngCleanCoalGR, lngCleanCoalRILD, lngCleanCoalPHIN;

//4 Mineral Parameters & Endpoint Values...
//Declare input parameters
double P1D, P2D, P3D, P4D;
double P1U, P2U, P3U, P4U;

//Declare input parameter indices
int lngP1Den, lngP2Den, lngP3Den, lngP4Den;
int lngP1Uma, lngP2Uma, lngP3Uma, lngP4Uma;

double U = 0.0;
double Sum = 0.0;
int i, numSamples, N, NN, ZnParChg;

        //Declare "Thickness" parameters                          //5

        int indtopH, aindtopH, bindtopH, cindtopH, indbottomH, indexH=0, indexDA=0, Tstep=0;
        BOOL L2H=FALSE;
        double ThicknessA[300];
        int indtopHA[300], indbottomHA[300];
        double Rsum=0, Resolution, Ravg;

        //Declare interface R parameters                          //Declare the parameters
        int s, stepdown=0, stepup=0, Mstepdown, Mstepup;
        double prevR = 1000.0, Rb, RLL;
        BOOL downR = FALSE;
        int indexDAR=0;

        //Declare "CRHOB" parameters        //6
BOOL L2 = FALSE, down = FALSE;
double prev = 2.1, min, resolution;
int indmin, indtop, indbottom, aindex=0;
        int indexDAD=0;

        //dynamic array indices
        //int indexDAR=0, indexDAC=0, indexDAG=0, indexDACD=0;

        double mina[1000];
        int indtopa[1000];
        int indbottoma[1000];
        int indexb;

        //Declare "CSH_CRHOB" parameters
        BOOL L3 = FALSE;
        int indtop2, indbottom2, diff;
        double sumcsh=0.0;
        int indexDAC=0;

        //Corrected GR
        int indexDAG=0;

        //corrected rhob for thickness
        int indexDACD=0;

        //normalize gr
        double GRmin=100.0;

        //coal thickness output
        BOOL TH=FALSE;
        int Thtopind, Thbottomind;
```

147

```
//GR correction
BOOL LGR=FALSE;


//csh GR
BOOL GRup=FALSE;
double GRpre=0.0;
int indGRM, stepGR;

//Coal thickness output
int CoalThInd = 0;
double CoalThA[50];
double CoalThk = 0;

//Coal thickness output
int HGRCThInd = 0;
double HGRCThA[50];
double HGRCThk = 0;

//Coal thickness output
int AshyCThInd = 0;
double AshyCThA[50];
double AshyCThk = 0;

//Coal thickness output
int CSHThInd = 0;
double CSHThA[50];
double CSHThk = 0;

//Coal thickness output
int BCSHThInd = 0;
double BCSHThA[50];
double BCSHThk = 0;

//select the thickest coal bed
int MaxCoalThInd=0;
int      Coalbedind=0;
double MaxCoalTh, Minirhob;
int TopOfThikCoal;
int BottomOfThikCoal;

int TopOfThikCoal2;
int BottomOfThikCoal2;

int TopIndex;
int BottomIndex;

int cshtop;

//Washout calculation

int TopCali, BottomCali;
double SumCali = 0;
double AvgCali;
int CaliStep=0;

//output information for horizontal drilling design
int coalind;
int numcoal=0;
double coal;
double coalA[100];
```

148

```
int coaltopind[100], coalbottomind[100];

int atop, abottom, atop1, abottom1, thickstep =0;
double coal percent[100];

double topdepth[100];

int coalthickstep=0, HGRCthickstep=0;
double cleancoalB[100], HGRCB[100];

double Fpressure, Fdensity, gascontent, gasinplace=0, gasinplace1=0, gasinplace2=0, gasinplace3=0, gasinplace4=0;

double Thcoal, Thhgr, Thhash, Thcsh, Thbcsh;

double CO2content;

//GR humps

BOOL GRup2=FALSE;
int MinGRind2, MinGRind, MaxGRind2;
double MinGR2=0, MaxGR2=0, GRprev2=300, GRboundary2;

// sand and water

double PHIN, PHIDs, PHIAs, Vshls, PHIEs, Swms;

//RILD NORMALIZATION

int Rinterval, RILDstep=0;
double RILDsum=0;

//calculate ro

double PHIEavg, RILDsavg, PHIEsum=0, RILDssum=0, Ro;
int RILDsstep=0, PHIEstep=0;

//desensitize resistivity curve

double PreviousR, Resistivity, Rmax;
int start, RmaxN;
BOOL ResistivityUP=FALSE;

//select high resolution curves

double stepgr1, stepgr2, steprhob1=0, steprhob2=0, pr1, pr2;
int steprhob=0;

//pick gr, rild, and phin of coal

int seamtop, seambottom;

//Get the indices for the input parameters
lngGRcln = PDK_GetParameterIndex("GRcln");
lngGRshl = PDK_GetParameterIndex("GRshl");
lngRhoM = PDK_GetParameterIndex("RhoM");
lngRhoF = PDK_GetParameterIndex("RhoF");
lngRw = PDK_GetParameterIndex("Rw");
lngRwBnd = PDK_GetParameterIndex("RwBnd");
lngRshl = PDK_GetParameterIndex("Rshl");
lnga = PDK_GetParameterIndex("a");
lngm = PDK_GetParameterIndex("m");
```

```
lngGasContent = PDK_GetParameterIndex("GasContent");

//Get the indices for the input parameters
lngP1Den = PDK_GetParameterIndex("P1Den");
lngP2Den = PDK_GetParameterIndex("P2Den");
lngP3Den = PDK_GetParameterIndex("P3Den");
lngP4Den = PDK_GetParameterIndex("P4Den");
lngP1Uma = PDK_GetParameterIndex("P1Uma");
lngP2Uma = PDK_GetParameterIndex("P2Uma");
lngP3Uma = PDK_GetParameterIndex("P3Uma");
lngP4Uma = PDK_GetParameterIndex("P4Uma");


//Get the indices for the input curves
lngRHOB = PDK_GetCurveIndex(PRIZM_SDK_INPUT, "RHOB");
    lngRHOZ = PDK_GetCurveIndex(PRIZM_SDK_INPUT, "RHOZ");
    lngRHOB_MAIN = PDK_GetCurveIndex(PRIZM_SDK_INPUT, "RHOB_MAIN");
lngDPHI = PDK_GetCurveIndex(PRIZM_SDK_INPUT, "DPHI");
lngRT  = PDK_GetCurveIndex(PRIZM_SDK_INPUT, "RT");
lngNPHI = PDK_GetCurveIndex(PRIZM_SDK_INPUT, "NPHI");
lngGR  = PDK_GetCurveIndex(PRIZM_SDK_INPUT, "GR");
lngPEF = PDK_GetCurveIndex(PRIZM_SDK_INPUT, "PEF");
    lngRLL3 = PDK_GetCurveIndex(PRIZM_SDK_INPUT, "RLL3");      //1
lngGR_MAIN  = PDK_GetCurveIndex(PRIZM_SDK_INPUT, "GR_MAIN");
    lngSHALLOW_RT = PDK_GetCurveIndex(PRIZM_SDK_INPUT, "SHALLOW_RT");
lngAO30  = PDK_GetCurveIndex(PRIZM_SDK_INPUT, "AO30");
lngAHT30  = PDK_GetCurveIndex(PRIZM_SDK_INPUT, "AHT30");
    lngAT30 = PDK_GetCurveIndex(PRIZM_SDK_INPUT, "AT30");      //1
lngSGRD  = PDK_GetCurveIndex(PRIZM_SDK_INPUT, "SGRD");
    lngCALI  = PDK_GetCurveIndex(PRIZM_SDK_INPUT, "CALI");
lngDCAL  = PDK_GetCurveIndex(PRIZM_SDK_INPUT, "DCAL");
    lngHCAL  = PDK_GetCurveIndex(PRIZM_SDK_INPUT, "HCAL");      //1
lngCALI_MAIN  = PDK_GetCurveIndex(PRIZM_SDK_INPUT, "CALI_MAIN");
    lngSFLU = PDK_GetCurveIndex(PRIZM_SDK_INPUT, "SFLU");      //1
lngDFL  = PDK_GetCurveIndex(PRIZM_SDK_INPUT, "DFL");
    lngRHO8  = PDK_GetCurveIndex(PRIZM_SDK_INPUT, "RHO8");


    lngRHOB2  = PDK_GetCurveIndex(PRIZM_SDK_INPUT, "RHOB2");  //DW
lngRHOB3  = PDK_GetCurveIndex(PRIZM_SDK_INPUT, "RHOB3");
    lngCGR = PDK_GetCurveIndex(PRIZM_SDK_INPUT, "CGR");
lngEHGR  = PDK_GetCurveIndex(PRIZM_SDK_INPUT, "EHGR");
lngHGR  = PDK_GetCurveIndex(PRIZM_SDK_INPUT, "HGR");
    lngAHO30  = PDK_GetCurveIndex(PRIZM_SDK_INPUT, "AHO30");  //1
lngAHF30  = PDK_GetCurveIndex(PRIZM_SDK_INPUT, "AHF30");
    lngAF30  = PDK_GetCurveIndex(PRIZM_SDK_INPUT, "AF30");
lngLL3  = PDK_GetCurveIndex(PRIZM_SDK_INPUT, "LL3");
    lngRSHAL  = PDK_GetCurveIndex(PRIZM_SDK_INPUT, "RSHAL");  //1
lngRXOZ  = PDK_GetCurveIndex(PRIZM_SDK_INPUT, "RXOZ");
    lngRXO8  = PDK_GetCurveIndex(PRIZM_SDK_INPUT, "RXO8");      //1
lngCALI_1  = PDK_GetCurveIndex(PRIZM_SDK_INPUT, "CALI_1");
    lngCALIPER  = PDK_GetCurveIndex(PRIZM_SDK_INPUT, "CALIPER");
    lngGR2  = PDK_GetCurveIndex(PRIZM_SDK_INPUT, "GR2");
    lngGR3  = PDK_GetCurveIndex(PRIZM_SDK_INPUT, "GR3");
    lngHMRS  = PDK_GetCurveIndex(PRIZM_SDK_INPUT, "HMRS");

    lngDPSS  = PDK_GetCurveIndex(PRIZM_SDK_INPUT, "DPSS");
    lngNPSS  = PDK_GetCurveIndex(PRIZM_SDK_INPUT, "NPSS");
    lngDPOR  = PDK_GetCurveIndex(PRIZM_SDK_INPUT, "DPOR");
    lngCNPOR  = PDK_GetCurveIndex(PRIZM_SDK_INPUT, "CNPOR");

    lngRILD  = PDK_GetCurveIndex(PRIZM_SDK_INPUT, "RILD");
```

150

```
//Get the indices for the output curves
lngPHIDout = PDK_GetCurveIndex(PRIZM_SDK_OUTPUT, "PHIDout");
lngPHIA = PDK_GetCurveIndex(PRIZM_SDK_OUTPUT, "PHIA");
lngPHIE = PDK_GetCurveIndex(PRIZM_SDK_OUTPUT, "PHIE");
lngVshl = PDK_GetCurveIndex(PRIZM_SDK_OUTPUT, "Vshl");
lngRoDW = PDK_GetCurveIndex(PRIZM_SDK_OUTPUT, "RoDW");
lngSwE = PDK_GetCurveIndex(PRIZM_SDK_OUTPUT, "SwE");
lngSwA = PDK_GetCurveIndex(PRIZM_SDK_OUTPUT, "SwA");
lngSwT = PDK_GetCurveIndex(PRIZM_SDK_OUTPUT, "SwT");
lngBVW = PDK_GetCurveIndex(PRIZM_SDK_OUTPUT, "BVW");
lngSwMS = PDK_GetCurveIndex(PRIZM_SDK_OUTPUT, "SwMS");
lngSwI = PDK_GetCurveIndex(PRIZM_SDK_OUTPUT, "SwI");
    lngThickness = PDK_GetCurveIndex(PRIZM_SDK_OUTPUT, "Thickness");        //6
    lngRint = PDK_GetCurveIndex(PRIZM_SDK_OUTPUT, "Rint");
    lngCRHOB = PDK_GetCurveIndex(PRIZM_SDK_OUTPUT, "CRHOB");
    lngCRHOBcsh = PDK_GetCurveIndex(PRIZM_SDK_OUTPUT, "CRHOBcsh");
    lngCCGR = PDK_GetCurveIndex(PRIZM_SDK_OUTPUT, "CCGR");
    lngCCRHOB = PDK_GetCurveIndex(PRIZM_SDK_OUTPUT, "CCRHOB");
    lngCleanCoal = PDK_GetCurveIndex(PRIZM_SDK_OUTPUT, "CleanCoal");
    lngHGRC = PDK_GetCurveIndex(PRIZM_SDK_OUTPUT, "HGRC");
    lngHash = PDK_GetCurveIndex(PRIZM_SDK_OUTPUT, "Hash");
    lngcsh = PDK_GetCurveIndex(PRIZM_SDK_OUTPUT, "csh");
    lngBentCSH = PDK_GetCurveIndex(PRIZM_SDK_OUTPUT, "BentCSH");
    lngNGR = PDK_GetCurveIndex(PRIZM_SDK_OUTPUT, "NGR");
    lngashcontent = PDK_GetCurveIndex(PRIZM_SDK_OUTPUT, "ashcontent");

    lngGRcsh = PDK_GetCurveIndex(PRIZM_SDK_OUTPUT, "GRcsh");

    lngCoalTh = PDK_GetCurveIndex(PRIZM_SDK_OUTPUT, "CoalTh");
    lngHGRCTh = PDK_GetCurveIndex(PRIZM_SDK_OUTPUT, "HGRCTh");
    lngAshyCTh = PDK_GetCurveIndex(PRIZM_SDK_OUTPUT, "AshyCTh");
    lngCSHTh = PDK_GetCurveIndex(PRIZM_SDK_OUTPUT, "CSHTh");
    lngBCSHTh = PDK_GetCurveIndex(PRIZM_SDK_OUTPUT, "BCSHTh");
    lngWashout = PDK_GetCurveIndex(PRIZM_SDK_OUTPUT, "Washout");
    lngGRcoal = PDK_GetCurveIndex(PRIZM_SDK_OUTPUT, "GRcoal");

    lngcoal1 = PDK_GetCurveIndex(PRIZM_SDK_OUTPUT, "coal1");
    lngtopdepth1 = PDK_GetCurveIndex(PRIZM_SDK_OUTPUT, "topdepth1");
    lngcoal percent1 = PDK_GetCurveIndex(PRIZM_SDK_OUTPUT, "coal percent1");

    lngcoal2 = PDK_GetCurveIndex(PRIZM_SDK_OUTPUT, "coal2");
    lngtopdepth2 = PDK_GetCurveIndex(PRIZM_SDK_OUTPUT, "topdepth2");
    lngcoal percent2 = PDK_GetCurveIndex(PRIZM_SDK_OUTPUT, "coal percent2");

    lngcoal3 = PDK_GetCurveIndex(PRIZM_SDK_OUTPUT, "coal3");
    lngtopdepth3 = PDK_GetCurveIndex(PRIZM_SDK_OUTPUT, "topdepth3");
    lngcoal percent3 = PDK_GetCurveIndex(PRIZM_SDK_OUTPUT, "coal percent3");

    lngcoal4 = PDK_GetCurveIndex(PRIZM_SDK_OUTPUT, "coal4");
    lngtopdepth4 = PDK_GetCurveIndex(PRIZM_SDK_OUTPUT, "topdepth4");
    lngcoal percent4 = PDK_GetCurveIndex(PRIZM_SDK_OUTPUT, "coal percent4");

    lngcoal5 = PDK_GetCurveIndex(PRIZM_SDK_OUTPUT, "coal5");
    lngtopdepth5 = PDK_GetCurveIndex(PRIZM_SDK_OUTPUT, "topdepth5");
    lngcoal percent5 = PDK_GetCurveIndex(PRIZM_SDK_OUTPUT, "coal percent5");

    lngcoal6 = PDK_GetCurveIndex(PRIZM_SDK_OUTPUT, "coal6");
    lngtopdepth6 = PDK_GetCurveIndex(PRIZM_SDK_OUTPUT, "topdepth6");
    lngcoal percent6 = PDK_GetCurveIndex(PRIZM_SDK_OUTPUT, "coal percent6");

    lngcoal7 = PDK_GetCurveIndex(PRIZM_SDK_OUTPUT, "coal7");
    lngtopdepth7 = PDK_GetCurveIndex(PRIZM_SDK_OUTPUT, "topdepth7");
```

```
lngcoal percent7 = PDK_GetCurveIndex(PRIZM_SDK_OUTPUT, "coal percent7");

lngcoal8 = PDK_GetCurveIndex(PRIZM_SDK_OUTPUT, "coal8");
lngtopdepth8 = PDK_GetCurveIndex(PRIZM_SDK_OUTPUT, "topdepth8");
lngcoal percent8 = PDK_GetCurveIndex(PRIZM_SDK_OUTPUT, "coal percent8");

lngcleancoal1 = PDK_GetCurveIndex(PRIZM_SDK_OUTPUT, "cleancoal1");
lngHGRC1 = PDK_GetCurveIndex(PRIZM_SDK_OUTPUT, "HGRC1");

lngcleancoal2 = PDK_GetCurveIndex(PRIZM_SDK_OUTPUT, "cleancoal2");
lngHGRC2 = PDK_GetCurveIndex(PRIZM_SDK_OUTPUT, "HGRC2");

lngcleancoal3 = PDK_GetCurveIndex(PRIZM_SDK_OUTPUT, "cleancoal3");
lngHGRC3 = PDK_GetCurveIndex(PRIZM_SDK_OUTPUT, "HGRC3");

lngcleancoal4 = PDK_GetCurveIndex(PRIZM_SDK_OUTPUT, "cleancoal4");
lngHGRC4 = PDK_GetCurveIndex(PRIZM_SDK_OUTPUT, "HGRC4");

lngcleancoal5 = PDK_GetCurveIndex(PRIZM_SDK_OUTPUT, "cleancoal5");
lngHGRC5 = PDK_GetCurveIndex(PRIZM_SDK_OUTPUT, "HGRC5");

lngcleancoal6 = PDK_GetCurveIndex(PRIZM_SDK_OUTPUT, "cleancoal6");
lngHGRC6 = PDK_GetCurveIndex(PRIZM_SDK_OUTPUT, "HGRC6");

lngcleancoal7 = PDK_GetCurveIndex(PRIZM_SDK_OUTPUT, "cleancoal7");
lngHGRC7 = PDK_GetCurveIndex(PRIZM_SDK_OUTPUT, "HGRC7");

lngcleancoal8 = PDK_GetCurveIndex(PRIZM_SDK_OUTPUT, "cleancoal8");
lngHGRC8 = PDK_GetCurveIndex(PRIZM_SDK_OUTPUT, "HGRC8");

lngGIP = PDK_GetCurveIndex(PRIZM_SDK_OUTPUT, "GIP");
lngGIPcleancoal = PDK_GetCurveIndex(PRIZM_SDK_OUTPUT, "GIPcleancoal");
lngGIPhgrc = PDK_GetCurveIndex(PRIZM_SDK_OUTPUT, "GIPhgrc");
lngGIPashycoal = PDK_GetCurveIndex(PRIZM_SDK_OUTPUT, "GIPashycoal");
lngGIPshales = PDK_GetCurveIndex(PRIZM_SDK_OUTPUT, "GIPshales");

lngCO2 = PDK_GetCurveIndex(PRIZM_SDK_OUTPUT, "CO2");
lngDPORO = PDK_GetCurveIndex(PRIZM_SDK_OUTPUT, "DPORO");

lngsandgas = PDK_GetCurveIndex(PRIZM_SDK_OUTPUT, "sandgas");
lngGIPsandgas = PDK_GetCurveIndex(PRIZM_SDK_OUTPUT, "GIPsandgas");
lngSW = PDK_GetCurveIndex(PRIZM_SDK_OUTPUT, "SW");

lngsand = PDK_GetCurveIndex(PRIZM_SDK_OUTPUT, "sand");
lngsandphih = PDK_GetCurveIndex(PRIZM_SDK_OUTPUT, "sandphih");

lngRILDavg = PDK_GetCurveIndex(PRIZM_SDK_OUTPUT, "RILDavg");

lnggascontentcurve = PDK_GetCurveIndex(PRIZM_SDK_OUTPUT, "gascontentcurve");

lngTGIPclean = PDK_GetCurveIndex(PRIZM_SDK_OUTPUT, "TGIPclean");
lngTGIPhgr = PDK_GetCurveIndex(PRIZM_SDK_OUTPUT, "TGIPhgr");
lngTGIPashy = PDK_GetCurveIndex(PRIZM_SDK_OUTPUT, "TGIPashy");
lngTGIPcsh = PDK_GetCurveIndex(PRIZM_SDK_OUTPUT, "TGIPcsh");
lngTGIPbcsh = PDK_GetCurveIndex(PRIZM_SDK_OUTPUT, "TGIPbcsh");
lngTGIP = PDK_GetCurveIndex(PRIZM_SDK_OUTPUT, "TGIP");


lngCleanCoalGR = PDK_GetCurveIndex(PRIZM_SDK_OUTPUT, "CleanCoalGR");
lngCleanCoalRILD = PDK_GetCurveIndex(PRIZM_SDK_OUTPUT, "CleanCoalRILD");
lngCleanCoalPHIN = PDK_GetCurveIndex(PRIZM_SDK_OUTPUT, "CleanCoalPHIN");
```

```
//4 Mineral...
lngP1 = PDK_GetCurveIndex(PRIZM_SDK_OUTPUT, "P1");
lngP2 = PDK_GetCurveIndex(PRIZM_SDK_OUTPUT, "P2");
lngP3 = PDK_GetCurveIndex(PRIZM_SDK_OUTPUT, "P3");
lngP4 = PDK_GetCurveIndex(PRIZM_SDK_OUTPUT, "P4");
lngP1dsp = PDK_GetCurveIndex(PRIZM_SDK_OUTPUT, "P1dsp");
lngP2dsp = PDK_GetCurveIndex(PRIZM_SDK_OUTPUT, "P2dsp");
lngP3dsp = PDK_GetCurveIndex(PRIZM_SDK_OUTPUT, "P3dsp");
lngP4dsp = PDK_GetCurveIndex(PRIZM_SDK_OUTPUT, "P4dsp");
lngUMA = PDK_GetCurveIndex(PRIZM_SDK_OUTPUT, "UMA");
lngDGA = PDK_GetCurveIndex(PRIZM_SDK_OUTPUT, "DGA");

//Calculate coal thickness

numSamples = PDK_GetNumSamples();
    Resolution = PDK_GetStep();

    //arrays

    thicknessDA = (double *)malloc(numSamples*sizeof(double));

    //OTHERS ARRAYS

    rintDA= (double *)malloc(numSamples*sizeof(double));
    rhobDA= (double *)malloc(numSamples*sizeof(double));
    cshDA= (double *)malloc(numSamples*sizeof(double));
    cgrDA= (double *)malloc(numSamples*sizeof(double));
    crhobDA= (double *)malloc(numSamples*sizeof(double));

    //OTHER ARRAYS
    cleancoalA= (double *)malloc(numSamples*sizeof(double));
    HGRA= (double *)malloc(numSamples*sizeof(double));
    HASHA= (double *)malloc(numSamples*sizeof(double));
    BENTCSHA= (double *)malloc(numSamples*sizeof(double));
    CSHA= (double *)malloc(numSamples*sizeof(double));


    //input data curve array

    gr= (double *)malloc(numSamples*sizeof(double));
    rhob= (double *)malloc(numSamples*sizeof(double));
    res= (double *)malloc(numSamples*sizeof(double));
    cali= (double *)malloc(numSamples*sizeof(double));
    NGRA= (double *)malloc(numSamples*sizeof(double));
    GRcshA= (double *)malloc(numSamples*sizeof(double));

    Washouts= (double *)malloc(numSamples*sizeof(double));
    GRcoalA= (double *)malloc(numSamples*sizeof(double));
    RILDnm= (double *)malloc(numSamples*sizeof(double));

    //crhobDA=malloc(4*numSamples);

    //GR

    //identiy main path and high resolution curves

    for( N = 0; N <= numSamples - 1; N++)
    {
        RHOB=PDK_GetCurveValueAt(lngRHOB, N);
        RHOB2=PDK_GetCurveValueAt(lngRHOB2, N);

        if(PDK_IsNotNull(RHOB) && PDK_IsNotNull(RHOB2) && steprhob==0 )
```

```
            {
                    pr1=RHOB;
                    pr2=RHOB2;

                    steprhob++;
            }
            else if(PDK_IsNotNull(RHOB) && PDK_IsNotNull(RHOB2))
            {
                    steprhob1=steprhob1+ fabs(RHOB-pr1);
                    steprhob2=steprhob2+ fabs(RHOB2-pr2);

                    pr1=RHOB;
                    pr2=RHOB2;

                    steprhob++;
            }
            if(steprhob>100)
            {
                    goto outside;
            }
        }
outside:;

        stepgr1=steprhob1;
        stepgr2=steprhob2;

        for( N = 0; N <= numSamples - 1; N++)
        {
                GR=PDK_GetCurveValueAt(lngGR, N);
                GR_MAIN=PDK_GetCurveValueAt(lngGR_MAIN, N);
                CGR=PDK_GetCurveValueAt(lngCGR, N);
                EHGR=PDK_GetCurveValueAt(lngEHGR, N);
                HGR=PDK_GetCurveValueAt(lngHGR, N);
                GR2=PDK_GetCurveValueAt(lngGR2, N);
                GR3=PDK_GetCurveValueAt(lngGR3, N);

                if(PDK_IsNotNull(GR2) && PDK_IsNotNull(GR) )
                {
                        if(stepgr1>stepgr2)
                        {
                                *(gr+N) = GR;
                        }
                        else
                        {
                                *(gr+N) = GR2;
                        }
                }
                else if(PDK_IsNotNull(GR3))
                {
                        *(gr+N) = GR3;
                }
                else if(PDK_IsNotNull(GR2))
                {
                        *(gr+N) = GR2;
                }
                else if(PDK_IsNotNull(EHGR))
                {
                        *(gr+N) = EHGR;
                }
                else if(PDK_IsNotNull(HGR))
                {
                        *(gr+N) = HGR;
```

```
        }
        else if(PDK_IsNotNull(GR))
        {
                *(gr+N) = GR;
        }
        else if(PDK_IsNotNull(GR_MAIN))
        {
                *(gr+N) = GR_MAIN;
        }
        else if(PDK_IsNotNull(CGR))
        {
                *(gr+N) = CGR;
        }

        else
        {
                *(gr+N) = PDK_GetNull();
        }
}

//Normalizing GR

for( N = 0; N <= numSamples - 1; N++)
{
        if(*(gr+N)>0 && *(gr+N)<=GRmin)
        {
                GRmin=*(gr+N);
        }
}

for( N = 0; N <= numSamples - 1; N++)
{
        *(gr+N)=15+*(gr+N)-GRmin;
        NGR=*(gr+N);
        PDK_SetCurveValueAt(lngNGR, N, NGR);
}

//RHOB

for( N = 0; N <= numSamples - 1; N++)
{
        RHOB=PDK_GetCurveValueAt(lngRHOB, N);
        RHOB_MAIN=PDK_GetCurveValueAt(lngRHOB_MAIN, N);
        RHOZ=PDK_GetCurveValueAt(lngRHOZ, N);
        RHO8=PDK_GetCurveValueAt(lngRHO8, N);
        RHOB2=PDK_GetCurveValueAt(lngRHOB2, N);
        RHOB3=PDK_GetCurveValueAt(lngRHOB3, N);

        if(PDK_IsNotNull(RHOB) && PDK_IsNotNull(RHOB2) )
        {
                if(steprhob1>steprhob2)
                {
                        *(rhob+N) = RHOB;
                }
                else
                {
                        *(rhob+N) = RHOB2;
                }
        }
        else if(PDK_IsNotNull(RHOB3))
        {
                *(rhob+N) = RHOB3;
```

```
            }
            else if(PDK_IsNotNull(RHOB2))
            {
                    *(rhob+N) = RHOB2;
            }
            else if(PDK_IsNotNull(RHO8))
            {
                    *(rhob+N) = RHO8;
            }
            else if(PDK_IsNotNull(RHOB_MAIN))
            {
                    *(rhob+N) = RHOB_MAIN;
            }
            else if(PDK_IsNotNull(RHOZ))
            {
                    *(rhob+N) = RHOZ;
            }
            else if(PDK_IsNotNull(RHOB))
            {
                    *(rhob+N) = RHOB;
            }
            else
            {
                    *(rhob+N) = PDK_GetNull();
            }

    }

// correct the artificial number at the top or the bottom of a curve

NN = 0;

if( *(rhob +NN) < 2.3)
{
        while(*(rhob+NN)<2.3 && NN<numSamples)
        {
                *(rhob+NN) = PDK_GetNull();
                NN++;
        }
}

NN = numSamples -1;

if( *(rhob +NN) < 2.3)
{
        while(*(rhob+NN)<2.3 && NN>0)
        {
                *(rhob+NN) = PDK_GetNull();
                NN--;
        }
}

//RILD

//Rinterval=20/Resolution;

//for( N = 0; N <= Rinterval; N++)
//{
        //RILD=PDK_GetCurveValueAt(lngRILD, N);
        //if(RILD>0.1 && RILD<100)
        //{
        //      RILDsum=RILDsum+RILD;
```

156

```
            //      RILDstep++;
            //}
//}

//RILDavg = RILDsum/RILDstep;

//for( N = 0; N <= numSamples - 1; N++)
//{
//      RILDavg = RILDsum/RILDstep;

//      PDK_SetCurveValueAt( lngRILDavg, N, RILDavg);
//}

for( N = 0; N <= numSamples - 1; N++)
{
        RILD=PDK_GetCurveValueAt(lngRILD, N);

        if(RILD>0)
        {
                *(RILDnm+N)=RILD;
        }
}


//Calculate DPORO

for( N = 0; N <= numSamples - 1; N++)
{
        DPORO=(2.64-*(rhob+N))/(2.64-1.02)*100;

        PDK_SetCurveValueAt( lngDPORO, N, DPORO);
}

//Calculate gas sand, SW, AND GAS IN SAND


for( N = 0; N <= numSamples - 1; N++)
{
        //Gas sand
        DPSS=PDK_GetCurveValueAt(lngDPSS, N);
        NPSS=PDK_GetCurveValueAt(lngNPSS, N);
        DPOR=PDK_GetCurveValueAt(lngDPOR, N);
        CNPOR=PDK_GetCurveValueAt(lngCNPOR, N);
        DPHI=PDK_GetCurveValueAt(lngDPHI, N);
        NPHI=PDK_GetCurveValueAt(lngNPHI, N);

        DPORO=(2.64-*(rhob+N))/(2.64-1.02)*100;
        if(DPOR <0)
        {
                DPOR=DPORO;
        }

        if(*(gr +N)<50 && *(rhob +N)>2.35 && NPSS<DPSS && NPSS>0 && *(gr +N)>0 && DPSS>0.12)
        {
                sandgas=sandgas+Resolution;

                Vshls=(*(gr +N)-15)/82;
                DPSS=DPSS*(1-Vshls);

                SW=sqrt(0.17/( *(RILDnm +N) *DPSS*DPSS));

                if(SW>1 || SW<0.35)
```

157

```
                    {
                        SW=1;
                    }

                PDK_SetCurveValueAt( lngSW, N, SW);

                    GIPsandgas=GIPsandgas+Resolution*43560*160*(1-
SW)*DPSS/1000000/(0.2829*0.93*555/(0.43*(PDK_GetStart()+Resolution*N)));
            }
            else if(*(gr +N)<50 && *(rhob +N)>2.35 && CNPOR<DPOR && CNPOR>0 && DPOR>12)
            {
                sandgas=sandgas+Resolution;

                Vshls=(*(gr +N)-15)/82;
                DPOR=DPOR*(1-Vshls);

                SW=sqrt(0.17/( *(RILDnm +N) *DPOR*DPOR/10000));

                if(SW>1 || SW<0.35)
                {
                        SW=1;
                }

                PDK_SetCurveValueAt( lngSW, N, SW);

                    GIPsandgas=GIPsandgas+Resolution*43560*160*(1-
SW)*DPOR/1000000/(0.2829*0.93*555/(0.43*(PDK_GetStart()+Resolution*N)));
            }
            else if(*(gr +N)<50 && *(rhob +N)>2.35 && NPHI<DPHI && NPHI>0 && DPHI>0.12)
            {
                sandgas=sandgas+Resolution;

                Vshls=(*(gr +N)-15)/82;
                DPHI=DPHI*(1-Vshls);

                SW=sqrt(0.17/( *(RILDnm +N) *DPHI*DPHI));

                if(SW>1 || SW<0.35)
                {
                        SW=1;
                }

                PDK_SetCurveValueAt( lngSW, N, SW);

                    GIPsandgas=GIPsandgas+Resolution*43560*160*(1-
SW)*DPHI/1000000/(0.2829*0.93*555/(0.43*(PDK_GetStart()+Resolution*N)));
            }

            PDK_SetCurveValueAt( lngsandgas, N, sandgas);
            PDK_SetCurveValueAt( lngGIPsandgas, N, GIPsandgas);
        }

        //SAND AND SAND PHIH

        for( N = 0; N <= numSamples - 1; N++)
        {
            DPSS=PDK_GetCurveValueAt(lngDPSS, N);
            NPSS=PDK_GetCurveValueAt(lngNPSS, N);
            DPOR=PDK_GetCurveValueAt(lngDPOR, N);
            CNPOR=PDK_GetCurveValueAt(lngCNPOR, N);
            DPHI=PDK_GetCurveValueAt(lngDPHI, N);
            NPHI=PDK_GetCurveValueAt(lngNPHI, N);
```

```
DPORO=(2.64-*(rhob+N))/(2.64-1.02)*100;
if(DPOR <0)
{
        DPOR=DPORO;
}

if(*(gr +N)<50 && *(rhob +N)>2.35 && DPOR>0.09)
{
        sand=sand+Resolution;
        sandphih=sandphih+Resolution*DPOR/100;
}
else if(*(gr +N)<50 && *(rhob +N)>2.35 && DPSS>9)
{
        sand=sand+Resolution;
        sandphih=sandphih+Resolution*DPSS;
}
else if(*(gr +N)<50 && *(rhob +N)>2.35 && DPHI>0.09)
{
        sand=sand+Resolution;
        sandphih=sandphih+Resolution*DPHI;
}

}

for( N = 0; N <= numSamples - 1; N++)
{
        PDK_SetCurveValueAt( lngsand, N, sand);
        PDK_SetCurveValueAt( lngsandphih, N, sandphih);
}

//resistivity

for( N = 0; N <= numSamples - 1; N++)
{
        SHALLOW_RT=PDK_GetCurveValueAt(lngSHALLOW_RT, N);
        AO30=PDK_GetCurveValueAt(lngAO30, N);
        AHT30=PDK_GetCurveValueAt(lngAHT30, N);
        AT30=PDK_GetCurveValueAt(lngAT30, N);
        SGRD=PDK_GetCurveValueAt(lngSGRD, N);
        SFLU=PDK_GetCurveValueAt(lngSFLU, N);
        RLL3=PDK_GetCurveValueAt(lngRLL3, N);
        DFL=PDK_GetCurveValueAt(lngDFL, N);
        AHO30=PDK_GetCurveValueAt(lngAHO30, N);
        AHF30=PDK_GetCurveValueAt(lngAHF30, N);
        AF30=PDK_GetCurveValueAt(lngAF30, N);
        LL3=PDK_GetCurveValueAt(lngLL3, N);
        RSHAL=PDK_GetCurveValueAt(lngRSHAL, N);
        RXOZ=PDK_GetCurveValueAt(lngRXOZ, N);
        RXO8=PDK_GetCurveValueAt(lngRXO8, N);
        HMRS=PDK_GetCurveValueAt(lngHMRS, N);

        if(PDK_IsNotNull(RLL3))
        {
                *(res+N) = RLL3;
        }

        else if(PDK_IsNotNull(AO30))
        {
                *(res+N) = AO30;
        }
        else if(PDK_IsNotNull(AHO30))
```

```
        {
                *(res+N) = AHO30;
        }
        else if(PDK_IsNotNull(AHT30))
        {
                *(res+N) = AHT30;
        }
        else if(PDK_IsNotNull(AT30))
        {
                *(res+N) = AT30;
        }
        else if(PDK_IsNotNull(SGRD))
        {
                *(res+N) = SGRD;
        }
        else if(PDK_IsNotNull(SFLU))
        {
                *(res+N) = SFLU;
        }
        else if(PDK_IsNotNull(DFL))
        {
                *(res+N) = DFL;
        }
        else if(PDK_IsNotNull(AHF30))
        {
                *(res+N) = AHF30;
        }
        else if(PDK_IsNotNull(AF30))
        {
                *(res+N) = AF30;
        }
        else if(PDK_IsNotNull(LL3))
        {
                *(res+N) = LL3;
        }
        else if(PDK_IsNotNull(RSHAL))
        {
                *(res+N) = RSHAL;
        }
        else if(PDK_IsNotNull(SHALLOW_RT))
        {
                *(res+N) = SHALLOW_RT;
        }
        else if(PDK_IsNotNull(RXOZ))
        {
                *(res+N) = RXOZ;
        }
        else if(PDK_IsNotNull(RXO8))
        {
                *(res+N) = RXO8;
        }
        else if(PDK_IsNotNull(HMRS))
        {
                *(res+N) = HMRS;
        }

        else
        {
                *(res+N) = PDK_GetNull();
        }

}
```

```
//CALI

for( N = 0; N <= numSamples - 1; N++)
{
        CALI=PDK_GetCurveValueAt(lngCALI, N);
        DCAL=PDK_GetCurveValueAt(lngDCAL, N);
        HCAL=PDK_GetCurveValueAt(lngHCAL, N);
        CALI_MAIN=PDK_GetCurveValueAt(lngCALI_MAIN, N);
        CALI_1=PDK_GetCurveValueAt(lngCALI_1, N);
        CALIPER=PDK_GetCurveValueAt(lngCALIPER, N);


        if(PDK_IsNotNull(DCAL))
        {
              *(cali+N) = DCAL;
        }
        else if(PDK_IsNotNull(HCAL))
        {
              *(cali+N) = HCAL;
        }
        else if(PDK_IsNotNull(CALIPER))
        {
              *(cali+N) = CALIPER;
        }
        else if(PDK_IsNotNull(CALI_MAIN))
        {
              *(cali+N) = CALI_MAIN;
        }
        else if(PDK_IsNotNull(CALI_1))
        {
              *(cali+N) = CALI_1;
        }
        else if(PDK_IsNotNull(CALI))
        {
              *(cali+N) = CALI;
        }
        else
        {
              *(cali+N) = PDK_GetNull();
        }
}

resolution = PDK_GetStep();

// Calculate the washout amounts

if(resolution > 0.2 )
{
        TopCali = numSamples -150;
        BottomCali = numSamples - 100;
}

else
{
        TopCali = numSamples -500;
        BottomCali = numSamples - 450;
}

if(PDK_IsNotNull(*(cali + TopCali)))
{
```

```
            while( PDK_IsNotNull(*(cali + TopCali)) && (TopCali < BottomCali))
            {
                   SumCali = SumCali + *(cali + TopCali);
                   TopCali++;
                   CaliStep++;
            }

            AvgCali = SumCali/CaliStep;


    }

    else if(PDK_IsNull(*(cali + TopCali)) && TopCali>0)
    {
            while(PDK_IsNull(*(cali + TopCali)))
            {
                   TopCali--;
            }
            if(TopCali>0)
            {
                   AvgCali = *(cali + TopCali);
            }
    }

    for( N = 0; N <= numSamples - 1; N++)
    {
            if(PDK_IsNotNull(*(cali + N)))
            {
                   Washout = *(cali +N) - AvgCali;
                   PDK_SetCurveValueAt( lngWashout, N, Washout );
                   *(Washouts +N)=Washout;
            }
    }

    //calculate csh GR
    for( N = 0; N <= numSamples - 1; N++)
    {
            NGR=*(gr+N);

            if(PDK_IsNull(NGR))
            {
                   GRcsh = PDK_GetNull();
            }
            else if((GRup==TRUE)  && (NGR<= GRpre) && (NGR >90))
            {
                   GRup=FALSE;
                   indGRM=N-1;
                   stepGR=ceil((NGR) * 0.43 / 150 / resolution);
                   GRcsh=146;
                   GRpre=NGR;
                   while(stepGR>=0 && indGRM-stepGR >=0 && indGRM+stepGR < numSamples)
                   {
                          PDK_SetCurveValueAt( lngGRcsh, indGRM-stepGR, GRcsh );
                          PDK_SetCurveValueAt( lngGRcsh, indGRM+stepGR, GRcsh );
                          stepGR--;
                          *(GRcshA+(indGRM-stepGR))=GRcsh;
                          *(GRcshA+(indGRM+stepGR))=GRcsh;
                   }


            }
            else if((NGR)>GRpre)
            {
```

```
                          GRup=TRUE;
                          GRpre=NGR;
                  }
              GRpre=NGR;
      }

      for( N = 0; N <= numSamples - 1; N++)
      {
              if(*(GRcshA+N)<0)
              {
                      *(GRcshA+N)=PDK_GetNull();
              }
      }


      //calculate coal thickness

      for( N = 0; N <= numSamples - 1; N++)                              //7
{
              RHOB = *(rhob +N);

              if( PDK_IsNull(RHOB) )
              {
goto EndOfThickness;
              }
              else if(L2H == FALSE && RHOB <= 2.0)
              {
                      L2H = TRUE;
                      indtopH = N;
              }
              else if((L2H == TRUE) && (RHOB > 2.0))
              {
                      L2H = FALSE;
                      indbottomH = N-1;
                      Thickness = (indbottomH - indtopH)* Resolution;

                      ThicknessA[indexH]=Thickness;
                      indtopHA[indexH]=indtopH;
                      indbottomHA[indexH]=indbottomH;
                      indexH++;

                      //Correct GR for thickness
                      aindtopH = indtopH;
                      bindtopH = indtopH;
                      cindtopH = indtopH;

                      if(Thickness <=3)
                      {
                              CCGR=*(gr+aindtopH);

                              while(aindtopH<indbottomH)
                              {
                                      aindtopH++;

                                      if (CCGR> *(gr+aindtopH))
                                      {
                                              CCGR=*(gr+aindtopH);
                                      }
                              }

                              while(bindtopH<=indbottomH)
```

```
                        {
                                *(cgrDA+bindtopH) = CCGR;
                                PDK_SetCurveValueAt( lngCCGR, bindtopH, CCGR );
                                bindtopH++;
                        }
                }

                //output the coal thickness
                while(indbottomH>=cindtopH)
                {
                        *(thicknessDA+cindtopH)=Thickness;
                        PDK_SetCurveValueAt(lngThickness, cindtopH, Thickness);
                        cindtopH++;
                }

        }

        EndOfThickness:;
}

//identify the GR humps

for( N = 0; N <= numSamples - 1; N++)
{
        if(PDK_IsNull(*(gr+N)))
        {
                goto ENDOFGR;
        }
        else if(GRup2 == FALSE && *(gr+N)>GRprev2 && MaxGR2>0)
        {
                GRup2 = TRUE;
                MinGRind2 = N-1;
                MinGRind=N-1;
                MinGR2 = *(gr+MinGRind2);

                if(MaxGR2>0)
                {
                        GRboundary2 = (MaxGR2 + MinGR2)/2;

                        while(*(gr+MinGRind2)<=GRboundary2)
                        {
                                *(gr+MinGRind2)=65;
                                MinGRind2--;
                        }
                }

                GRprev2 = *(gr+N);
        }
        else if(GRup2 == TRUE && *(gr+N)<GRprev2)
        {
                GRup2 = FALSE;
                MaxGRind2 = N-1;
                MaxGR2 = *(gr+MaxGRind2);

                if(MinGR2>0)
                {
                        GRboundary2 = (MaxGR2 + MinGR2)/2;

                        while(*(gr+MinGRind)<=GRboundary2)
                        {
                                *(gr+MinGRind)=65;
                                MinGRind++;
```

164

```
                        }
                }

                GRprev2 = *(gr+N);
        }
        else if(*(gr+N)>GRprev2)
        {
                GRprev2 = *(gr+N);
                GRup2 = TRUE;
        }
        else
                GRprev2 = *(gr+N);

ENDOFGR:;
        }




        //select the thickest coal bed for rhob check

        if(indexH>0)
        {
                Coalbedind = indexH -1;
        }

        MaxCoalTh = ThicknessA[Coalbedind];
        MaxCoalThInd = Coalbedind;

        while(Coalbedind>0)
        {
                Coalbedind--;

                if(ThicknessA[Coalbedind] >= MaxCoalTh)
                {
                        MaxCoalTh = ThicknessA[Coalbedind];
                        MaxCoalThInd = Coalbedind;
                }
        }


        //select the thickest coal bed for rhob check

        TopOfThikCoal = indtopHA[MaxCoalThInd];
        BottomOfThikCoal = indbottomHA[MaxCoalThInd];

        TopOfThikCoal2 = indtopHA[MaxCoalThInd];
        BottomOfThikCoal2 = indbottomHA[MaxCoalThInd];



        for( N = 0; N <= numSamples - 1; N++)
        {
                if(*(cgrDA+N)<0)
                {
                        *(cgrDA+N)=PDK_GetNull();
                }
        }

        for( N = 0; N <= numSamples - 1; N++)
        {
                if(*(thicknessDA+N)<0)
```

```
            {
                *(thicknessDA+N)=PDK_GetNull();
            }
    }


//Select the thickest coal interval and calculate its average resistivity


    while(TopOfThikCoal2 < BottomOfThikCoal2)
    {
            RLL3 = *(res+ TopOfThikCoal2);
            if( PDK_IsNull(RLL3) )
            {
                    TopOfThikCoal2++;
            }
            else if(RLL3>2600)
            {
                    TopOfThikCoal2++;
            }
            else
            {
                    Rsum=Rsum+RLL3;
                    TopOfThikCoal2++;
                    Tstep++;
            }
    }


    Ravg = Rsum/Tstep;

    //Calculate the interface resistivity


    if(Resolution<0.1)
    {
            Mstepdown = 15;
            Mstepup = 15;
    }
    else if(Resolution >0.06 && Resolution<0.15)
    {
            Mstepdown = 7;
            Mstepup = 7;
    }
else if(Resolution >0.15 && Resolution<0.3)
    {
            Mstepdown = 3;
            Mstepup = 3;
    }
    else if(Resolution >0.3)
    {
            Mstepdown = 2;
            Mstepup = 2;
    }
for( N = 0; N <= numSamples - 1; N++)
    {
            RLL3 = *(res +N);
            PreviousR=RLL3;
            start=N;
            RmaxN=N+100;
```

```
while(start<=numSamples-1 && start<RmaxN)
{
        start++;
        Resistivity=*(res +start);

        if(ResistivityUP==TRUE && Resistivity<PreviousR && Resistivity<3000)
        {
                ResistivityUP=FALSE;
                Rmax=*(res +(start-1));
                RmaxN=start;
        }
        else if(Resistivity>PreviousR)
        {
                ResistivityUP=TRUE;
                PreviousR=Resistivity;
        }
        else
        {
                PreviousR=Resistivity;
        }
}


if(PDK_IsNull(RLL3))
{
        goto EndOfRint;
}

else if((prevR < RLL3) && (downR == TRUE) && (*(res+(N-1))<0.5*Rmax))
{
        downR = FALSE;
        s = N-1;
        Rint = 0;
        Rb=1.26*(*(res+s));
        RLL=*(res+s);

        while( RLL<= Rb && s<numSamples && stepdown<=Mstepdown)
        {
                stepdown++;
                s++;
                RLL=*(res+s);
        }

        N=s;
        prevR = RLL;

        s=s-stepdown;
        RLL = *(res+s);

        while(RLL<= Rb && s>0 && stepup <=Mstepup)
        {
                stepup++;
                s--;
                RLL=*(res+s);
        }
        s=s+stepup;

        while( stepup >=0 && s>stepup)
        {
                indexDAR=s-stepup;
                *(rintDA+indexDAR)=Rint;
```

167

```
                            PDK_SetCurveValueAt( lngRint, s-stepup, Rint );
                            stepup--;
            }
            while( stepdown >0 && (s+stepdown) < numSamples)
            {
                        indexDAR=s+stepdown;
                        *(rintDA+indexDAR)=Rint;
                        PDK_SetCurveValueAt( lngRint, s+stepdown, Rint );
                        stepdown--;
            }
      }

      else if(prevR > RLL3)
      {
            downR = TRUE;
            prevR = RLL3;
      }
      else
      {
            prevR=RLL3;
      }
EndOfRint:;
      }

      for( N = 0; N <= numSamples - 1; N++)
      {
            if(*(rintDA+N)<0)
            {
                  *(rintDA+N)=PDK_GetNull();
            }
      }
//Correct RHOB

 resolution = PDK_GetStep();                  //7

  for( N = 0; N <= numSamples - 1; N++)
  {
            RHOB = *(rhob +N);

            if( PDK_IsNull(RHOB) )
            {
      goto EndOfRHOB;
            }
            else if(L2 == FALSE && RHOB <= 2.0)
            {
                        indtop = N;
                        prev = RHOB;
                        L2=TRUE;
                        down = TRUE;
                        indtopa[aindex]=indtop;
      }
            else if(L2==TRUE && down == TRUE && prev < RHOB)
            {
                  down = FALSE;
                  indmin = N-1;
                  prev = RHOB;

                  if(resolution > 0.4 && (indmin-2)>0 && (indmin+4)<numSamples)
                  {
                        min = (*(rhob+indmin)
            + *(rhob+(indmin+1)))/2;
                  }
```

168

```
            else if(resolution <0.4 && resolution >0.2 && (indmin-2)>0 && (indmin+4)<numSamples)
            {
                    min = (*(rhob+(indmin-1))
                    + *(rhob+indmin))/2;
            }
            else if(resolution <0.2 && resolution >0.06 && (indmin-2)>0 && (indmin+4)<numSamples)
            {
                    min = (*(rhob+(indmin-1))+*(rhob+(indmin))+*(rhob+(indmin+1))+*(rhob+(indmin+2)))/4;
            }
            else if(resolution <0.06 && (indmin-2)>0 && (indmin+4)<numSamples)
            {
                    min = (*(rhob+(indmin-2))+*(rhob+(indmin-1))+*(rhob+(indmin))+*(rhob+(indmin+1))+
                            *(rhob+(indmin+2))+*(rhob+(indmin+3))+*(rhob+(indmin+4)))/7;


            }



    }
    else if(L2==TRUE && down==FALSE && prev >RHOB)
    {
                    down = TRUE;
                    L2 = TRUE;
                    indbottom = N-1;
                    prev = RHOB;

                    mina[aindex]=min;

                    indbottoma[aindex]=indbottom;
                    aindex++;
                    indtopa[aindex] = indbottom;
    }
    else if(L2 == TRUE && RHOB >2)
    {
            indbottom = N-1;

            mina[aindex]=min;
            indbottoma[aindex]=indbottom;


            L2 = FALSE;
            prev = RHOB;
            aindex++;



    }
    else if(RHOB > 2.0)
    {
            L2 = FALSE;
            prev = RHOB;
    }
    prev = RHOB;

EndOfRHOB:;
}
    for( indexb=0; indexb < aindex; indexb++)
    {
            TopIndex = indtopa[indexb];
            BottomIndex = indbottoma[indexb];

            while(TopIndex <= BottomIndex)
            {
                    CRHOB=mina[indexb];
```

169

```
                    *(crhobDA+ TopIndex) = CRHOB;
                    PDK_SetCurveValueAt( lngCRHOB, TopIndex, CRHOB );
                    TopIndex++;


            }
    }

    for( N = 0; N <= numSamples - 1; N++)
    {
            if(*(crhobDA+N)<0)
            {
                    *(crhobDA+N)=PDK_GetNull();
            }
    }

    //Calculate CSH density

    for( N = 0; N <= numSamples - 1; N++)
{
            RHOB = *(rhob +N);

            if( PDK_IsNull(RHOB) )
            {
    goto EndOfRHOB2;
            }
            else if(L3 == FALSE && RHOB < 2.25 && RHOB>=2.0)
            {
                    L3 = TRUE;
                    indtop2=N;
                    cshtop=N;
            }
            else if(L3==TRUE && RHOB <=2.0)
            {
                    L3 = FALSE;
                    indbottom2=N;

                    diff=indbottom2-indtop2;

                    while(indtop2<indbottom2)
                    {
                            sumcsh = sumcsh + *(rhob+indtop2);
                            indtop2++;
                    }

                    CRHOBcsh = sumcsh/diff;
                    while(cshtop <= indbottom2)
                    {
                            *(cshDA+cshtop)=CRHOBcsh;
                            PDK_SetCurveValueAt( lngCRHOBcsh, cshtop, CRHOBcsh);
                            cshtop++;
                    }
                    sumcsh=0;
            }
            else if(L3 == FALSE && RHOB >=2.0 && RHOB <2.25)
            {
                    L3=TRUE;
                    indtop2=N-1;
                    cshtop = N-1;
            }
            else if(L3==TRUE && RHOB >= 2.25)
```

```
                {
                        L3 = FALSE;
                        indbottom2 = N-1;
                        diff = indbottom2-indtop2;

                        while(indtop2<indbottom2)
                        {
                                sumcsh = sumcsh + *(rhob+indtop2);
                                indtop2++;
                        }

                        CRHOBcsh = sumcsh/diff;

                        while(cshtop <= indbottom2)
                        {
                                *(cshDA+cshtop)=CRHOBcsh;
                                PDK_SetCurveValueAt( lngCRHOBcsh, cshtop, CRHOBcsh);
                                cshtop++;
                        }
                        sumcsh=0;
                }
EndOfRHOB2:;
}

for( N = 0; N <= numSamples - 1; N++)
{
        if(*(cshDA+N)<0)
        {
                *(cshDA+N)=PDK_GetNull();
        }
}
//Correct rhob for thickness

for( N = 0; N <= numSamples - 1; N++)
{
        if(*(crhobDA +N)>0 && *(thicknessDA +N)>0 && *(thicknessDA +N) <=3 && resolution <0.2)
        {
                CCRHOB = *(crhobDA +N) * (0.0267*(*(thicknessDA +N))+0.9333);
                PDK_SetCurveValueAt(lngCCRHOB, N, CCRHOB);
                *(crhobDA+N)=CCRHOB;
        }

        else if(*(crhobDA +N)>0 && *(thicknessDA +N)>0 && *(thicknessDA +N) <=3 && resolution >=0.2 )
        {
                CCRHOB = *(crhobDA +N) * (0.0211*(*(thicknessDA +N))+0.88);
                PDK_SetCurveValueAt(lngCCRHOB, N, CCRHOB);
                *(crhobDA+N)=CCRHOB;
        }

}

for( N = 0; N <= numSamples - 1; N++)
{
        if(*(crhobDA+N)<0)
        {
                *(crhobDA+N)=PDK_GetNull();
        }
}

//Combine rhob, crhob, and rhob_csh

for( N = 0; N <= numSamples - 1; N++)
```

```
    {
        if(*(crhobDA +N)>0)
        {
            *(rhob +N) = *(crhobDA +N);
        }
    }

    for( N = 0; N <= numSamples - 1; N++)
    {
        if(*(cshDA +N)>0)
        {
            *(rhob +N) = *(cshDA +N);
        }
    }

    //combine cgrDA with NGRA

    for( N = 0; N <= numSamples - 1; N++)
    {
        if(*(cgrDA +N)>0 && *(cgrDA+N)<*(gr+N))
        {
            *(gr +N) = *(cgrDA +N);
        }
    }

    //CALCULATE ASHCONTENTS
    for( N = 0; N <= numSamples - 1; N++)
    {
        if(*(rhob +N)>0)
        {
            ashcontent=(0.7879-1/(*(rhob +N)))/0.0043;
            PDK_SetCurveValueAt(lngashcontent, N, ashcontent);
        }
    }

//Check the minimum bulk density of the thickest coal bed

    Minirhob = *(rhob + TopOfThikCoal);

    while(TopOfThikCoal < BottomOfThikCoal)
    {
        TopOfThikCoal++;

        if(*(rhob + TopOfThikCoal) <= Minirhob)
        {
            Minirhob = *(rhob + TopOfThikCoal);
        }
    }

//coal lithology category

    for( N = 0; N <= numSamples - 1; N++)
    {
        if(PDK_IsNull(*(rhob+N)))
        {
            goto endoflithology;
        }

        else if(PDK_IsNotNull(*(rhob+N)) && *(Washouts+N)<=0.5 && *(thicknessDA+N)<=1.5) // Prevent thin bed been
overshadowed high GR
        {
```

```
if(*(rhob +N)<=1.55 )
{
        CleanCoal = 2.2;
        PDK_SetCurveValueAt( lngCleanCoal, N, CleanCoal);
        *(cleancoalA +N)=2.2;
}

else if( *(rhob +N)<=1.75)
{
        HGRC = 2.2;
        *(HGRA +N)=2.2;
        PDK_SetCurveValueAt( lngHGRC, N, HGRC);
}

else if( *(rhob +N)<=1.9)
{
        Hash = 2.2;
        *(HASHA +N)=2.2;
        PDK_SetCurveValueAt( lngHash, N, Hash);
}
else if( *(rhob +N)<=2.1)
{
        csh = 2.2;
        *(CSHA +N)=2.2;
        PDK_SetCurveValueAt( lngcsh, N, csh);
}


}

else if(PDK_IsNotNull(*(res+N)) && PDK_IsNotNull(*(gr+N)) && PDK_IsNotNull(*(rhob+N)) && Minirhob >=
1.55 )
{
        if(*(rhob +N)<=2.2 && *(res +N)<=30)
        {
                BentCSH = 2.2;
                *(BENTCSHA +N)=2.2;
                PDK_SetCurveValueAt( lngBentCSH, N, BentCSH);
        }
        else if(*(rhob +N)<=2.0 && *(rintDA+N)==0)
        {
                csh = 2.2;
                *(CSHA +N)=2.2;
                PDK_SetCurveValueAt( lngcsh, N, csh);
        }
        else if( *(rhob +N)<=2.2 && *(GRcshA+N)>0)
        {
                csh = 2.2;
                *(CSHA +N)=2.2;
                PDK_SetCurveValueAt( lngcsh, N, csh);
        }


        else if(*(rhob +N)<=1.75 && *(gr +N)<=70)
        {
                CleanCoal = 2.2;
                PDK_SetCurveValueAt( lngCleanCoal, N, CleanCoal);
                *(cleancoalA +N)=2.2;
        }

        else if( *(rhob +N)<=1.75)
        {
                HGRC = 2.2;
```

173

```
                              *(HGRA +N)=2.2;
                              PDK_SetCurveValueAt( lngHGRC, N, HGRC);
                    }

          else if( *(rhob +N)<=2.0)
          {
                    Hash = 2.2;
                    *(HASHA +N)=2.2;
                    PDK_SetCurveValueAt( lngHash, N, Hash);
          }
          else if( *(rhob +N)<=2.2 && *(rintDA+N)!=0)
          {
                    csh = 2.2;
                    *(CSHA +N)=2.2;
                    PDK_SetCurveValueAt( lngcsh, N, csh);
          }
}

else if(PDK_IsNotNull(*(res+N)) && PDK_IsNotNull(*(rhob+N)) && Minirhob >= 1.55 )
{
          if(*(rhob +N)<=2.2 && *(res +N)<=30)
          {
                    BentCSH = 2.2;
                    *(BENTCSHA +N)=2.2;
                    PDK_SetCurveValueAt( lngBentCSH, N, BentCSH);
          }
          else if(*(rhob +N)<=2.0 && *(rintDA+N)==0)
          {
                    csh = 2.2;
                    *(CSHA +N)=2.2;
                    PDK_SetCurveValueAt( lngcsh, N, csh);
          }
          else if( *(rhob +N)<=2.22)
          {
                    csh = 2.2;
                    *(CSHA +N)=2.2;
                    PDK_SetCurveValueAt( lngcsh, N, csh);
          }


          else if(*(rhob +N)<=1.75 )
          {
                    CleanCoal = 2.2;
                    PDK_SetCurveValueAt( lngCleanCoal, N, CleanCoal);
                    *(cleancoalA +N)=2.2;
          }


          else if( *(rhob +N)<=2.0)
          {
                    Hash = 2.2;
                    *(HASHA +N)=2.2;
                    PDK_SetCurveValueAt( lngHash, N, Hash);
          }
          else if( *(rhob +N)<=2.2 && *(rintDA+N)!=0)
          {
                    csh = 2.2;
                    *(CSHA +N)=2.2;
                    PDK_SetCurveValueAt( lngcsh, N, csh);
          }

}
```

174

```
else if(PDK_IsNotNull(*(gr+N)) && PDK_IsNotNull(*(rhob+N)) && Minirhob >= 1.55)
{


        if( *(rhob +N)<=2.2 && *(GRcshA+N)>0)
        {
                csh = 2.2;
                *(CSHA +N)=2.2;
                PDK_SetCurveValueAt( Ingcsh, N, csh);
        }


        else if(*(rhob +N)<=1.75 && *(gr +N)<=70)
        {
                CleanCoal = 2.2;
                PDK_SetCurveValueAt( IngCleanCoal, N, CleanCoal);
                *(cleancoalA +N)=2.2;
        }

        else if( *(rhob +N)<=1.75)
        {
                HGRC = 2.2;
                *(HGRA +N)=2.2;
                PDK_SetCurveValueAt( IngHGRC, N, HGRC);
        }

        else if( *(rhob +N)<=2.0)
        {
                Hash = 2.2;
                *(HASHA +N)=2.2;
                PDK_SetCurveValueAt( IngHash, N, Hash);
        }
        else if( *(rhob +N)<=2.1)
        {
                csh = 2.2;
                *(CSHA +N)=2.2;
                PDK_SetCurveValueAt( Ingcsh, N, csh);
        }


}

else if(PDK_IsNotNull(*(rhob+N)) && Minirhob >= 1.55)
{

        if(*(rhob +N)<=1.75 )
        {
                CleanCoal = 2.2;
                PDK_SetCurveValueAt( IngCleanCoal, N, CleanCoal);
                *(cleancoalA +N)=2.2;
        }

        else if( *(rhob +N)<=2.0)
        {
                Hash = 2.2;
                *(HASHA +N)=2.2;
                PDK_SetCurveValueAt( IngHash, N, Hash);
        }
        else if( *(rhob +N)<=2.2)
        {
                csh = 2.1;
```

175

```
                    *(CSHA +N)=2.2;
                    PDK_SetCurveValueAt( lngcsh, N, csh);
            }

    }


    else if(PDK_IsNotNull(*(res+N)) && PDK_IsNotNull(*(gr+N)) && PDK_IsNotNull(*(cali+N)) &&
PDK_IsNotNull(*(rhob+N)))
        {
            if( *(rhob +N)<=2.22 && *(res +N)<=30 )
            {
                    BentCSH = 2.2;
                    *(BENTCSHA +N)=2.2;
                    PDK_SetCurveValueAt( lngBentCSH, N, BentCSH);
            }
            else if(*(rhob +N)<=2.0 && *(rintDA+N)==0)
            {
                    csh = 2.2;
                    *(CSHA +N)=2.2;
                    PDK_SetCurveValueAt( lngcsh, N, csh);
            }
            else if(*(rhob +N)<=2.22 && *(GRcshA+N)>0)
            {
                    csh = 2.2;
                    *(CSHA +N)=2.2;
                    PDK_SetCurveValueAt( lngcsh, N, csh);
            }

            else if(*(rhob +N)<=1.55 &&  *(gr +N)<=70)
            {
                    CleanCoal = 2.2;
                    PDK_SetCurveValueAt( lngCleanCoal, N, CleanCoal);
                    *(cleancoalA +N)=2.2;
            }
            else if(*(rhob +N)<=1.75)
            {
                    HGRC = 2.2;
                    *(HGRA +N)=2.2;
                    PDK_SetCurveValueAt( lngHGRC, N, HGRC);
            }

            else if( *(rhob +N)<=2.0 && *(Washouts +N)<=2.5)
            {
                    Hash = 2.2;
                    *(HASHA +N)=2.2;
                    PDK_SetCurveValueAt( lngHash, N, Hash);
            }
            else if( *(rhob +N)<=2.2 && *(rintDA+N)!=0)
            {
                    csh = 2.2;
                    *(CSHA +N)=2.2;
                    PDK_SetCurveValueAt( lngcsh, N, csh);
            }

    }

    else if(PDK_IsNotNull(*(res+N)) && PDK_IsNotNull(*(gr+N)) && PDK_IsNotNull(*(rhob+N)) )
        {
            if(*(rhob +N)<=2.2 && *(res +N)<=30)
            {
```

```
                          BentCSH = 2.2;
                          *(BENTCSHA +N)=2.2;
                          PDK_SetCurveValueAt( lngBentCSH, N, BentCSH);
                  }
                  else if(*(rhob +N)<=2.0 && *(rintDA+N)==0)
                  {
                          csh = 2.2;
                          *(CSHA +N)=2.2;
                          PDK_SetCurveValueAt( lngcsh, N, csh);
                  }
                  else if( *(rhob +N)<=2.2 && *(GRcshA+N)>0)
                  {
                          csh = 2.2;
                          *(CSHA +N)=2.2;
                          PDK_SetCurveValueAt( lngcsh, N, csh);
                  }


                  else if(*(rhob +N)<=1.55 && *(gr +N)<=70)
                  {
                          CleanCoal = 2.2;
                          PDK_SetCurveValueAt( lngCleanCoal, N, CleanCoal);
                          *(cleancoalA +N)=2.2;
                  }

                  else if( *(rhob +N)<=1.75)
                  {
                          HGRC = 2.2;
                          *(HGRA +N)=2.2;
                          PDK_SetCurveValueAt( lngHGRC, N, HGRC);
                  }

                  else if( *(rhob +N)<=2.0)
                  {
                          Hash = 2.2;
                          *(HASHA +N)=2.2;
                          PDK_SetCurveValueAt( lngHash, N, Hash);
                  }
                  else if( *(rhob +N)<=2.2 && *(rintDA+N)!=0)
                  {
                          csh = 2.2;
                          *(CSHA +N)=2.2;
                          PDK_SetCurveValueAt( lngcsh, N, csh);
                  }
          }

          else if(PDK_IsNotNull(*(res+N)) && PDK_IsNotNull(*(rhob+N)) )
          {
                  if(*(rhob +N)<=2.2 && *(res +N)<=30)
                  {
                          BentCSH = 2.2;
                          *(BENTCSHA +N)=2.2;
                          PDK_SetCurveValueAt( lngBentCSH, N, BentCSH);
                  }
                  else if(*(rhob +N)<=2.0 && *(rintDA+N)==0)
                  {
                          csh = 2.2;
                          *(CSHA +N)=2.2;
                          PDK_SetCurveValueAt( lngcsh, N, csh);
                  }
                  else if( *(rhob +N)<=2.22)
                  {
```

```
                csh = 2.2;
                *(CSHA +N)=2.2;
                PDK_SetCurveValueAt( lngcsh, N, csh);
        }


        else if(*(rhob +N)<=1.55 )
        {
                CleanCoal = 2.2;
                PDK_SetCurveValueAt( lngCleanCoal, N, CleanCoal);
                *(cleancoalA +N)=2.2;
        }

        else if( *(rhob +N)<=1.75)
        {
                HGRC = 2.2;
                *(HGRA +N)=2.2;
                PDK_SetCurveValueAt( lngHGRC, N, HGRC);
        }


        else if( *(rhob +N)<=2.0)
        {
                Hash = 2.2;
                *(HASHA +N)=2.2;
                PDK_SetCurveValueAt( lngHash, N, Hash);
        }
        else if( *(rhob +N)<=2.2 && *(rintDA+N)!=0)
        {
                csh = 2.2;
                *(CSHA +N)=2.2;
                PDK_SetCurveValueAt( lngcsh, N, csh);
        }

}

else if(PDK_IsNotNull(*(gr+N)) && PDK_IsNotNull(*(rhob+N)))
{


        if( *(rhob +N)<=2.2 && *(GRcshA+N)>0)
        {
                csh = 2.2;
                *(CSHA +N)=2.2;
                PDK_SetCurveValueAt( lngcsh, N, csh);
        }


        else if(*(rhob +N)<=1.55 &&  *(gr +N)<=70)
        {
                CleanCoal = 2.2;
                PDK_SetCurveValueAt( lngCleanCoal, N, CleanCoal);
                *(cleancoalA +N)=2.2;
        }

        else if( *(rhob +N)<=1.75)
        {
                HGRC = 2.2;
                *(HGRA +N)=2.2;
                PDK_SetCurveValueAt( lngHGRC, N, HGRC);
        }
```

```
                    else if( *(rhob +N)<=2.0)
                    {
                            Hash = 2.2;
                            *(HASHA +N)=2.2;
                            PDK_SetCurveValueAt( lngHash, N, Hash);
                    }
                    else if( *(rhob +N)<=2.1)
                    {
                            csh = 2.2;
                            *(CSHA +N)=2.2;
                            PDK_SetCurveValueAt( lngcsh, N, csh);
                    }

            }
            else if(PDK_IsNotNull(*(rhob+N)))
            {

                    if(*(rhob +N)<=1.55 )
                    {
                            CleanCoal = 2.2;
                            PDK_SetCurveValueAt( lngCleanCoal, N, CleanCoal);
                            *(cleancoalA +N)=2.2;
                    }

                    else if( *(rhob +N)<=1.75)
                    {
                            HGRC = 2.2;
                            *(HGRA +N)=2.2;
                            PDK_SetCurveValueAt( lngHGRC, N, HGRC);
                    }

                    else if( *(rhob +N)<=1.9)
                    {
                            Hash = 2.2;
                            *(HASHA +N)=2.2;
                            PDK_SetCurveValueAt( lngHash, N, Hash);
                    }
                    else if( *(rhob +N)<=2.1)
                    {
                            csh = 2.2;
                            *(CSHA +N)=2.2;
                            PDK_SetCurveValueAt( lngcsh, N, csh);
                    }

            }


endoflithology:;

    }
    //Calculate and output GAS IN PLACE

    for( N = 0; N <= numSamples - 1; N++)
    {
        if(TH==FALSE && *(cleancoalA +N)>0)
        {
            Thtopind=N;
            TH=TRUE;
        }
        else if(TH==TRUE && *(cleancoalA +N)<0 && N <= numSamples -1)
        {
            TH=FALSE;
```

```
                    Thbottomind=N-1;
                    Thcoal=(Thbottomind-Thtopind)*Resolution;

                    Fpressure=(PDK_GetStart()+Thcoal)*0.45;
                    Fdensity=(*(rhob+Thbottomind)+*(rhob+Thtopind))/2;

                    if(Fdensity<1.3 || Fdensity>1.55)
                    {
                            ashcontent=0.16;
                    }
                    else
                    {
                            ashcontent=(0.7879-1/Fdensity)/0.43;
                    }

                    gascontent=651*Fpressure/(Fpressure+604)*(1-ashcontent);

                    CO2content=1050*Fpressure/(Fpressure+380)*(1-ashcontent);

                    CO2=CO2+160*Thcoal*1800*CO2content/1000000;

                    gasinplace=gasinplace+160*Thcoal*1800*gascontent/1000000;

            }
    }

gasinplace1=gasinplace;

TH=FALSE;

//Calculate and output coal thickness

for( N = 0; N <= numSamples - 1; N++)
{
        if(TH==FALSE && *(HGRA +N)>0)
        {
                Thtopind=N;
                TH=TRUE;
        }
        else if(TH==TRUE && *(HGRA +N)<0 && N <= numSamples -1)
        {
                TH=FALSE;
                Thbottomind=N-1;

                Thhgr=(Thbottomind-Thtopind)*Resolution;

                Fpressure=(PDK_GetStart()+Thhgr)*0.45;

                ashcontent=0.42;

                gascontent=651*Fpressure/(Fpressure+604)*(1-ashcontent);

                gasinplace=gasinplace+160*Thhgr*1800*gascontent/1000000;

                gasinplace2=gasinplace2+160*Thhgr*1800*gascontent/1000000;

                CO2content=1050*Fpressure/(Fpressure+380)*(1-ashcontent);

                CO2=CO2+160*Thhgr*1800*CO2content/1000000;


        }
```

```
}

TH=FALSE;

//Calculate and output coal thickness

for( N = 0; N <= numSamples - 1; N++)
{
        if(TH==FALSE && *(HASHA +N)>0)
        {
                Thtopind=N;
                TH=TRUE;
        }
        else if(TH==TRUE && *(HASHA +N)<0 && N <= numSamples -1)
        {
                TH=FALSE;
                Thbottomind=N;

                Thhash=(Thbottomind-Thtopind)*Resolution;

                Fpressure=(PDK_GetStart()+Thhash)*0.45;

                ashcontent=0.58;

                gascontent=651*Fpressure/(Fpressure+604)*(1-ashcontent);

                gasinplace=gasinplace+160*Thhash*1800*gascontent/1000000;

                gasinplace3=gasinplace3+160*Thhash*1800*gascontent/1000000;

                CO2content=1050*Fpressure/(Fpressure+380)*(1-ashcontent);

                CO2=CO2+160*Thhash*1800*CO2content/1000000;

        }
}

TH=FALSE;

//Calculate and output coal thickness

for( N = 0; N <= numSamples - 1; N++)
{
        if(TH==FALSE && *(CSHA +N)>0)
        {
                Thtopind=N;
                TH=TRUE;
        }
        else if(TH==TRUE && *(CSHA +N)<0 && N <= numSamples -1)
        {
                TH=FALSE;
                Thbottomind=N;

                Thcsh=(Thbottomind-Thtopind)*Resolution;

                Fpressure=(PDK_GetStart()+Thcsh)*0.45;

                ashcontent=0.71;

                gascontent=651*Fpressure/(Fpressure+604)*(1-ashcontent);
```

```
                    gasinplace=gasinplace+160*Thcsh*1800*gascontent/1000000;

                    gasinplace4=gasinplace4+160*Thcsh*1800*gascontent/1000000;

                    CO2content=1050*Fpressure/(Fpressure+380)*(1-ashcontent);

                    CO2=CO2+160*Thcsh*1800*CO2content/1000000;


            }
    }


    TH=FALSE;

    //Calculate and output coal thickness

    for( N = 0; N <= numSamples - 1; N++)
    {
            if(TH==FALSE && *(BENTCSHA +N)>0)
            {
                    Thtopind=N;
                    TH=TRUE;
            }
            else if(TH==TRUE && *(BENTCSHA +N)<0 && N <= numSamples -1)
            {
                    TH=FALSE;
                    Thbottomind=N;

                    Thbcsh=(Thbottomind-Thtopind)*Resolution;

                    Fpressure=(PDK_GetStart()+Thbcsh)*0.45;

                    ashcontent=0.71;

                    gascontent=651*Fpressure/(Fpressure+604)*(1-ashcontent);

                    gasinplace=gasinplace+160*Thbcsh*1800*gascontent/1000000;

                    gasinplace4=gasinplace4+160*Thbcsh*1800*gascontent/1000000;

                    CO2content=1050*Fpressure/(Fpressure+380)*(1-ashcontent);

                    CO2=CO2+160*Thbcsh*1800*CO2content/1000000;


            }
    }

    for( N = 0; N <= numSamples - 1; N++)
    {
            GIP=gasinplace;
            PDK_SetCurveValueAt(lngGIP, N, GIP);
            GIPcleancoal = gasinplace1;
            PDK_SetCurveValueAt(lngGIPcleancoal, N, GIPcleancoal);
            GIPhgrc = gasinplace2;
            PDK_SetCurveValueAt(lngGIPhgrc, N, GIPhgrc);
            GIPashycoal = gasinplace3;
            PDK_SetCurveValueAt(lngGIPashycoal, N, GIPashycoal);
            GIPshales = gasinplace4;
            PDK_SetCurveValueAt(lngGIPshales, N, GIPshales);
            PDK_SetCurveValueAt(lngCO2, N, CO2);
```

182

```
}

//use gascontent_core to calculate gascontent curve and gip

for( N = 0; N <= numSamples - 1; N++)
{
        GasContent = PDK_GetParameterValueAt(lngGasContent, N);

        if(*(cleancoalA +N)>0)
        {
                if(*(rhob +N) <=1.32 || *(rhob +N)>=1.55)
                {
                        ashcontent=0.14;
                }
                else
                {
                        ashcontent=(0.7879-1/ *(rhob +N))/0.43;
                }

                gascontentcurve = GasContent * (1-ashcontent)/0.86;

                TGIPclean=TGIPclean+160*Resolution*1800*gascontentcurve/1000000;
        }
        else if(*(HGRA +N)>0)
        {

                ashcontent=0.42;

                gascontentcurve = GasContent * (1-ashcontent)/0.86;

                TGIPhgr=TGIPhgr+160*Resolution*1800*gascontentcurve/1000000;
        }
        else if( *(HASHA +N)>0)
        {

                ashcontent=0.58;

                gascontentcurve = GasContent * (1-ashcontent)/0.86;

                TGIPashy=TGIPashy+160*Resolution*1800*gascontentcurve/1000000;
        }

        else if(*(CSHA +N)>0 )
        {
                ashcontent=0.82;

                gascontentcurve = GasContent * (1-ashcontent)/0.86;

                TGIPcsh=TGIPcsh+160*Resolution*1800*gascontentcurve/1000000;
        }
        else if(*(BENTCSHA +N)>0)
        {
                ashcontent=0.82;

                gascontentcurve = GasContent * (1-ashcontent)/0.86;

                TGIPbcsh=TGIPbcsh+160*Resolution*1800*gascontentcurve/1000000;
        }
        else

                gascontentcurve=0;
```

183

```
            PDK_SetCurveValueAt(lnggascontentcurve, N, gascontentcurve);
}

TGIP=TGIPclean+TGIPhgr+TGIPashy+TGIPcsh;

for( N = 0; N <= numSamples - 1; N++)
{
        PDK_SetCurveValueAt(lngTGIPclean, N, TGIPclean);
        PDK_SetCurveValueAt(lngTGIPhgr, N, TGIPhgr);
        PDK_SetCurveValueAt(lngTGIPashy, N, TGIPashy);
        PDK_SetCurveValueAt(lngTGIPcsh, N, TGIPcsh);
        PDK_SetCurveValueAt(lngTGIPbcsh, N, TGIPbcsh);
        PDK_SetCurveValueAt(lngTGIP, N, TGIP);
}

//output coalbed thickness, top depth, and coal  percentage

while(numcoal<indexH)
{
        coal=0;

        for(int i=0; i<indexH; i++)
        {
                if(ThicknessA[i]>coal)
                {
                        coal=ThicknessA[i];
                        coalind=i;
                }
        }

        coalA[numcoal]=coal;
        coaltopind[numcoal]=indtopHA[coalind];
        coalbottomind[numcoal]=indbottomHA[coalind];
        numcoal++;
        ThicknessA[coalind]=0;
}

for(int ii=0; ii<indexH; ii++)
{
        atop=coaltopind[ii];
        abottom=coalbottomind[ii];

        atop1=coaltopind[ii];
        abottom1=coalbottomind[ii];

        while(atop<abottom)
        {
                if(*(cleancoalA+atop)>0)
                {
                        coalthickstep++;
                }
                else if(*(HGRA+atop)>0)
                {
                        HGRCthickstep++;
                }
                atop++;
        }

        while(atop1<abottom1)
        {

                if(*(cleancoalA+atop1)>0 || *(HGRA+atop1)>0 || *(HASHA+atop1)>0)
```

184

```
                        {
                                thickstep++;
                        }
                        atop1++;

                }
                if(coalA[ii]>0)
                {
                coal percent[ii]=thickstep*resolution/coalA[ii]*100;
                }
                cleancoalB[ii]=coalthickstep*resolution;
                HGRCB[ii]=HGRCthickstep*resolution;

                thickstep=0;
                HGRCthickstep=0;
                coalthickstep=0;
        }

        for(int iii=0; iii<indexH; iii++)
        {
                topdepth[iii]=PDK_GetStart()+resolution*coaltopind[iii];
        }

        for(int aa=0; aa<indexH; aa++)
        {
                if(PDK_IsNotNull(coalA[aa]) && coal percent[aa]>30)
                {
                        coal1 = coalA[aa];
                        topdepth1=topdepth[aa];
                        coal percent1=coal percent[aa];
                        cleancoal1=cleancoalB[aa];
                        HGRC1=HGRCB[aa];

                        for( N = 0; N <= numSamples - 1; N++)
                        {

                        PDK_SetCurveValueAt( lngcoal1, N, coal1);
                        PDK_SetCurveValueAt( lngtopdepth1, N, topdepth1);
                        PDK_SetCurveValueAt( lngcoal percent1, N, coal percent1);
                        PDK_SetCurveValueAt( lngcleancoal1, N, cleancoal1);
                        PDK_SetCurveValueAt( lngHGRC1, N, HGRC1);
                        }

                        coalA[aa]=PDK_GetNull();
                        goto nextcoal;
                }
        }
nextcoal:;

//pick gr, rild, and neutron of clean coal

        seamtop = ceil((topdepth1-PDK_GetStart())/Resolution);
        seambottom=ceil((topdepth1+coal1-PDK_GetStart())/Resolution);

        for(int zz=seamtop; zz<seambottom; zz++)
        {
                GR= *(gr +zz);
                RILD=PDK_GetCurveValueAt(lngRILD, zz);
                CNPOR=PDK_GetCurveValueAt(lngCNPOR, zz);

                if(GR<CleanCoalGR && GR>0)
                {
```

185

```
                    CleanCoalGR=GR;
            }
            if(RILD>CleanCoalRILD)
            {
                    CleanCoalRILD=RILD;
            }
            if(CNPOR>CleanCoalPHIN)
            {
                    CleanCoalPHIN=CNPOR;
            }
    }

    for( N = 0; N <= numSamples - 1; N++)
    {
            PDK_SetCurveValueAt( lngCleanCoalGR, N, CleanCoalGR);
            PDK_SetCurveValueAt( lngCleanCoalRILD, N, CleanCoalRILD);
            PDK_SetCurveValueAt( lngCleanCoalPHIN, N, CleanCoalPHIN);
    }

    for(int bb=0; bb<indexH; bb++)
    {
            if(PDK_IsNotNull(coalA[bb]) && coal percent[bb]>30)
            {
                    coal2 = coalA[bb];
                    topdepth2=topdepth[bb];
                    coal percent2=coal percent[bb];
                    cleancoal2=cleancoalB[bb];
                    HGRC2=HGRCB[bb];

                    for( N = 0; N <= numSamples - 1; N++)
                    {

                    PDK_SetCurveValueAt( lngcleancoal2, N, cleancoal2);
                    PDK_SetCurveValueAt( lngHGRC2, N, HGRC2);

                    PDK_SetCurveValueAt( lngcoal2, N, coal2);
                    PDK_SetCurveValueAt( lngtopdepth2, N, topdepth2);
                    PDK_SetCurveValueAt( lngcoal percent2, N, coal percent2);
                    }

                    coalA[bb]=PDK_GetNull();
                    goto nextcoal1;
            }
    }
nextcoal1:;

    for(int cc=0; cc<indexH; cc++)
    {
            if(PDK_IsNotNull(coalA[cc]) && coal percent[cc]>30)
            {
                    coal3 = coalA[cc];
                    topdepth3=topdepth[cc];
                    coal percent3=coal percent[cc];

                    cleancoal3=cleancoalB[cc];
                    HGRC3=HGRCB[cc];

                    for( N = 0; N <= numSamples - 1; N++)
                    {

                    PDK_SetCurveValueAt( lngcleancoal3, N, cleancoal3);
                    PDK_SetCurveValueAt( lngHGRC3, N, HGRC3);
```

186

```
                                    PDK_SetCurveValueAt( lngcoal3, N, coal3);
                                    PDK_SetCurveValueAt( lngtopdepth3, N, topdepth3);
                                    PDK_SetCurveValueAt( lngcoal percent3, N, coal percent3);
                                    }

                                    coalA[cc]=PDK_GetNull();
                                    goto nextcoal2;
                        }
                }
nextcoal2:;

            for(int dd=0; dd<indexH; dd++)
            {
                    if(PDK_IsNotNull(coalA[dd]) && coal percent[dd]>30)
                    {
                            coal4 = coalA[dd];
                            topdepth4=topdepth[dd];
                            coal percent4=coal percent[dd];

                            cleancoal4=cleancoalB[dd];
                            HGRC4=HGRCB[dd];

                            for( N = 0; N <= numSamples - 1; N++)
                            {

                                    PDK_SetCurveValueAt( lngcleancoal4, N, cleancoal4);
                                    PDK_SetCurveValueAt( lngHGRC4, N, HGRC4);

                                    PDK_SetCurveValueAt( lngcoal4, N, coal4);
                                    PDK_SetCurveValueAt( lngtopdepth4, N, topdepth4);
                                    PDK_SetCurveValueAt( lngcoal percent4, N, coal percent4);
                                    }

                                    coalA[dd]=PDK_GetNull();
                                    goto nextcoal3;
                        }
                }
nextcoal3:;

            for(int ee=0; ee<indexH; ee++)
            {
                    if(PDK_IsNotNull(coalA[ee]) && coal percent[ee]>30)
                    {
                            coal5 = coalA[ee];
                            topdepth5=topdepth[ee];
                            coal percent5=coal percent[ee];

                            cleancoal5=cleancoalB[ee];
                            HGRC5=HGRCB[ee];

                            for( N = 0; N <= numSamples - 1; N++)
                            {

                                    PDK_SetCurveValueAt( lngcleancoal5, N, cleancoal5);
                                    PDK_SetCurveValueAt( lngHGRC5, N, HGRC5);

                                    PDK_SetCurveValueAt( lngcoal5, N, coal5);
                                    PDK_SetCurveValueAt( lngtopdepth5, N, topdepth5);
                                    PDK_SetCurveValueAt( lngcoal percent5, N, coal percent5);
                                    }
```

```
                                    coalA[ee]=PDK_GetNull();
                                    goto nextcoa4;
                    }
        }
nextcoa4:;

        for(int ff=0; ff<indexH; ff++)
        {
                if(PDK_IsNotNull(coalA[ff]) && coal percent[ff]>30)
                {
                        coal6 = coalA[ff];
                        topdepth6=topdepth[ff];
                        coal percent6=coal percent[ff];

                        cleancoal6=cleancoalB[ff];
                        HGRC6=HGRCB[ff];

                        for( N = 0; N <= numSamples - 1; N++)
                        {

                        PDK_SetCurveValueAt( lngcleancoal6, N, cleancoal6);
                        PDK_SetCurveValueAt( lngHGRC6, N, HGRC6);

                        PDK_SetCurveValueAt( lngcoal6, N, coal6);
                        PDK_SetCurveValueAt( lngtopdepth6, N, topdepth6);
                        PDK_SetCurveValueAt( lngcoal percent6, N, coal percent6);
                        }

                        coalA[ff]=PDK_GetNull();
                        goto nextcoal5;
                }
        }
nextcoal5:;

        for(int gg=0; gg<indexH; gg++)
        {
                if(PDK_IsNotNull(coalA[gg]) && coal percent[gg]>30)
                {
                        coal7 = coalA[gg];
                        topdepth7=topdepth[gg];
                        coal percent7=coal percent[gg];

                        cleancoal7=cleancoalB[gg];
                        HGRC7=HGRCB[gg];

                        for( N = 0; N <= numSamples - 1; N++)
                        {

                        PDK_SetCurveValueAt( lngcleancoal7, N, cleancoal7);
                        PDK_SetCurveValueAt( lngHGRC7, N, HGRC7);

                        PDK_SetCurveValueAt( lngcoal7, N, coal7);
                        PDK_SetCurveValueAt( lngtopdepth7, N, topdepth7);
                        PDK_SetCurveValueAt( lngcoal percent7, N, coal percent7);
                        }

                        coalA[gg]=PDK_GetNull();
                        goto nextcoal6;
                }
        }
nextcoal6:;
```

188

```
for(int hh=0; hh<indexH; hh++)
{
        if(PDK_IsNotNull(coalA[hh]) && coal percent[hh]>30)
        {
                coal8 = coalA[hh];
                topdepth8=topdepth[hh];
                coal percent8=coal percent[hh];

                cleancoal8=cleancoalB[hh];
                HGRC8=HGRCB[hh];

                for( N = 0; N <= numSamples - 1; N++)
                {

                PDK_SetCurveValueAt( lngcleancoal8, N, cleancoal8);
                PDK_SetCurveValueAt( lngHGRC8, N, HGRC8);

                PDK_SetCurveValueAt( lngcoal8, N, coal8);
                PDK_SetCurveValueAt( lngtopdepth8, N, topdepth8);
                PDK_SetCurveValueAt( lngcoal percent8, N, coal percent8);
                }

                coalA[hh]=PDK_GetNull();
                goto nextcoal7;
        }
}
nextcoal7:;


        //release memory

        free(gr);
        free(res);
        free(rhob);
        free(cali);
        free(NGRA);
        free(GRcshA);

        //
        free(thicknessDA);
        free(rintDA);
        free(rhobDA);
        free(cshDA);
        free(cgrDA);
        free(crhobDA);

        //
        free(cleancoalA);
        free(HGRA);
        free(HASHA);
        free(BENTCSHA);
        free(CSHA);

        free(Washouts);
        free(GRcoalA);
```

189